ISSN 1881-7815 Online ISSN 1881-7823

BST BioScience Trends

Volume 8, Number 6
December, 2014

IRCA BSSA

IACMHR

www.biosciencetrends.com

BST
BioScience Trends

ISSN: 1881-7815
Online ISSN: 1881-7823
CODEN: BTIRCZ
Issues/Year: 6
Language: English
Publisher: IACMHR Co., Ltd.

BioScience Trends is one of a series of peer-reviewed journals of the International Research and Cooperation Association for Bio & Socio-Sciences Advancement (IRCA-BSSA) Group and is published bimonthly by the International Advancement Center for Medicine & Health Research Co., Ltd. (IACMHR Co., Ltd.) and supported by the IRCA-BSSA and Shandong University China-Japan Cooperation Center for Drug Discovery & Screening (SDU-DDSC).

BioScience Trends devotes to publishing the latest and most exciting advances in scientific research. Articles cover fields of life science such as biochemistry, molecular biology, clinical research, public health, medical care system, and social science in order to encourage cooperation and exchange among scientists and clinical researchers.

BioScience Trends publishes Original Articles, Brief Reports, Reviews, Policy Forum articles, Case Reports, News, and Letters on all aspects of the field of life science. All contributions should seek to promote international collaboration.

Editorial Board

Editorial Office

Pearl City Koishikawa 603,
2-4-5 Kasuga, Bunkyo-ku,
Tokyo 112-0003, Japan
Tel: +81-3-5840-8764
Fax: +81-3-5840-8765
E-mail: office@biosciencetrends.com

BioScience Trends

Editorial and Head Office

Pearl City Koishikawa 603, 2-4-5 Kasuga, Bunkyo-ku,
Tokyo 112-0003, Japan

Tel: +81-3-5840-8764, Fax: +81-3-5840-8765
E-mail: office@biosciencetrends.com
URL: www.biosciencetrends.com

Editorial Board Members

CONTENTS

Volume 8, Number 6, 2014

Original Articles

Commentary

Subject Index

Guide for Authors

Copyright

Original Article

DOI: 10.5582/bst.2014.01138

A systematic review of social capital and chronic non-communicable diseases

Fuyong Hu[1,2,*], Bo Hu[3,*], Ren Chen[2], Ying Ma[2], Li Niu[3], Xia Qin[2], Zhi Hu[1,2,]**

[1] *Department of Epidemiology and Biostatistics, School of Public Health, Anhui Medical University, Hefei, China;*
[2] *School of Health Services Management, Anhui Medical University, Hefei, China;*
[3] *The First Affiliated Hospital of Anhui Medical University, Hefei, China.*

Summary **Nowadays, chronic non-communicable diseases have become a significant social problem of healthcare which threatens human health along with their rapid progress of morbidity and mortality. How to develop potential, intangible resources to compensate for insufficient physical resources is urgent. By analyzing literature reporting the association between social capital and chronic non-communicable diseases systematically, evidence was found for a positive association between social capital and chronic non-communicable disease prevention and control. The social capital theory may provide a new idea to solve the problem.**

Keywords: Social capital, chronic non-communicable diseases, systematic review

1. Introduction

Chronic non-communicable diseases (NCDs), also known as chronic diseases, are a series of diseases which don't pass from person to person. They are of long duration and generally have slow progression (*1*). The four main types of NCDs are cardiovascular diseases (CVD), cancers, chronic respiratory diseases (COPD), and diabetes, which make the largest contribution to morbidity and mortality of NCDs (*2*). Along with the rapid development of social economy, lifestyle changes, urbanization speeding up and population aging, NCDs constitute the largest burden of morbidity and mortality (*3*), especially in low and middle income countries (LMICs) (*4*). NCDs pose a heavy financial burden on many affected residents, which impose insurmountable barriers to access essential healthcare for the poor (*5*). How to effectively prevent and control NCDs is no longer a simple health problem, but a social problem. Addressing primary prevention and equity of health systems by national NCD policies needs a long time to wait in most LMICs. How to develop potential, intangible resources to compensate for insufficient physical resources is urgent.

With growing recognition of the social determinants of health, social capital is an increasingly important construct in healthcare (*6*). Social capital theory originated from the interdisciplinary union of sociology and economics, activated in every field of social development. There are many definitions of social capital according to systematic review. Bourdier seemed to be the first to dedicate an entire work to the concept, while further refinements came from Coleman, Putnam, Leonardi, Nanetti, Portes and others (*7*). The most accessible definition of social capital used in healthcare originated with Putnam (*8*).

According to Putnam, social capital is defined as "features of social organization, such as trust, norms and networks, which can improve the efficacy of society by facilitating coordinated actions" (*9*). The concept represents the resources available to members of tightly knit communities, and tends to emphasize social capital as a group attribute or contextual concept (*10*), which may work on individual health by contextual influence. The contextual level can be further divided into 4 analytic levels: the "macro" level (social, political and economic context), the "meso" level (neighborhood or community), individual-level behaviors, and individual-level attitudes (*7*). The former 2 levels can be summarized as the ecological level, and the latter as individual level. Meanwhile, the concept of social capital can be defined as the "network" theory,

*These authors contributed equally to this works.

**Address correspondence to:*
Dr. Zhi Hu, School of Health Services Management, Anhui Medical University, No. 81, Meishan Road, Hefei 230032, Anhui, China.
E-mail: aywghz@126.com

and is equal to resources which may be acquired through individual's social networks (*6*). This resource concept also can be summarized as individual level.

There are enough consensuses to draw some important generalizations about the nature of social capital (*10*). The behavioral manifestations of civic engagement or members participation can be classified as structural social capital, and those subjective attitudes (interpersonal trust and norms of reciprocity) as cognitive social capital (*11*). Social capital also can be broken down into bonding, bridging, and linking social capital by the interpersonal relationship between different social identity (*12*). Bonding social capital represents the strong ties between homogeneous groups, such as family and company. In contrast, bridging social capital represents the weak ties between heterogeneous groups, differing by age, ethnic group, class, etc. Linking social capital refers to norms of respect and trusting relationships across power or authority gradients in society (*13*). No matter how to classify, social capital has still been measured via individual cognition and behavior in the health field.

In this paper, we present a systematic review of the quantitative studies that have investigated the association between social capital and NCDs (the four main types), and explore the role of social capital in NCD prevention and control.

2. Methods

2.1. *Literature search*

In order to identify all quantitative studies investigating the association between social capital and NCDs published up to 1 July 2014, a review protocol was developed. 6 electronic databases (PubMed, Biosis Previews, EBSCO, ELSEVIER ScienceDirect, Wiley Online Library, SCIE, JCR) in our school library were searched using Medical Subject Headings ("Chronic Disease" or Cancer or Diabetes or "Cardiovascular Diseases" or COPD) and keywords "Social Capital" . The search strategy is shown in Supplementary Data. First, duplicated studies were excluded. Second, the abstracts of all studies were reviewed, and those against inclusion criteria were removed. The inclusion criteria were as follows: studies were included if they had a NCDs outcome, but excluded if NCDs were confounding factors. Studies were included if they measured social capital, and analyzed the association between social capital and NCDs. The references of included studies were identified in the same way.

2.2. *Data extraction and analysis*

The full texts of included studies were reviewed. The data of setting, study design, population, sample size, social capital measurement, health outcomes, validity and results of each study was extracted. Effect estimates were extracted separately and later classified by the four types of NCDs and two types (structural/cognitive) and two levels (ecological/individual) of social capital. Because differences in the measurement of social capital and NCDs made meta-analysis impossible, we adopted the method of grouping results developed by Ramirez *et al*. (*14*). The association between social capital and NCDs of each included study was classified into one of three categories as follows: an inverse association between social capital and NCDs significant at the 5% level (high levels of social capital associated with lower risk of NCDs), no association between social capital and NCDs not statistically significant at the 5% level, and a positive association between social capital and NCDs significant at the 5% level (high levels of social capital associated with higher risk of NCDs). The combined association between social capital and the risk of NCDs was evaluated after the number of included studies in each category was counted. Each study was evaluated using a 9 point validity checklist covering problems (*8*).

3. Results

3.1. *Studies selection*

Figure 1 shows the procedure of studies selection. Totally 316 studies from 6 databases were searched, 87 studies were excluded as duplicates. After reviewing the abstract of the rest of the studies, only 15 studies met inclusion criteria. Two studies were identified through reference searching, making a total of 17 studies in this review.

3.2. *Characteristics of the included studies*

Characteristics of included studies measuring NCDs and social capital are shown in Table 1. Only 1 study

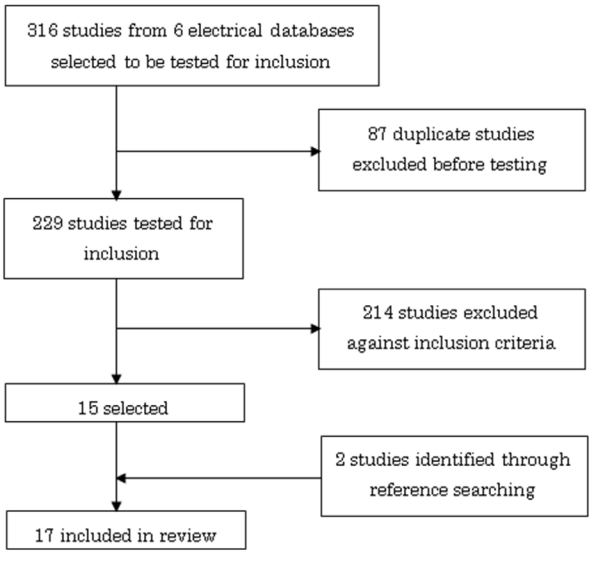

Figure 1. Procedure of studies selection.

Table 1. Characteristics of the 17 studies measuring NCDs and social capital

Reference	Setting	Study design	Population	Sample size	Social capital measure	NCDs measure	Validity
Kawachi *et al*., 1997 (*15*)	USA 39 states	Cross-sectional ecologic study	18+ years	7654	trust, fairness, help group membership aggregated to state level	Age-adjusted mortality rates of CVD and cancer	1, 3, 5
Lynch *et al*., 2001 (*16*)	16 OECD countries	Cross-national study	All years	N.S.	trust belonging to organizations, volunteering aggregated to countries level	Mortality rates of CVD, cancer, diabetes, COPD	1, 3, 5, 7
Lochner *et al*., 2003 (*17*)	USA, Chicago	Cross-sectional study	45-64 years in 342 neighborhood	N.S.	reciprocity, trust civic participation aggregated to neighborhood-level	Mortality rates of CVD and cancer	1, 3, 5
Franzini *et al*., 2003 (*18*)	USA, Texas	Cross-level analyses	25 + years	50268	homeownership, crime index county level	Years of potential life lost to cardiovascular disease	1, 2, 3, 4
Veenstra *et al*., 2005 (*19*)	Canada, Hamilton	Cross-sectional study	Adult	1504	involvement individual level	The number of chronic conditions	2, 3, 5, 8, 9
Ahern *et al*., 2005 (*20*)	USA	Cross-sectional study	25 + years	769	reciprocity, trust at collective level amount of social support, quality of social support at individual level	Diabetes	1, 3, 4, 6, 8
Ali *et al*., 2006 (*21*)	Southern Sweden, Scania	Prospective cohort study	18-80 years	13322	trust, social participation the combination of C and S individual level	The incidence of CVD	3, 6
Holtgrave *et al*., 2006 (*22*)	USA, 48 states	Cross-sectional study	18+ years	Nearly 500000	a combination of 14 variables aggregated to state level	Percentage of diabetes	1, 2, 3
Sundquist *et al*., 2006 (*23*)	Sweden	Prospective cohort study	45–74 years	2805679	proportions of individuals voting in local government elections at neighborhood level	Incidence of CVD	1, 2, 3
Hyyppa *et al*., 2007 (*24*)	Finland	Prospective cohort study	30–99 years	7217	interpersonal trust, residential stability, leisure participation individual level	CVD mortality	1, 3, 4
Scheffler *et al*., 2008 (*25*)	USA, Northern California	Retrospective cohort study	30–85 years hospitalized for acute coronary syndrome	34752 residents in 35 counties	the Petris Social Capital Index (PSCI) county level	Recurrence of acute coronary syndrome	1, 2, 3
Islam *et al*., 2008 (*26*)	Sweden	Retrospective cohort study	20–84 years	94537	election participation rate crime rate municipal level	Cancer and CVD mortality	1, 2, 3

Key to methodological limitations: Measurement of social capital: 1, secondary analysis of survey questions to measure social capital; 2, combined all aspects of social capital into one score, or only measured one aspect of social capital; 3, didn't mention the validity of social capital measurement; 4, can't represent respondents' views of their community. Methodological limitations: 5, tested the relationship between social capital and NCDs not a stated objective of the study; 6, response rate less than 60%. Features of analysis limitations: 7, lacked control for confounding by socioeconomic status; 8, used only single level modeling while hierarchical data structure (individual and contextual level variables) existed; 9, contextual level disorder, violence or psychological resources adjusted for.

(To continue)

Table 1. Characteristics of the 17 studies measuring NCDs and social capital (Continued)

Reference	Setting	Study design	Population	Sample size	Social capital measure	NCDs measure	Validity
Long *et al.*, 2010 (*27*)	USA, Philadelphia, 69 neighborhoods	Cross-sectional study	29+ years Black veterans with diabetes	294	COMM, HELP, IMPROVE, BELONG, TRUST, PARTICP aggregated to neighborhood level	HbA1c level	1, 3
Farajzadegan *et al.*,2013 (*28*)	Iran, Isfahan	Cross-sectional study	30+ years Patients with type 2 diabetes	120	trust and solidarity, collective action and cooperation, information and communication, social cohesion and inclusion, empowerment and political action, groups and networks individual level	HbA1c level	3, 4
Muennig *et al.*, 2013 (*29*)	USA	Retrospective cohort study	18-65 years	12626, 12625, 12626, 3480, 12630	visit friends or relatives, visit neighbors, attend church, attend meetings, belong to clubs individual level	CVD mortality	1, 2, 3, 4, 5
Riumallo-Herr *et al.*, 2014 (*30*)	Chile	Cross-sectional study	30+ years	4956	social support, generalized trust, neighborhood trust individual level	Diabetes	2, 3, 4
Sundquist *et al.*, 2014 (*31*)	Sweden	Prospective cohort study	65+ years	1517336	rate of voting in local government elections neighborhood level	Mortality of CVD, Cancer, COPD and diabetes	1, 2, 3

Key to methodological limitations: Measurement of social capital: 1, secondary analysis of survey questions to measure social capital; 2, combined all aspects of social capital into one score, or only measured one aspect of social capital; 3, didn't mention the validity of social capital measurement; 4, can't represent respondents' views of their community. Methodological limitations: 5, tested the relationship between social capital and NCDs not a stated objective of the study; 6, response rate less than 60%. Features of analysis limitations: 7, lacked control for confounding by socioeconomic status; 8, used only single level modeling while hierarchical data structure (individual and contextual level variables) existed; 9, contextual level disorder, violence or psychological resources adjusted for.

was set in LMIC according to the World Bank database, the majority of the studies were set in European and American countries, and nearly one half of the studies were set in USA. Seven studies used cohort study, and 10 used cross-sectional study. Sixteen studies chose adults as respondents, and 1 all years. Two studies didn't show sample size as they used secondary statistic data at the ecological level. Compared to ordinary data, sample size of studies referred to respondents with NCDs was much less.

Even though measurement of social capital was diverse, they can be concluded as cognitive and structural social capital. Variables of individual cognition can be summarized as cognitive social capital, like trust, fairness, help, support and reciprocity *et al*. Other variables of individual behavior can be summarized as structural social capital, like membership, participation, voting or election, homeownership and crime rate *et al*. Ten studies measured social capital at the ecological level, and 6 at the individual level, and 1 at both levels. The way to measure social capital was usually by questionnaire.

Seven studies used mortality as health outcomes, and 8 used morbidity, and 2 used glycosylated hemoglobin (HbA1c) level. Eleven studies examined CVD, 7 studies examined diabetes, 5 studies examined cancer, and 2 studies examined COPD. Eight studies used ICD-9 or ICD-10 to classify NCDs, and the remainder used clinic diagnosis.

Table 1 shows the methodological validity of each study. All included studies had a number of methodological limitations. No information in validity of social capital measurement was the common problem in each study. Thirteen studies were secondary analyses of survey data not specifically designed to measure social capital, 8 studies only measured one aspect of social capital or combined different aspects of social capital into one score, 5 studies included problem 4 and 5, and other limitations were in the minority. The sample sizes were not summarized in the late analysis as 2 studies did not mention their sample size.

3.3. *The association between social capital and NCDs*

The results of included studies are extracted and summarized in Table 2. There was a little evidence of an inverse association between social capital (cognitive/ structural) and cardiovascular diseases, with 9 of 15 effected estimates reporting high levels of social capital associated with lower risk level of cardiovascular diseases. Four of 6 effected estimates showed a significant inverse association between cognitive social capital and diabetes, while 1 study reported a significant positive association, and the association between structural social capital and diabetes was inclined to have no association, while 1 reported a significant inverse association. The association between cognitive

Table 2. Summary of data on the association between social capital (cognitive/structural) and NCDs

Items	Number of effect estimates			
	Number of effect estimates	Inverse association	No association	Positive association
Cognitive social capital				
CVD	5	3	2	0
Diabetes	6	4	1	1
Cancer	3	1	2	0
COPD	1	0	1	0
Total	15	8	6	1
Structural social capital				
CVD	10	6	4	0
Diabetes	3	1	2	0
Cancer	5	3	2	0
COPD	2	1	1	0
Total	20	11	9	0

Combined social capital and the number of chronic conditions not included.

Table 3. Summary of data on the association between social capital (individual/ecological level) and NCDs

Items	Number of effect estimates			
	Number of effect estimates	Inverse association	No association	Positive association
Individual level				
CVD	3	2	1	0
Diabetes	4	3	0	1
Cancer	0	0	0	0
COPD	0	0	0	0
Total	7	5	1	1
Ecological level				
CVD	8	7	1	0
Diabetes	4	3	1	0
Cancer	5	3	2	0
COPD	2	1	1	0
Total	19	14	5	0

social capital and cancer was a little inclined to have no association, and structural social capital to have an inverse association. The association between social capital (cognitive/structural) and COPD was inclined to have no association.

The results of included studies summarized in Table 3 according to individual and ecological levels of social capital, and most of the effected estimates were at the ecological level. While at the individual level, there was a little evidence of inverse associations between social capital and NCDs (CVD and diabetes), and studies which referred to cancer and COPD were not found. While at the ecological level, there was strong evidence of an inverse association between social capital and CVD, and a little evidence of inverse associations with diabetes and cancer, and no association with COPD.

4. Discussion

In this review, most studies are from Occident in 17 included articles, while in LMIC these kinds of studies are rare (*15-31*), so the effect of social capital on NCDs in these countries is not known. Social capital was measured by individual cognition and behavior, and the ecological data were aggregated from the individual level, and there is no effective method to measure social capital precisely and directly at present. As affected by individual subject and object factors, the included studies had more or less methodological limitations, and there is a need to pay attention in future research.

According to Table 2, cognitive social capital was inclined to be inversely associated with CVD and diabetes, and structural social capital was inclined to be inversely associated with CVD and cancer. When classified at individual and ecological levels, social capital was strong evidence of an inverse association with NCDs. The quantitative studies of social capital and NCDs are few, on the other hand, as the set of included studies, residents may have high level of healthcare, and the effect of social capital may not emerge in some NCDs. The more healthy people are more likely to join in leisure participation or organizations (*32*). These biases may influence the association between structural social capital and NCDs.

Social capital is the product of human socialization, some research have even regarded it as a public

commodity (*33,34*). Investment in social capital is the result of conscious or unconscious human investment strategy, and aimed at minimizing survival risk. Even though causal mechanisms through which social capital could affect NCDs were unclear. The mechanisms that social capital exerts a contextual effect on human health may conclude diffusing the knowledge of health promotion, keeping healthy behavior by informal social control, access to healthcare services and amenities, and receiving emotional or material support and mutual respect based on social network and participation (*11*). The higher the stocks of social capital the higher appearance to health achievement of a given area (*35*). Local residents could increase exposure to health messages, influence health promotion by informal social control, and eventually result in public health outcomes (*36*). Strengthening the stocks of social capital in communities may provide an important buffer for reducing socioeconomic disparities and affording a relatively equal healthcare system, especially in LMIC.

This review was subject to a number of limitations. First, 6 electronic databases were searched, other published studies which followed our criterion in unselected databases may not be included. Still there might be unpublished studies by research groups who have not published material about social capital and NCDs and may be under-represented. All included studies in English, and language bias may be overlooked. Second, differences in the measurement of social capital and NCDs made formal meta-analysis impossible. Each effected estimate was not given a weight to all included studies and that equivalent effect of each study was summarized in this review.

In conclusion, evidence was found for a positive association between social capital and NCD prevention and control despite various measurements. The social capital theory may provide a new idea to solve the shortage problem of physical resources in NCD prevention and control, especially in LMIC. Further study is urgently required to explore the effect of social capital in NCD prevention, control and management in LMIC.

Acknowledgements

This project was supported by the National Natural Science Foundation of China (Grant No. 71273011).

References

1. WHO Noncommunicable diseases. *http://www.who.int/mediacentre/factsheets/fs355/en/ (accessed December 1, 2014).*
2. Hunter DJ, Reddy KS. Noncommunicable diseases. N Engl J Med. 2013; 369:1336-1343.
3. Probst-Hensch N, Kunzli N. Preventing noncommunicable diseases-beyond lifestyle. Epidemiology. 2012; 23:181-183.
4. Stuckler D. Population causes and consequences of leading chronic diseases: A comparative analysis of prevailing explanations. Milbank Q. 2008; 86:273-326.
5. Kankeu HT, Saksena P, Xu K, Evans DB. The financial burden from non-communicable diseases in low- and middle-income countries: A literature review. Health Res Policy Syst. 2013; 11:31.
6. Ma Y, Qin X, Chen R, Li N, Chen R, Hu Z. Impact of individual-level social capital on quality of life among AIDS patients in China. PloS one. 2012; 7:e48888.
7. Macinko J, Starfield B. The utility of social capital in research on health determinants. Milbank Q. 2001; 79:387-427, IV.
8. De Silva MJ, McKenzie K, Harpham T, Huttly SR. Social capital and mental illness: A systematic review. J Epidemiol Community Health. 2005; 59:619-627.
9. Putnam RD, Leonardi R, Nanetti R. Making democracy work: Civic traditions in modern Italy. Princeton University Press, Princeton, USA, 1993, p:258.
10. Lochner K, Kawachi I, Kennedy BP. Social capital: A guide to its measurement. Health place. 1999; 5:259-270.
11. Murayama H, Fujiwara Y, Kawachi I. Social capital and health: A review of prospective multilevel studies. J Epidemiol. 2012; 22:179-187.
12. Szreter S, Woolcock M. Health by association? Social capital, social theory, and the political economy of public health. Int J Epidemiol. 2004; 33:650-667.
13. Poortinga W. Community resilience and health: The role of bonding, bridging, and linking aspects of social capital. Health place. 2012; 18:286-295.
14. Ramirez AJ, Westcombe AM, Burgess CC, Sutton S, Littlejohns P, Richards MA. Factors predicting delayed presentation of symptomatic breast cancer: A systematic review. Lancet. 1999; 353:1127-1131.
15. Kawachi I, Kennedy BP, Lochner K, Prothrow-Stith D. Social capital, income inequality, and mortality. Am J Public Health. 1997; 87:1491-1498.
16. Lynch J, Smith GD, Hillemeier M, Shaw M, Raghunathan T, Kaplan G. Income inequality, the psychosocial environment, and health: Comparisons of wealthy nations. Lancet. 2001; 358:194-200.
17. Lochner KA, Kawachi I, Brennan RT, Buka SL. Social capital and neighborhood mortality rates in Chicago. Soc Sci Med. 2003; 56:1797-1805.
18. Franzini L, Spears W. Contributions of social context to inequalities in years of life lost to heart disease in Texas, USA. Soc Sci Med. 2003; 57:1847-1861.
19. Veenstra G, Luginaah I, Wakefield S, Birch S, Eyles J, Elliott S. Who you know, where you live: Social capital, neighbourhood and health. Soc Sci Med. 2005; 60:2799-2818.
20. Ahern MM, Hendryx MS. Social capital and risk for chronic illnesses. Chronic illness. 2005; 1:183-190.
21. Ali SM, Merlo J, Rosvall M, Lithman T, Lindstrom M. Social capital, the miniaturisation of community, traditionalism and first time acute myocardial infarction: A prospective cohort study in southern Sweden. Soc Sci Med. 2006; 63:2204-2217.
22. Holtgrave DR, Crosby R. Is social capital a protective factor against obesity and diabetes? Findings from an exploratory study. Ann Epidemiol. 2006; 16:406-408.
23. Sundquist J, Johansson SE, Yang M, Sundquist K. Low linking social capital as a predictor of coronary heart disease in Sweden: A cohort study of 2.8 million people. Soc Sci Med. 2006; 62:954-963.

24. Hyyppa MT, Maki J, Impivaara O, Aromaa A. Individual-level measures of social capital as predictors of all-cause and cardiovascular mortality: A population-based prospective study of men and women in Finland. Eur J Epidemiol. 2007; 22:589-597.
25. Scheffler RM, Brown TT, Syme L, Kawachi I, Tolstykh I, Iribarren C. Community-level social capital and recurrence of acute coronary syndrome. Soc Sci Med. 2008; 66:1603-1613.
26. Islam MK, Gerdtham UG, Gullberg B, Lindstrom M, Merlo J. Social capital externalities and mortality in Sweden. Econ Hum Biol. 2008; 6:19-42.
27. Long JA, Field S, Armstrong K, Chang VW, Metlay JP. Social capital and glucose control. J Community Health. 2010; 35:519-526.
28. Farajzadegan Z, Jafari N, Nazer S, Keyvanara M, Zamani A. Social capital – a neglected issue in diabetes control: A cross-sectional survey in Iran. Health Soc Care Community. 2013; 21:98-103.
29. Muennig P, Cohen AK, Palmer A, Zhu W. The relationship between five different measures of structural social capital, medical examination outcomes, and mortality. Soc Sci Med. 2013; 85:18-26.
30. Riumallo-Herl CJ, Kawachi I, Avendano M. Social capital, mental health and biomarkers in Chile: Assessing the effects of social capital in a middle-income country. Soc Sci Med. 2014; 105:47-58.
31. Sundquist K, Hamano T, Li X, Kawakami N, Shiwaku K, Sundquist J. Linking social capital and mortality in the elderly: A Swedish national cohort study. Exp Gerontol. 2014; 55:29-36.
32. Sundquist K, Lindstrom M, Malmstrom M, Johansson SE, Sundquist J. Social participation and coronary heart disease: A follow-up study of 6900 women and men in Sweden. Soc Sci Med. 2004; 58:615-622.
33. Harpham T, Grant E, Thomas E. Measuring social capital within health surveys: Key issues. Health Policy Plan. 2002; 17:106-111.
34. Bolin K, Lindgren B, Lindstrom M, Nystedt P. Investments in social capital – implications of social interactions for the production of health. Soc Sci Med. 2003; 56:2379-2390.
35. Kawachi I. Social capital and community effects on population and individual health. Ann N Y Acad Sci. 1999; 896:120-130.
36. Viswanath K, Randolph Steele W, Finnegan JR, Jr. Social capital and health: Civic engagement, community size, and recall of health messages. Am J Public Health. 2006; 96:1456-1461.

(Received December 4, 2014; Revised December 14, 2014; Accepted December 18, 2014)

Original Article

DOI: 10.5582/bst.2014.01031

Combination of microRNA expression profiling with genome-wide SNP genotyping to construct a coronary artery disease-related miRNA-miRNA synergistic network

Lin Hua[1,2,*,], Hong Xia[1,2,*], Ping Zhou[1,2], Dongguo Li[1,2], Lin Li[1,2]**

[1] *School of Biomedical Engineering, Capital Medical University, Beijing, China;*
[2] *Beijing Key Laboratory of Fundamental Research on Biomechanics in Clinical Application, Capital Medical University, Beijing, China.*

Summary **In recent years, microRNAs (miRNAs) were found to play critical roles in many important biological processes. On the other hand, the rapid development of genome-wide association studies (GWAS) help identify potential genetic variants associated with the disease phenotypic variance. Therefore, we suggested a combined analysis of microRNA expression profiling with genome-wide Single Nucleotide Polymorphism (SNP) genotyping to identify potential disease-related biomarkers. Considering functional SNPs in miRNA genes or target sites might be important signals associated with human complex diseases, we constructed a miRNA-miRNA synergistic network related to coronary artery disease (CAD) by performing a genome-wide scan for SNPs in human miRNA 3' -untranslated regions (UTRs) target sites and computed potential SNP cooperation effects contributing to disease based on potential miRNA-SNP interactions reported recently. Furthermore, we identified some potential CAD-related miRNAs by analyzing the constructed miRNA-miRNA synergistic network. As a result, the predicted miRNA-miRNA network and miRNA clusters were validated by significantly high interaction effects of CAD-related miRNAs. Accurate classification performances were obtained for all of the identified miRNA clusters, and the sensitivity and specificity were all more than 90%. The network topological analysis confirmed some novel CAD-related miRNAs identified recently by experiments. Our method might help to understand miRNA function and CAD disease, as well as to explore the novel mechanisms involved.**

Keywords: GWAS, target, sites, interaction

1. Introduction

MicroRNAs (miRNAs) are endogenous small non-coding RNA molecules that can regulate gene expression at the posttranscriptional level by binding with 3'-untranslated regions (UTRs) of the target mRNAs through base pairing. About 80% of miRNA genes are located within introns of defined transcription units, and their expression is frequently correlated with expression profiles of their host genes (*1*). Currently, it is estimated that a miRNA may regulate hundreds of target genes and most of human protein coding genes are regulated by miRNAs. miRNA plays critical roles in many important biological processes, and it is therefore suggested that miRNAs are also involved in human complex diseases such as cancers (*2*), heart diseases (*3*), nervous system damage (*4*) and so on.

On the other hand, in recent years, genome-wide association studies (GWAS) have become an increasingly effective tool to identify genetic variation associated with the risk of complex diseases (*5,6*). However, currently identified genetic variants collectively can explain only a small proportion of disease phenotypic variance, and the noise causes many of the identified signals to be false positive loci. A noteworthy observation is that miRNAs are wide and key regulators of gene expression,

*These authors contributed equally to this works.
***Address correspondence to:*
Dr. Lin Hua, School of Biomedical Engineering, Capital Medical University, Beijing, 100069, China.
E-mail: hualin7750@139.com

miRNA-related Single Nucleotide Polymorphisms (SNPs) including SNPs in miRNA genes and target sites therefore may function as regulatory SNPs through modifying miRNA regulation to affect phenotypes and disease susceptibility (*7,8*). More and more evidence has shown that SNPs in target sites or miRNA genes are associated with diseases (*7,8*). For example, Chen and Rajewsky uncovered that SNP density in conserved miRNA sites was lower than in conserved control sites, suggesting that a large class of computationally predicted conserved miRNA target sites is under significant negative selection (*9*). Their results also implicate that SNPs located in miRNA binding sites are likely to affect the expression of the miRNA target and might contribute to the susceptibility of humans to complex diseases. Recent advances in genetic studies have systematically identified and analyzed human polymorphisms in miRNAs and/or miRNA target sites (*8,10*). However, most of them focus on SNPs in target sites and their effects or disease-related miRNAs, while few of them mentioned the understanding of the synergistic regulation of miRNAs and their potential targeted SNPs cooperative effects contributing to disease. With the rapid accumulation of disease-related miRNAs, it is increasingly needed to uncover their functional relationships contributing to diseases at a system biology level.

Different from those constructed miRNA-miRNA networks depending on co-occurrence in 3'-UTRs of the same miRNA target genes (*11*), or using the correlations between the gene silencing scores of individual miRNAs or the combinatorial effects of co-expressed miRNAs in the modulation of a given pathway (*12*), or using the functional information and protein interaction data of predicted miRNA targets (*13*), we attempted to construct a miRNA-miRNA synergistic network related to coronary artery disease (CAD) by performing a genome-wide scan for SNPs in human miRNA 3'-UTR target sites and computed SNP cooperative effects contributing to disease based on the potential miRNA-SNPs interactions reported recently (*7*). In this process, miRNA expression profiling data and genome-wide SNP genotype data were integrated. As a result, predicted a miRNA-miRNA network was validated by significantly high interaction effects of CAD-related miRNAs. Our method can help to understand miRNA function and CAD disease, as well as to explore novel miRNA biomarkers and infer novel mechanisms connecting miRNAs to functions.

2. Materials and Methods

2.1. *Data Source*

2.1.1. *CAD related genome-wide SNP genotype data*

For GWAS data, we selected the genome-wide Wellcome Trust Case Control Consortium (WTCCC) data (*http://www.wtccc.org.uk*), which examined about 2000 individuals for seven major diseases, using a shared set of about 3000 controls. In the current study, only CAD data was used. As a part of the WTCCC, 482, 428 genome-wide SNPs were genotyped. The Standard WTCCC thresholds were applied for SNP quality control (genotype call rate > 95%, Hardy Weinberg equilibrium p-value > 5×10^{-7}, Minor Allele Frequency (MAF) > 0.01). In this analysis, we took those SNPs with $p < 0.01$ in single association tests as potential risk SNPs in consideration of relaxing the cutoff which can avoid losing some true positive loci. In fact, we have found some significant CAD-related risk SNPs confirmed by experiment, such as rs4299376 ($p = 0.004$), rs2505083 ($p = 0.008$) and rs46522 ($p = 0.008$) (*14*), have become non-risk SNPs in GWAS according to the significant level of 0.0001 in previous studies (*15*).

2.1.2. *CAD-related miRNA expression profiling data*

For miRNA expression profiling data, we selected the platform evaluated by Illumina (Illumina Inc, San Diego, CA, USA) Human v2 miRNA expression beadchip (GEO association: GPL8179, *http://www.ncbi.nlm.nih.gov/geo/*). The dataset GSE28858 includes 1,146 miRNA expression values of 12 CAD patients and 12 controls. We downloaded miRNA expression values after log2 transformation.

2.2. *Scan of 3'-UTR SNPs from the WTCCC CAD-related GWAS data*

In this analysis, we used an update SNPnexus (*http://www.snpnexus.org*) tool to perform the scan of 3'-UTR SNPs from the WTCCC CAD-related GWAS data. SNPnexus database provides annotation and genomic location on clones, contigs or chromosomes for both novel and public SNPs by incorporating a broader range of variations such as insertions/deletions block substitutions, and region-based analysis. In addition, we referred to the enhanced functional annotation involved in the update SNPnexus tool (*16*).

2.3. *Identification of differentially expressed miRNAs*

In this analysis, we applied Significance Analysis of Microarrays (SAM) method (*http://otl.stanford.edu*) to extract the statistical significance miRNAs between CAD and control groups. SAM can identify statistically significant miRNAs by carrying out miRNA specific t-tests and computing a statistic for each miRNA, which measures the strength of the relationship between miRNA expression and the phenotype (*17*). In this method, repeated permutations of the data are used to determine if the expression of any miRNA is significant

related to the phenotype. In this analysis, we used the criterion of $p < 0.05$ and False Discovery Rates (FDR) < 0.1 to determine miRNAs variously differentially expressed.

2.4. *Identification of differentially expressed miRNA and 3'-UTR SNP pairs*

In this analysis, consider that the gain of a functional miRNA target site will repress protein expression and affect physiological function and clinical phenotype, and thus we used miRNA and 3'-UTR SNP target gain predicted by the MiRNASNP tool (*http:// www.bioguo.org/miRNASNP*) (*7*) to extract differentially expressed miRNA and 3'-UTR SNP pairs. MiRNASNP tool combined results of two popular tools, TargetScan (*http://www.TargetScan.org/*) and miRanda *(http:// www.microrna.org*), which are regularly updated and considered to have relatively good performance. In this tool, the UTR sequences were divided into wild type and corresponding mutant type, and miRNA and 3'-UTR SNP target gain was defined as follows:

$$\text{Gain} = (\text{ST} \cap \text{SM}) - (\text{WT} \cup \text{WM}), \quad (1)$$

where ST are the target genes of SNP-miRNAs processed by TargetScan and SM are the target genes of SNP-miRNAs processed by miRanda; whereas WT are the target genes of wild-type miRNAs processed by TargetScan and WM are the target genes of wild-type miRNAs processed by miRanda (*7*). That means, if one miRNA-SNP pair was predicted in both ST and SM, but neither in WT nor WM, this pair is called miRNA and 3'-UTR SNP target gain. For each of miRNA-SNP pair, minimum hybridization energy of the miRNA–target interaction is calculated using RNAhybrid (*http:// bibiserv.techfak.uni-bielefeld.de/rnahybrid*) (*7,18*). In this analysis, we used the binding energy changes between wild-type miRNA/target and SNP-miRNA/target to evaluate the interaction strength of each miRNA-SNP pair. More energy change means sharper interaction.

2.5. *Construction of miRNA-miRNA synergistic network*

Here, for those 3'-UTR SNPs regulated by differentially expressed miRNAs, we used logistic regression methods based on PLINK software (*http://pngu.mgh.harvard.edu/~purcell/plink/*) to detect SNP-SNP cooperation effects contributing to coronary artery disease. We used 0.05 as the cutoff of significant interaction effect between two SNPs, and the multiple test corrections were not performed to avoid the loss. On one hand, we consider that Bonferroni correction assumes that the tests are independent, yet many interaction tests are highly correlated. Multiple test corrections might be overly conservative due to high correlations among the interaction tests, and adjusting for multiple testing may result in a decrease in power to detect weaker associations of susceptibility SNPs. On the other hand, when considering interaction effect in the logistic regression analysis, such as gene-gene interaction or gene-environment interaction, p-values can be relaxed (*19*).

For two given miRNA-SNP pairs: $miRNA_1$-SNP_1 and $miRNA_2$-SNP_2, if SNP_1 interacted with SNP_2 ($p_{12} < 0.05$), we defined an interaction score of $miRNA_1$ and $miRNA_2$:

$$S_{12} = E_1 \times E_2 \times (-\log(p_{12})) \quad (2)$$

where E_1 and E_2 are binding energy changes of $miRNA_1$-SNP_1 and $miRNA_2$-SNP_2, respectively. The greater S score means stronger interaction between two miRNAs. After assembling all miRNA pairs identified above, we generated the miRNA-miRNA synergistic network related to CAD disease. A node represents a miRNA, and two nodes are connected if the corresponding miRNA pair has an interaction action. Figure 1 shows the workflow to construct the miRNA-miRNA synergistic network.

2.6. *Extraction of miRNA clusters and Randomization tests*

To validate the constructed miRNA-miRNA network, we extracted miRNA clusters to evaluate their co-expression or combined strength. Note that highly connected nodes (*hubs*) characterized by those nodes with high degrees are often considered as important targets of networks (*20*), and sub-networks implicated by *hubs* have also been shown to be highly conserved in maintaining the housekeeping biological functions of cells (*15*). We therefore examined all of the miRNA clusters implicated by *hub* miRNAs to see their characteristics. Considering *hubs* might be different in terms of the network size, we did not directly define *hubs* as nodes with more than five interactions in the network like Taylor's study (*21*). Instead, we assumed the degree of nodes followed a Poisson distribution in a random network (*22*). To determine whether a miRNA is a *hub* miRNA, the following formula was used to compute its probability of degree $\geq t$ (*23*):

$$P(x \geq t) = 1 - P(x < t) = 1 - \sum^{t-1} \lambda^k \exp(-\lambda)/k! \ (\lambda = np_1, p_1 = m/C_n^2), \quad (3)$$

where n is the number of miRNAs and m is the number of interacting miRNA-pairs in the miRNA-miRNA network. In our analysis, a miRNA was considered as a *hub* when its P value was smaller than the probability of this rare event. This filtering criteria was supported by some previous studies (*15,24*).

Then, we extracted miRNA clusters implicated by *hubs*, which include all miRNAs linked to the *hubs* directly. We computed the average S scores for each of

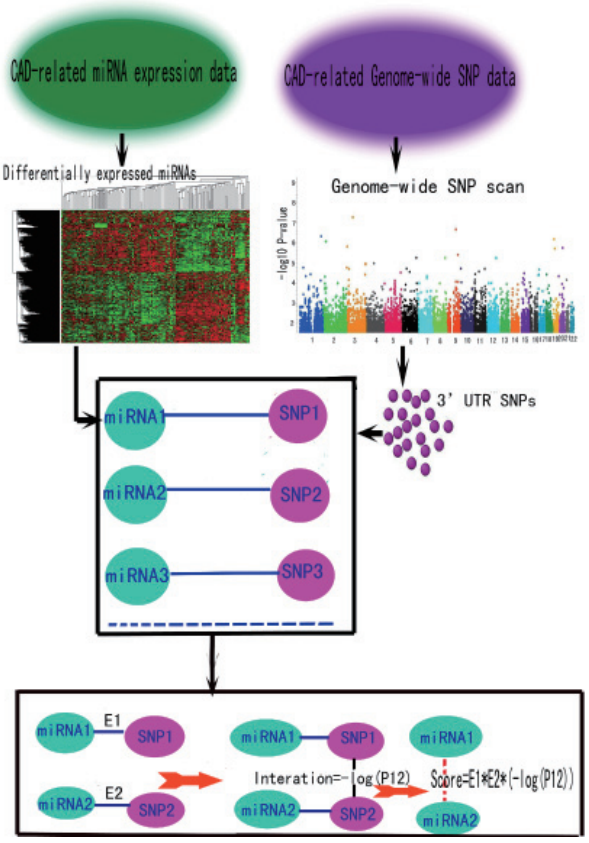

Figure 1. The workflow to construct the miRNA-miRNA network. The process involves three main steps. First, we identified differentially expressed miRNAs using CAD-related miRNA expression profiling data, and performed a scan of 3'-UTR SNPs from the WTCCC CAD-related genome-wide SNP genotype data. Second, we used the MiRNASNP tool to extract differentially expressed miRNA and 3'-UTR SNP pairs and their corresponding binding energy changes. Finally, we performed logistic regression to detect the significant interaction of 3'-UTR target SNPs of differentially expressed miRNAs, and then identified miRNA pairs based on the corresponding SNP-pairs. After assembling all miRNA pairs identified, we constructed the miRNA-miRNA synergistic network related to CAD disease.

the miRNA clusters. To evaluate the significance of co-expression or combined strength of miRNAs involved in these clusters, we performed the randomization tests. For each miRNA cluster, we randomly selected the same number of miRNA pairs from all SNP (miRNA)-SNP (miRNA) pairs, and calculated the corresponding average S score. This procedure was repeated 1,000 times, and the significant *P*-value is the fraction of the average S scores under random conditions, which is greater than the value in the real condition.

3. Results

3.1. *Identification of differentially expressed miRNAs*

According to the criterion of $p < 0.05$ and FDR < 0.1, we applied the SAM method to identify 398 significantly differentially expressed miRNAs. Where, 6 out of the 12 previously identified CAD-related miRNAs in miRNA disease association database-HMDD (Human MicroRNA Disease Database, *http://202.38.126.151/hmdd/tools/hmdd2.html*) (*25*) exhibited statistically significant differential expression between cases and controls, and they were miR-126 ($p = 0.0007$), miR-130a ($p = 0.0278$), miR-21 ($p = 0.0005$), miR-222 ($p = 0.0181$), miR-340 ($p = 6.11E-05$) and miR-624 ($p = 0.0012$). A growing amount of evidence has shown their association with CAD. For example, a recent report suggested that vascular miR-126 is consumed during transcoronary passage, and the differential regulation of circulating miRs during the transcoronary passage might provide important insights to exploit their role as cardiac biomarkers (*26*). We listed those significantly up-regulated (Fold_change > 1.5) or down-regulated (Fold_change < 1/1.5) differentially expressed miRNAs in Table S1 (*http://www.biosciencetrends.com/docindex.php?year=2014&kanno=5*).

3.2. *Identification of differentially expressed miRNA and 3'-UTR SNP pairs*

Using the SNPnexus tool, we performed a scan of 3'-UTR SNPs from the WTCCC CAD-related GWAS data, and 3,521 3'-UTR SNPs were identified. Among these 3'-UTR SNPs, only 43 (1.2%) were significant ($p < 0.01$). Then, we used miRNA and 3'-UTR SNP target gain predicted by the MiRNASNP tool to extract 126 differentially expressed miRNA and 3'-UTR SNP pairs. Among these miRNA and 3'-UTR SNP pairs, the average of binding energy changes caused by SNPs in 3'-UTR was 12.32 kcal/mol, where the miR-770-5p and rs9991 pair was up to 36.3 kcal/mol, suggesting a greater affect of the differentially expressed miRNA-target SNP binding.

3.3. *Construction of miRNA-miRNA synergistic network*

In this analysis, we used logistic regression methods based on PLINK software to detect SNP-SNP cooperative effects contributing to coronary artery disease. As a result, 7,875 SNP-pairs arose from 126 3'-UTR SNPs targeted by differentially expressed miRNAs. According to our criterion of significant interaction, 281 SNP-SNP pairs were selected. While, one pair of SNPs: rs175634 and rs1043515 showed the most significant interaction ($p = 0.000113$). There are a certain number of SNPs showing interaction with multiple other SNPs. For example, SNP rs10802805 interacts with another 10 SNPs, such as rs2112812 ($p = 0.0017$), rs9537 ($p = 0.0083$), rs6052935 ($p = 0.0236$) and so on.

For two given miRNA-SNP pairs: $miRNA_1$-SNP_1 and $miRNA_2$-SNP_2, and the corresponding interaction effect of SNP_1 and SNP_2, we computed the interaction score of $miRNA_1$ and $miRNA_2$ using the S measure as defined in the Methods section. For overlapped

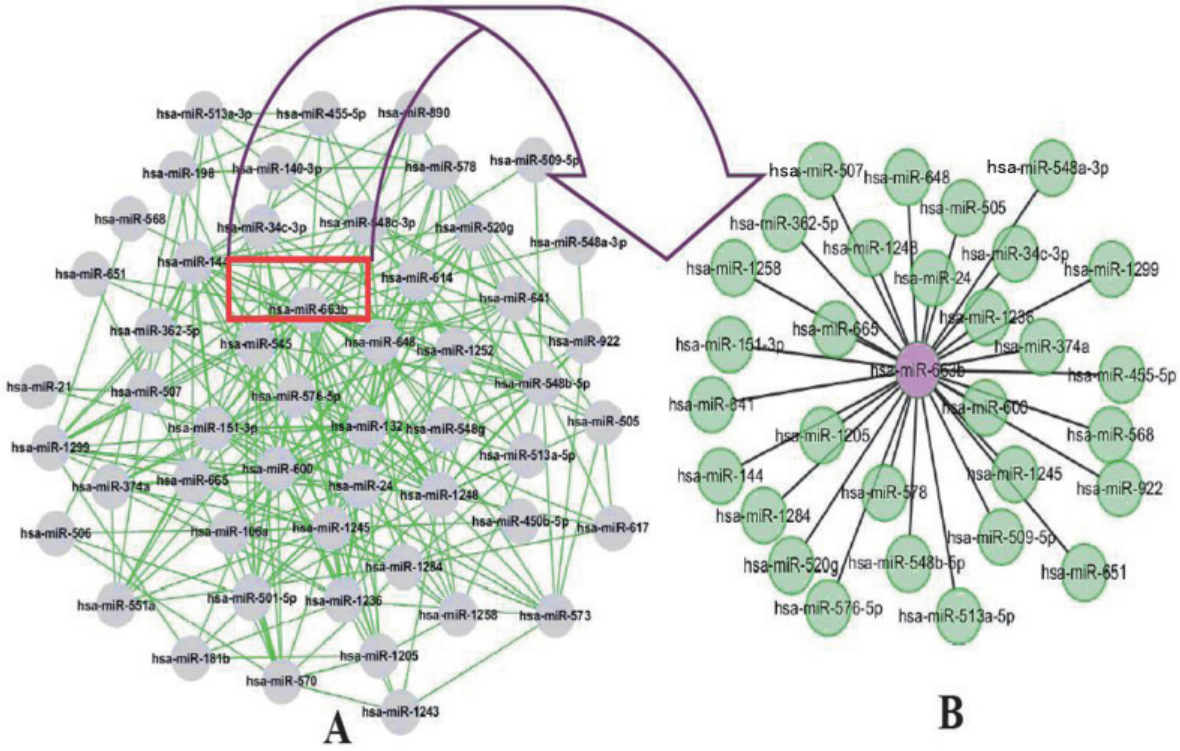

Figure 2. The constructed miRNA-miRNA synergistic network related to CAD. (A) CAD-related miRNA-miRNA network. Each node represents a miRNA, and two nodes are connected if the corresponding miRNA pair has an interaction. **(B)** A special example: miR-663b related miRNA cluster.

miRNA pairs, we took the maximum S scores as their interaction strength. After assembling all miRNA pairs, we can see that interacting miRNAs formed a miRNA-miRNA synergistic network related to CAD disease (See Figure 2A). For the whole network, the maximum interaction strength was seen from miR-665 and miR-132 (S = 1355.46), followed by miR-140-3p and miR-198 (S = 1319.96). The average S score was 188.68. To determine if this network is a small-world network, we constructed 1,000 random small-world networks using Cytoscape software (*http://www.cytoscape.org*) (*27*), and computed the average clustering coefficient and average diameter. We found that the network had a short diameter of 2.983, which is similar to that of a random small world network (2.987 ± 0.091, p = 0.144). In addition, we calculated the average clustering coefficient of the network, and obtained an average clustering coefficient of 0.322 which was much higher than for random networks (0.166 ± 0.014, **p** < 0.001) and approved the dense local neighborhoods of the network. This result suggests that immediate neighbors of a miRNA tend to be synergistic and contribute to disease (*28*).

With the topological characteristic analysis of this constructed miRNA-miRNA network, we can see that there were more poorly connected nodes than *hubs*. More than 60% of the nodes had degrees of ≤ 10. In other words, the degree shows a scale-free distribution, which means that most miRNAs only have a few connected miRNAs, but some miRNAs show an outstanding degree property. For example, miR-663b showed the highest degree (degree = 30, $p < 10^{-5}$), suggesting it can connect to a greater number of miRNAs than others. This is supported by newly published research in which they found miR-663b showed the highest sensitivity and specificity for discrimination of acute myocardial infarction cases from health controls of miRNA expression in peripheral total blood samples (*29*). In addition, miR-144 also showed a greater degree (degree = 18, $p = 0.0187$). A recent study has reported that ectopic expression of miR-144 augmented cardiomyocyte survival, which was further improved by over-expression of miR-144, compared to control cells in response to simulated ischemia (*30*). This result support our constructed networks not only shed light on the relationships between miRNAs, but also give insight into those *hub* miRNAs which are more evolutionarily conserved than non-*hub* miRNAs. It also can be explained that *hub* miRNAs are subject to selection pressure and constraints, due to their involvements in many biological processes and their multiple interacting miRNA partners.

3.4. *The validation of miRNA-miRNA network using miRNA expression value*

It is possible that miRNAs with similar functions tend to have similar expression profiles. To further

validate and evaluate the accuracy of our constructed miRNA-miRNA network and investigate the expression pattern of connecting miRNA-pairs, we analyzed their expression similarity using Pearson's correlation coefficients. As a result, we found that approximately 40% of miRNA pairs have positive or negative co-expression patterns ($p < 0.05$). In addition, we used logistic regression models based on miRNA expression values to analyze the cooperative effects of miRNA-pairs. Interestingly, more than half of miRNA-pairs (52.3%) are proved to be significant ($p < 0.05$). Specially, when investigating those miRNA-pairs including miR-663b; approximately 80% of them are significant (See Table 1 and Figure 2B). This result further supports that miR-663b is an important CAD association miRNA, which is more likely to interact with other miRNAs contributing to disease.

3.5. *Randomization test*

To evaluate the co-expression or combined strength of the miRNA groups involved in the network, we extracted miRNA clusters implicated by *hubs* from the constructed network. In our analysis, a *hub* miRNA with ≥ 17 partners in a random network ($p < 0.05$) was considered a rare event under the null hypothesis that *n* miRNAs were connected randomly. According to this criterion, when 6 *hub* miRNAs were extracted, they were miR-600 (degree = 17, $p = 0.034$), miR-548b-5p (degree = 17, $p = 0.034$), miR-1245 (degree = 19, $p = 0.0099$), miR-144 (degree = 18, $p = 0.0187$), miR-1248 (degree = 20, $p = 0.005$) and miR-663b (degree = 30, $p < 10\text{-}5$). For each miRNA cluster, we calculated the average S score to its 1000 random matched miRNA clusters. For miRNA clusters implicated by *hubs* miR-600, miR-548b-5p, miR-1245, miR-144, miR-1248, and miR-663b, each matched set consisted of 17, 17, 19, 18, 20, and 30 miRNAs randomly selected from 7,875 SNP (miRNA)-SNP(miRNA) pairs. According to the empirical distribution of S scores, we obtained a threshold value to determine the significance of each miRNA cluster. We found that excluding the miRNA cluster implicated by miR-548b-5p (S = 27.04, $p = 0.805$), other miRNA clusters implicated by *hubs* all showed outstanding S scores compared to random miRNA clusters: miR-600 (S = 138.48, $p < 0.001$), miR-1245 (S = 175.24, $p < 0.001$), miR-144 (S = 289.60, $p < 0.001$), miR-1248 (S = 206.52, $p < 0.001$) and miR-663b (S = 75.97, $p = 0.038$). In these identified miRNA clusters, some miRNAs have been proved to be associated with CAD. For example, in the miR-144 cluster, miR-545 has been found to show an up-regulation in premature CAD patients compared to controls in recent studies (*31*). In the miR-663b cluster,

Table 1. miR-663b related miRNA cluster

$miRNA_1$ (SNP_1)	$miRNA_2$ (SNP_2)	Logistic *p*-values based on miRNA expression values	Score = $E_1 \times E_2 \times P_{12}$
miR-663b (rs6052935)	miR-507 (rs4312485)	0.034	0.708
miR-663b (rs6052935)	miR-548a-3p (rs6654)	0.016	99.10
miR-663b (rs6052935)	miR-1205 (rs165345)	0.103	10.21
miR-663b (rs6052935)	miR-1236 (rs10894557)	0.012	27.12
miR-663b (rs175634)	miR-1245 (rs1043515)	0.866	3.63
miR-663b (rs6052935)	miR-1248 (rs12218073)	0.040	188.91
miR-663b (rs175634)	miR-1258 (rs198413)	0.024	2.53
miR-663b (rs6052935)	miR-1284 (rs1052912)	0.301	1.13
miR-663b (rs6052935)	miR-1299 (rs10260499)	0.019	25.25
miR-663b (rs6052935)	miR-144 (rs11543230)	0.514	149.46
miR-663b (rs6052935)	miR-151-3p (rs12174237)	0.035	130.08
miR-663b (rs175634)	miR-24 (rs12214037)	0.047	1.37
miR-663b (rs175634)	miR-34c-3p (rs2810)	0.033	10.04
miR-663b (rs6052935)	miR-362-5p (rs10521099)	0.040	145.19
miR-663b (rs6052935)	miR-374a (rs3811610)	0.302	0.70
miR-663b (rs6052935)	miR-455-5p (rs10933164)	0.028	3.16
miR-663b (rs6052935)	miR-505 (rs10864675)	0.040	154.42
miR-663b (rs6052935)	miR-509-5p (rs1064395)	0.043	6.58
miR-663b (rs6052935)	miR-513a-5p (rs11153074)	0.026	231.30
miR-663b (rs175634)	miR-520g (rs4151045)	0.021	20.04
miR-663b (rs6052935)	miR-548b-5p (rs3737933)	0.039	48.11
miR-663b (rs6052935)	miR-568 (rs8035733)	0.012	15.66
miR-663b (rs6052935)	miR-576-5p (rs435382)	0.026	2.73
miR-663b (rs6052935)	miR-578 (rs10165660)	0.022	141.50
miR-663b (rs6052935)	miR-600 (rs1045291)	0.030	191.84
miR-663b (rs6052935)	miR-641 (rs6880907)	0.376	4.62
miR-663b (rs6052935)	miR-648 (rs8713)	0.033	182.80
miR-663b (rs6052935)	miR-651 (rs10516139)	0.026	10.28
miR-663b (rs6052935)	miR-665 (rs16854011)	0.919	279.78
miR-663b (rs6052935)	miR-922 (rs7677472)	0.047	201.19

Note: P_{12} indicates the significant interaction *p*-value of SNP_1 and SNP_2.

an increased level of miR-24 was found in idiopathic end-stage failing human hearts by northern blot analysis of the hypertrophy-regulated miRNAs (32). Moreover, when we computed the average correlation coefficients using miRNA expression values for these five miRNA clusters, the average correlation coefficients were all approximately 0.5 (See Table 2). This result suggests the identified CAD-related miRNA clusters have greater average S scores and greater relevance than other miRNA clusters expected by chance (See Figure 3).

3.5. *Validation of classification performances of five identified miRNA clusters using miRNA expression values*

To validate whether the identified miRNA clusters have better classification performance, we applied Random Forests (RF) method (*33*) to miRNA expression profiling data in which those miRNAs involved in miRNA clusters are taken as predictor variables to classify samples. RF is an ensemble classifier that consists of many decision trees and each tree depends on the values of a random vector sampled independently. In this analysis, we used 5-fold cross validation to assess the classification accuracy rate. All samples were divided into five sets and in each analysis one set is considered as testing data, whereas the others are training data. For Random Forests program, 5,000 trees were constructed. As a result, accurate classification performances were obtained for all miRNA clusters, and the sensitivity and specificity were

Table 2. The characteristics of CAD related miRNA clusters

miRNA clusters implicated by *hubs*	Degree of *hub*	S (Scutoff)	**p*-value	Average correlation coefficient
miR-600	17	138.48 (105.50)	< 0.001	0.512
miR-1245	19	175.24 (84.40)	< 0.001	0.546
miR-144	18	289.60 (106.80)	< 0.001	0.479
miR-1248	20	206.52 (81.80)	< 0.001	0.464
miR-663b	30	75.97 (73.50)	0.038	0.489

Note: * Significant *p*-value is the fraction of the average S scores in random conditions, which is greater than the value in the real condition.

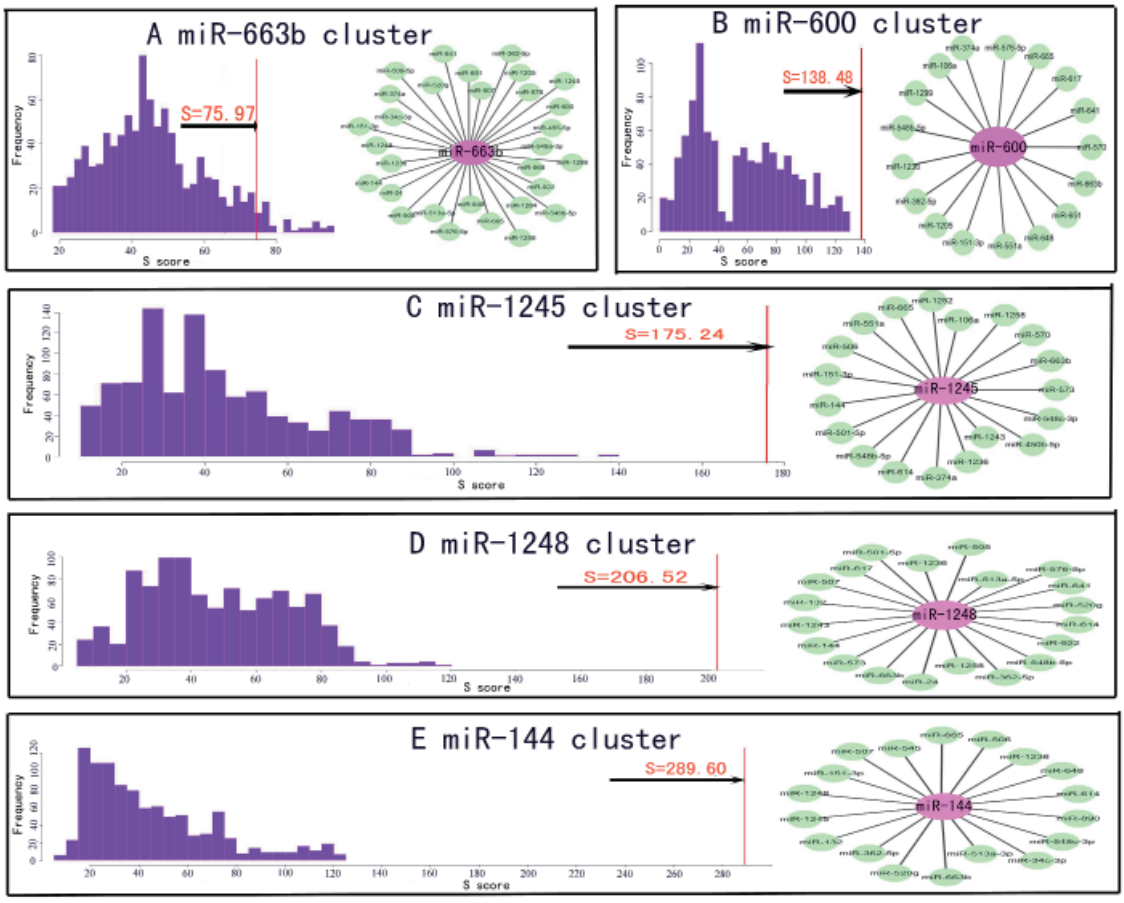

Figure 3. The distribution of average S scores for five miRNA clusters implicated by *hubs*. The random background distribution of average S scores for miRNA clusters implicated by miR-663b **(A)**, miR-600 **(B)**, miR-1245 **(C)**, miR-1248 **(D)** and miR-144 **(E)** are shown in purple colors. The red lines indicate the real average S scores of the corresponding miRNA clusters.

Table 3. Sensitivity, specificity, positive predictive value, negative predictive value, and area under ROC curve (AUC) for miRNA clusters used to detect CAD with Random Forest classifier

miRNA clusters implicated by *hubs*	The Prediction Property (95% Confidence Interval)					miRNA with the maximal MDG	MDG
	Sensitivity (%)	Specificity (%)	Positive predictive value (%)	Negative predictive value (%)	Area under ROC curve (AUC) (%)		
miR-600	92.3(64.0-99.8)	100.0(71.5-100.0)	100.0(73.5-100.0)	91.7(61.5-99.8)	95.8(86.4-105.3)	miR-1236	2.858
miR-1245	92.3(64.0-99.8)	90.9(58.7-99.8)	92.3(64.0-99.8)	90.9(58.7-99.8)	91.6(78.5-104.8)	miR-1236	2.314
miR-144	100.0(73.5-100.0)	91.7(61.5-99.8)	92.3(64.0-99.8)	100.0(71.5-100.0)	96.2(87.4-104.9)	miR-1236	2.864
miR-1248	100.0(71.5-100.0)	92.3(64.0-99.8)	91.7(61.5-99.8)	100.0(73.5-100.0)	95.8(86.4-105.3)	miR-1236	2.237
miR-663b	100.0(73.5-100.0)	91.7(61.5-99.8)	92.3(64.0-99.8)	100.0(71.5-100.0)	96.2(87.4-104.9)	miR-1236	2.062

all more than 90%. The sensitivity, specificity, positive predictive value, negative predictive value, and area under the ROC curve (AUC) for five miRNA clusters used to detect CAD with Random Forest classifier are shown in Table 3.

Note that it is often interesting to know which miRNAs are important in classification in Random Forests program. There are two measures of importance in RF program, the mean decrease in accuracy and the mean decrease Gini index (MDG) (*33*). In this analysis, we used MDG to measure the risk of miRNAs in each miRNA cluster. Greater MDG will indicate that the degree of impurity arising from a category could be reduced furthest by this miRNA, and thus suggests an important miRNA. Interestingly, miR-1236 ranked first for all miRNA clusters (See Table 3). Recent evidence showed that miR-1236 may function as a negative regulator of vascular endothelial growth factor receptor (VEGFR)-3 (*34*).

3.7. *Comparison with MISIM tool*

We also attempted to validate our results to see whether miRNAs involved in miRNA clusters have potential functional similarity. Currently, the functional similarities of miRNAs are often predicted by indirectly inferring similarities of their corresponding target genes. These prediction methods include Gene Ontology (GO) or pathway enrichment analysis for miRNA-targeted gene sets (*35*). However, these methods are not applicable for miRNA genes because the function of most miRNAs remains unknown and no such function annotation database is available. Therefore, in this analysis, we used a recent developed tool, MISIM (*http://210.73.221.6/*), which is used to measure miRNA functional similarity based on human miRNA-disease association data and structures of the corresponding disease relationships (*13*). We used 0.7 as the MISIM threshold to determine whether two miRNAs have a link. In other words, those miRNA pairs with a MISIM coefficient greater than or equal to 0.7 were selected. The results of MISIM showed that miR-106a, miR-144, miR-520g, miR-24, miR-132, miR-505, miR-507 and miR-600 had a similar function (See Figure 4). Indeed, recently published data have shown some of these miRNAs are

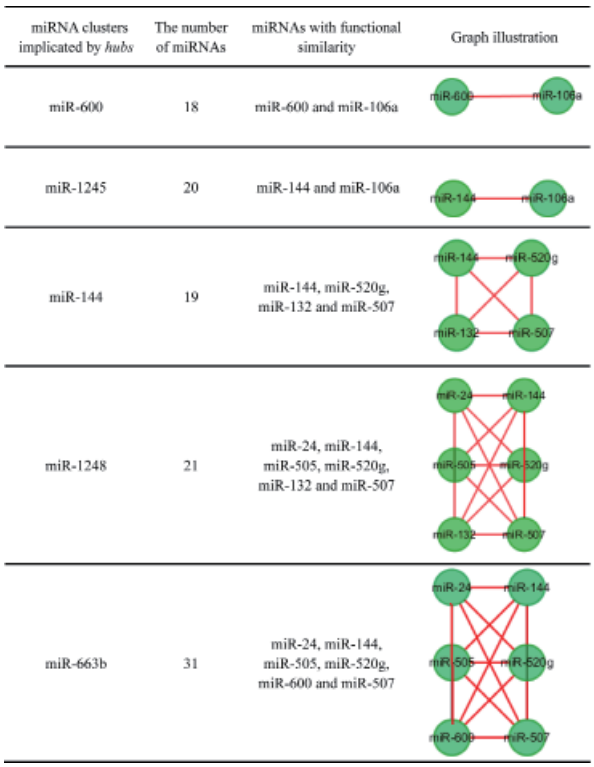

Figure 4. The evaluation of miRNA clusters based on functional similarity using MISIM tool. In graphical illustration, each green circle indicates a miRNA and each red line connects two miRNAs with similar function.

associated with CAD-related diseases, such as miR-132, miR-144, miR-106a and miR-24. For example, Katare *et al*. investigated the therapeutic activity and mechanistic targets of saphenous vein-derived pericyte progenitor cells (SVPs) in a mouse myocardial infarction model, and found SVP transplantation produced long-term improvement of cardiac function through a novel paracrine mechanism involving secretion of miR-132 and inhibition of its target genes (*36*). In addition, some miRNAs such as miR-24, were found to be up-regulated in human heart failure patients and transfection of neonatal cardiomyocytes with these miRNAs resulted in significant cardiomyocyte hypertrophy (*37*). These results suggest miRNA clusters identified by our method might have a potential functional aggregated trend related to CAD disease.

4. Discussion

Some recent studies have implicated that SNPs located at miRNA binding sites are likely to affect the expression of the miRNA target and might contribute to the susceptibility of humans to common diseases (*7,38*). In this paper, using the expression profiles of miRNAs and genome-wide SNP genotype data, we constructed a miRNA-miRNA synergistic network related to CAD by performing a genome-wide scan for SNPs in human miRNA 3'-UTR target sites and computed potential SNP cooperative effects contributing to disease based on the potential miRNA-SNPs interactions. Our method has effectively identified 5 miRNA clusters related to CAD, and a certain proportion of miRNAs identified have been reported to have association with coronary artery disease. For example, a recent study showed that loss of the miR-144 cluster limits ischemic preconditioning cardioprotection by up-regulating Rac-1-mediated oxidative stress signaling (*39*). Furthermore, some novel associations between miRNAs and CAD discovered recently have been predicted by our method, such as miR-663b.

It is worthy to note that the origin of our constructed miRNA-miRNA network is based on the genome-wide SNP-SNP interaction. In practice, when testing millions of SNP-pairs for interaction, novel statistic methods are required for getting high power, and a large sample size is required for estimating logistic regression parameters to avoid sparseness problems for modeling interaction effects. Fortunately, in our study, only 126 3'-UTR SNPs of approximately 5, 000 samples came into the interaction analysis, and therefore the "fast-epistasis" involved in PLINK could also perform well. Certainly, we have to point out that the absence of multiple testing corrections and the replication of interaction analysis might cause some false positive results. Therefore, further validation using other individual studies will be performed in the future.

Note that only 43 3'-UTR SNPs (1.2%) were significant ($p < 0.01$), which indicates that most SNPs involved in significant interactions have no marginal association. This result is consistent with those reported by Wu *et al*. (*40*), in which they found that 75% of interacting SNPs with *p*-values (for testing marginal association) larger than 0.2 and 44% of interacting SNPs with *p*-values (for testing marginal association) larger than 0.5. This strongly suggested that most significant SNP interactions have arisen from those SNPs with weak marginal association. However, an interesting observation was noted that the greatest binding energy changes was presented in miR-770-5p an rs9991 pair (36.3 kcal/mol), while miR-770-5p ($p = 0.0267$) and rs9991 ($p = 0.0043$) were all significantly associated with CAD. Although few matched data in this study can't prove the relevance between the binding energy changes and the significance of miRNAs or SNPs, this phenomenon suggests that those significant miRNAs or their corresponding targets should also be focused on when considering their interaction effects contributing to complex disease. Moreover, among 126 3'-UTR SNPs used in this analysis, 89 SNPs (70.6%) have relatively high MAF (MAF $\geq$ 0.10). Excluding 3 SNPs located in chromosome 18, 20, and 21 respectively, the average MAFs for the other 19 chromosomes were all greater than 0.14. Specially, SNP rs9991 which is significantly associated with CAD also has a relatively high MAF (MAF = 0.3115). This result agreed with a recent study in which Gong *et al*. demonstrated that those SNPs with a high population MAF, or high population frequency difference or undergoing positive selection pressure might be important candidates for population phenotype research and complex trait studies (*7*). Therefore, those SNP-associated miRNA target sites may be worthwhile to focus on in further experiments.

Furthermore, it should be pointed out when we investigated the relevance between S scores and the expression similarity for each connecting miRNA-pair involved in the constructed miRNA-miRNA network, we found there was no correlation between them ($p = 0.382$). This phenomenon also exists for identified miRNA clusters, such as miR-663b ($p = 0.920$) and miR-600 ($p = 0.963$). On one hand, this might be caused by the greater range of S scores (0.04-1355.46) due to the increased binding energy changes of miRNA-SNP pairs, or on the other hand, integration data might cause some potential errors due to different data types which contain different kinds of information. Moreover, we can see that some functionally similar miRNA pairs neither have high expression similarity nor belong to the same family or cluster.

Currently, although advanced laboratory instruments and computing systems developed to decipher the structure and function of genes, proteins, miRNAs and other substances in the human body, the limitations and the complexity of biomedical problems causes natural obstacles in understanding the etiology of complex diseases. Therefore, bioinformatics and computational data face a great challenge in discovering new biomarkers which can be used to detect, prevent and cure complex diseases by performing genomic data analysis. Fortunately, various high-throughput approaches such as genome sequencing technology, microarray technology and proteomic characterization of proteins and complexes have allowed us to gather vast amounts of data to construct cellular networks. Our future work will be enhanced by integrating more data types, such as miRNA expression profiling data, gene expression profiling data, protein-protein interaction data, disease data, genotype data and so on. Specially, we know that some novel findings obtained by bioinformatics analysis may not be the facts and need to be validated using experiment technologies. Therefore,

experiment validation is important and will further help confirm the identified biomarkers. In the past, we have used qRT-PCR, Western blots and luciferase assays to validate some breast cancer subtype-related miRNAs identified by silico analysis, and the report of this work is in press. In the future, we will use experimental technologies to further confirm these potential findings. We expect our study can provide more clues for other researchers to perform experiments and predictions for CAD-related biomarkers.

In conclusion, we have presented a framework to construct a miRNA-miRNA network using miRNA expression profiling data and genome-wide SNP genotype data. The network topological analysis confirmed some novel CAD-related miRNAs identified recently by experiment. Our method might help to undertand miRNA function and CAD disease, as well as explore the novel mechanisms connecting miRNAs and function.

Acknowledgements

This work is supported by Beijing Natural Science Foundation (Grant Nos. 7142015), National Science Foundation of China (Grant Nos. 31100905) and the Science Technology Development Project of Beijing Municipal Commission of Education (SQKM201210025008). This study is also funded by the excellent talent cultivation project of Beijing and the young backbone teacher's cultivation project of Beijing Municipal Commission of Education, and supported by the foundation-clinical cooperation project of Capital Medical University (11JL30, 11JL33 and 12JL75).

References

1. Stone N, Pangilinan F, Molloy AM, Shane B, Scott JM, Ueland PM, Mills JL, Kirke PN, Sethupathy P, Brody LC. Bioinformatic and genetic association analysis of microRNA target sites in one-carbon metabolism genes. PLoS ONE. 2011; 6:e21851.
2. Martins M, Rosa A, Guedes LC, *et al*. Convergence of miRNA expression profiling, a-synuclein interacton and GWAS in Parkinson's disease. PLoS ONE. 2011; 6:e25443.
3. Ikeda S, Kong SW, Lu J, Bisping E, Zhang H, Allen PD, Golub TR, Pieske B, Pu WT. Altered microRNA expression in human heart disease. Physiol Genomics. 2007; 31:367-373.
4. Hutchison ER, Okun E, Mattson MP. The Therapeutic Potential of microRNAs in nervous system damage, degeneration and repair. Neuromolecular Med. 2009; 11:153-161.
5. Hindorff LA, Sethupathy P, Junkins HA, Ramos EM, Mehta JP, Collins FS, Manolio TA. Potential etiologic and functional implications of genome-wide association loci for human diseases and traits. Proc Natl Acad Sci U S A. 2009; 106:9362-9367.
6. Spencer CC, Su Z, Donnelly P, Marchini J. Designing genome-wide association studies: Sample size, power, imputation, and the choice of genotyping chip. PLoS Genet. 2009; 5:e1000477.
7. Gong J, Tong Y, Zhang HM, Wang K, Hu T, Shan G, Sun J, Guo AY. Genome-wide identification of SNPs in microRNA genes and the SNP effects on microRNA target binding and biogenesis. Hum Mutat. 2012; 33:254-263.
8. Ryan BM, Robles AI, Harris CC. Genetic variation in microRNA networks: The implications for cancer research. Nat Rev Cancer. 2010; 10:389-402.
9. Chen K, Rajewsky N. Natural selection on human microRNA binding sites inferred from SNP data. Nat Genet. 2006; 38:1452-1456.
10. Bhartiya D, Laddha SV, Mukhopadhyay A, Scaria V. miRvar: A comprehensive database for genomic variations in microRNAs. Hum Mutat. 2011; 32:E2226-E2245.
11. Shalgi R, Lieber D, Oren M, Pilpel Y. Global and Local Architecture of the mammalian microRNA–transcription factor regulatory network. PLoS Comput Bio. 2007; 3:e131.
12. Boross G, Orosz K, Farkas IJ. Human microRNAs co-silence in well-separated groups and have different predicted essentialities. Bioinformatcis. 2009; 25:1063-1069.
13. Wang D, Wang J, Lu M, Song F, Cui Q. Inferring the human microRNA functional similarity and functional network based on microRNA-associated diseases. Bioinformatcis. 2010; 26:1644-1650.
14. Roberts R, Stewart AF. Genetics of coronary artery disease in the 21st century. Clin Cardiol. 2012; 35:536-540.
15. Huang W, Wang P, Liu Z, Zhang L. Identifying disease associations via genome-wide association studies. BMC Bioinformatcis. 2009; 10 (Suppl 1):S68.
16. Dayem Ullah AZ, Lemoine NR, Chelala C. SNPnexus: A web server for functional annotation of novel and publicly known genetic variants (2012 update). Nucleic Acids Res. 2012; 40:W65-W70.
17. Taylor J, Tibshirani R, Efron B. The 'miss rate' for the analysis of gene expression data. Biostatistics. 2005; 6:111-117.
18. Krüger J, Rehmsmeier M. RNAhybrid: MicroRNA target prediction easy, fast and flexible. Nucleic Acids Res. 2006; 34:W451-W454.
19. Hand BD, Kostek MC, Ferrell RE, Delmonico MJ, Douglass LW, Roth SM, Hagberg JM, Hurley BF. Influence of promoter region variants of insulin-like growth factor pathway genes on the strength-training response of muscle phenotypes in older adults. J Appl Physiol. 2007; 103:1678-1687.
20. Barabási AL, Oltvai ZN. Network biology: Understanding the cell's functional organization. Nat Rev Genet. 2004; 5:101-113.
21. Taylor IW, Linding R, Warde-Farley D, Liu Y, Pesquita C, Faria D, Bull S, Pawson T, Morris Q, Wrana JL. Dynamic modularity in protein interaction networks predicts breast cancer outcome. Nat Biotechnol. 2009; 27:199-204.
22. Blondel VD, Guillaume J-L, Hendrickx JM, Jungers RM. Distance distribution in random graphs and application to network exploration. Phys Rev E Stat Nonlin Soft Matter Phys. 2007; 76:101-108.
23. Jiang W, Li X, Rao S, Wang L, Du L, Li C, Wu C, Wang H, Wang Y, Yang B. Constructing disease-specific gene networks using pair-wise relevance metric: Application to colon cancer identifies interleukin 8, desmin and enolase

1 as the central elements. BMC Syst Biol. 2008; 2:1752-1766.
24. Shibolet O, Giallourakis C, Rosenberg I, Mueller T, Xavier RJ, Podolsky DK. AKAP13, a RhoA GTPase-specific guanine exchange factor, is a novel regulator of TLR2 signaling. J Biol Chem. 2007; 282:35308-35317.
25. Lu M, Zhang Q, Deng M, Miao J, Guo Y, Gao W, Cui Q. An Analysis of human microRNA and disease associations. PLoS One. 2008; 3:e3420.
26. De Rosa S, Fichtlscherer S, Lehmann R, Assmus B, Dimmeler S, Zeiher AM. Transcoronary concentration gradients of circulating microRNAs. Circulation. 2011; 124:1936-1944.
27. Shannon P, Markiel A, Ozier O, Baliga NS, Wang JT, Ramage D, Amin N, Schwikowski B, Ideker T. Cytoscape: A software environment for integrated models of biomolecular Interaction Networks. Genome Res. 2003; 13:2498-2504.
28. Xu J, Li CX, Li YS, Lv JY, Ma Y, Shao TT, Xu LD, Wang YY, Du L, Zhang YP, Jiang W, Li CQ, Xiao Y, Li X. MiRNA–miRNA synergistic network: Construction via co-regulating functional modules and disease miRNA topological features. Nucleic Acids Res. 2011; 39:825-836.
29. Meder B, Keller A, Vogel B, Haas J, Sedaghat-Hamedani F, Kayvanpour E, Just S, Borries A, Rudloff J, Leidinger P, Meese E, Katus HA, Rottbauer W. MicroRNA signatures in total peripheral blood as novel biomarkers for acute myocardial infarction. Basic Res Cardiol. 2011; 106:13-23.
30. Zhanga X, Wanga X, Zhua H, Zhu C, Wang Y, Pu WT, Jegga AG, Fan GC. Synergistic effects of the GATA-4-mediated miR-144/451 cluster in protection against simulated ischemia/reperfusion-induced cardiomyocyte death. J Mol Cell Cardiol. 2010; 49:841-850.
31. Bronze-da-Rocha E. MicroRNAs expression profiles in cardiovascular diseases. Biomed Res Int. 2014; 2014:985408.
32. van Rooij E, Sutherland LB, Liu N, Williams AH, McAnally J, Gerard RD, Richardson JA, Olson EN. A signature pattern of stress-responsive microRNAs that can evoke cardiac hypertrophy and heart failure. Proc Natl Acad Sci U S A. 2006; 103:18255-18260.
33. Pang H, Lin A, Holford M, Enerson BE, Lu B, Lawton MP, Floyd E, Zhao H. Pathway analysis using random forests classification and regression. Bioinformatcis. 2006; 22:2028-2036.
34. Jones D, Li Y, He Y, Xu Z, Chen H, Min W. Mirtron microRNA-1236 inhibits VEGFR-3 signaling during inflammatory lymphangiogenesis. Arterioscler Thromb Vasc Biol. 2012; 32:633-642.
35. Du Z, Li L, Chen CF, Yu PS, Wang JZ. G-SESAME: Web tools for GO-term-based gene similarity analysis and knowledge discovery. Nucleic Acids Res. 2009; 37:W345-W349.
36. Katare R, Riu F, Mitchell K, Gubernator M, Campagnolo P, Cui Y, Fortunato O, Avolio E, Cesselli D, Beltrami AP, Angelini G, Emanueli C, Madeddu P. Transplantation of human pericyte progenitor cells improves the repair of infarcted heart through activation of an angiogenic program involving micro-RNA-132. Circ Res. 2011; 109:894-906.
37. Catalucci D, Gallo P, Condorelli G. MicroRNAs in cardiovascular biology and heart disease. Circ Cardiovasc Genet. 2009; 2:402-408.
38. Yu Z, Li Z, Jolicoeur N, Zhang L, Fortin Y, Wang E, Wu M, Shen SH. Aberrant allele frequencies of the SNPs located in microRNA target sites are potentially associated with human cancers. Nucleic Acids Res. 2007; 35:4535-4541.
39. Wang X, Zhu H, Zhang X, Liu Y, Chen J, Medvedovic M, Li H, Weiss MJ, Ren X, Fan GC. Loss of the miR-144/451 cluster impairs ischaemic preconditioning-mediated cardioprotection by targeting Rac-1. Cardiovasc Res. 2012; 94:379-390.
40. Wu X, Dong H, Luo L, Zhu Y, Peng G, Reveille JD, Xiong M. A Novel statistic for genome-wide interaction analysis. PLoS Genet. 2010; 6:e1001131.

(Received February 26, 2014; Revised October 25, 2014; Accepted December 8, 2014)

Original Article

DOI: 10.5582/bst.2014.01084

Differentiation ability of multipotent hematopoietic stem/progenitor cells detected by a porcine specific anti-CD117 monoclonal antibody

Shino Ohshima[1], Syuuya Mori[1], Atsuko Shigenari[1], Asuka Miyamoto[1], Masaki Takasu[2], Noriaki Imaeda[2], Satoshi Nunomura[3], Yoshimichi Okayama[3], Masafumi Tanaka[1], Hitoshi Kitagawa[3], Jerzy K. Kulski[1,4], Hidetoshi Inoko[1], Asako Ando[1], Yoshie Kametani[1,*]

[1] *Department of Molecular Life Science, Division of Basic Medical Science and Molecular Medicine, Kanagawa, Japan;*
[2] *Department of Veterinary Medicine, Faculty of Applied Biological Sciences, Gifu University, Gifu, Japan;*
[3] *Division of Molecular Cell Immunology, Nihon University Graduate School of Medical Science, Tokyo, Japan;*
[4] *Centre for Forensic Science, The University of Western Australia, Perth, Western Australia, Australia.*

Summary **CD117 is a cytokine receptor expressed on the surface of hematopoietic stem cells with a likely role in cell survival, proliferation and differentiation. In order to study the differentiation activity of porcine CD117 hematopoietic cells *in vitro* and *in vivo* we prepared an anti-swine CD117 Mab (2A1) with high specificity for flow-cytometrical analysis. The 2A1 Mab did not recognize mouse or human mast cells suggesting that 2A1 is species-specific. Swine bone marrow (BM) CD117$^+$ cells differentiated *in vitro* mainly into erythroid and monocyte lineages in the methylcellulose-based colony assay. When the swine BM CD117$^+$ cells were transplanted *in vivo* into immunodeficient NOG (NOD/SCID/IL-2gc-null) mice, a significant amount of swine CD45$^+$ leukocytes, including CD3 positive T cells, were developed in the mice. These results revealed that the swine BM CD117$^+$ cells possess hematopoietic stem/progenitor activity and when monitored in immunodeficient mice or *in vitro* they can develop into lymphoid, erythroid, and myeloid cells efficiently with the new monoclonal antibody.**

Keywords: Swine, CD117, hematopoietic cell, monoclonal antibody, xeno-transplantation

1. Introduction

In transplantation studies, stem cells from various tissues such as from the heart or bone marrow have become an important alternative source to using donor organs or whole tissue for engraftment (*1-5*). The development of new reagents and methods are needed for the identification of stem cell markers and for monitoring their purification, transplantation and differentiation in foreign environments such as with the xeno-transplantation of stem cells between different animal species, because most of the tools today are cross-reactive monoclonal antibodies prepared against human antigens and not species specific (*6*). The swine has been an useful animal model for human medical science research and transplantation studies (*7*). For example, organ transplantation was extensively studied with major histocompatibility complex (MHC)-defined swine lines, alpha 1, 3-galactosyltransferase gene-knockout and/or human decay-accelerating factor transgenic swine (*8*). However, in recent years, experimental organ transplantation in swine is also gradually being replaced by stem cell transplantation involving hematopoietic and other tissue stem cells (*9-11*). Concomitant with the development of the swine stem cell transplantation research there is a continued need to produce stem cell marker-specific monoclonal antibodies (Mabs) (*6*).

Recently, a hematopoietic stem cell (HSC)-transplanted severe-immunodeficient mouse system (known as humanized mice) was extensively investigated for its efficacy of engraftment of foreign hematopoietic cells (*12*). Although this and other

**Address correspondence to:*
Dr. Yoshie Kametani, Department of Immunology, Tokai University School of Medicine, 143, Shimokasuya, Isehara, Kanagawa 259-1193, Japan.
E-mail: y-kametn@is.icc.u-tokai.ac.jp

mouse systems have limitations, they have been used efficiently to clarify the development pathway of hematopoietic cells, the efficacy of vaccination or drugs (*13*), and an improved humanized hematopoietic mouse system, human leukocyte antigen (HLA)-expressing mice, was recently reported (*14,15*). However, other animal stem cell models such as those using non-human primates or the swine also may be useful for evaluating xeno-reconstituted systems.

CD117 is a cytokine receptor tyrosine kinase type III expressed on the surface of wide variety of tissue stem cells including HSC, mesenchymal stem cells and multipotent progenitors (*16*). This molecule is also known as mast/stem cell growth factor receptor, proto-oncogene c-Kit or tyrosine-protein kinase kit and when activated by binding to a stem cell factor may play a role in regulating cell survival, proliferation and differentiation. As a cell surface marker, CD117 can be detected by using specific antibodies to identify and monitor the hematopoietic/mesenchymal stem/progenitor cell types and their stage of differentiation and activity in mice, humans and non-human primates. We have studied the xeno-transplantation of hematopoietic stem/progenitor cells of human, common marmoset and mouse and found that the cellularity of the reconstituted immune system in the transplantation environment was different among these animals, suggesting a significant diversity of hematopoietic cell characteristics (*17-19*). Thus, the stem cells of swine may have unique and different developmental potential compared to the mouse and non-human primates. Alternatively, they may have similar characteristics to the human and potentially could be used in experimental transplantation models for studying the pathogenesis and treatments of some human diseases. In this regard, Le Guern *et al.* (*20*) reported on the effect of long-term engraftment of swine stem cell factor (SCF)-positive cells in immunodeficient mice. However, because there were no species-specific Mabs readily available against swine CD117, researchers have tended to use the stem cell factor as a detectable stem cell differentiation marker and not CD117 (*21*).

In this study, we prepared a porcine-specific CD117 Mab and constructed a xeno-transplantation system for the engraftment of swine $CD117^+$ hematopoietic progenitor cells into immunodeficient NOG (NOD/SCID/IL-2gc-null) mice. In addition, we studied the differentiation of the swine $CD117^+$ hematopoietic progenitor cells after transplantation into the mice recipients by flow-cytometrical analysis.

2. Materials and Methods

2.1. *Animals and cells*

Newborn triple hybrid swine ((Landrace x Large While) x Duroc) were purchased from a commercial hog firm in Gifu prefecture, Japan and used for collection of bone-marrow (BM) cells. NOD/Shi-scid, IL-2gc-null (NOD/SCID/gc-null; NOG) mice were provided by Central Institute for Experimental Animals (CIEA, Kawasaki, Japan) and kept under specific pathogen-free conditions. Experiments using mice were approved by the Institutional Committee for Animal Care and Use and performed at Tokai University following the University guidelines.

Newborn swine or adult Duroc pigs were sacrificed under anesthesia (0.02 mg/kg Medetomidine Domitor; Nihon Zenyaku Kogyo Co. Koriyama, Japan, 0.2 mg/kg Midazolam; Dormicum injection 10mg, Astellas, Tokyo, Japan, 0.04 mg/kg Butophanol; Vetophale, Meiji Seika Pharma Co. Tokyo, Japan, intramuscular administration). After the birth of the piglets, the umbilical cord blood (CB) cells were collected from the umbilical cords of the expelled uterus using a 5ml syringe with 21Gx1 1/2 needle. The cells were centrifuged on Lymphocepal (IBL Co. Takasaki, Japan) at 2,000 rpm for 30 min. Mononuclear cells (MNCs) were collected and the remaining red blood cells (RBCs) were lysed with low osmotic buffer (20 mM Tris-HCl, pH7.4, 0.15 M NH4Cl). Femurs of the BMs were taken from the newborn swine and the cells were released from the tissues. RBCs were lysed and the cell suspension, prepared as mentioned above, was suspended in RPMI1640 medium (Nissui, Tokyo, Japan) containing 10% (v/v) heat-inactivated fetal calf serum (FCS; SAFC Biosciences, Tokyo, Japan) and used for the cytometric analyses.

2.2. *Preparation of CD117 transfectant*

The cDNA sequence of the swine CD117 gene used in this study was based on Sus scrofa KIT mRNA sequence (AB250963). RNA was extracted from cells by Isogen (Nippon Gene Co. LTD., Tokyo, Japan) and reverse-transcribed to cDNA by using the Superscript system (Invitrogen, Carlsbad, CA). A 2966 bp portion of the cDNA sequence that corresponds to an extracellular domain of the protein was amplified by PCR using cDNA as a template and AccuPrime Pfx DNA Polymerase (Invitrogen, Tokyo, Japan). The set of forward and reverse primers for PCR amplification of the CD117 gene used were as follows:

F, 5'-TAGAATTCGGTCTCACCGGTCGCCACCATG AGAGGCGCTCGCCGCGCCTGGGATT-3',
R, 5'-ATGATATCGGTCTCGGATCCTCAGACGTCT TCGTGGACAAGCA-3'.

Modified S/MAR-based episomal vectors (*22*) expressing swine CD117 cDNA were transfected into HEK293 or a mouse lymphoma cell line, A20, by electroporation using Gene Pulser (Neon® invitrogen,

Oregon, USA) according to the manufacturer's instructions.

2.3. *Monoclonal antibody preparation*

We initially immunized BALB/c mice with mitomycin C (MMC, Kyowahakko-Kirin, Tokyo Japan)-treated swine cord blood (CB) MNCs (1×10^6 cells/animal). For booster treatments, MMC-treated A20 transfectant was used biweekly for 3-6 times with 4×10^5 cells/animal with each immunization. MMC (final, 0.04 mg/mL) was added to the culture and incubated at 37°C for 30 min in 5% CO_2. The serum antibody titers of immunized mice were checked by flow cytometry analyses using CD117 cDNA-transfected HEK293 cells as a source of antigen. After 4 days of the final boost, mice were sacrificed and splenocytes were fused with the mouse myeloma cell line, P3-X63-Ag8-U1, according to a standard procedure. Positive clones were identified by using flow cytometry or an Imaging Analyzer (Array Scan, Thermo scientific, MA, USA). Briefly, CD117 transfected HEK293 cells were plated into the wells of 96 well plates. Culture supernatants were added to each well, incubated for 15 min and washed twice. APC-labeled (APC: allophycocyanin) anti-mouse IgG polyclonal antibody (Poly4053; Bio Legend, San Diego, US) was added and incubated for 15 min. Plates were washed and stained with Hoechst (Invitrogen, Oregon, USA) for 30 min at room temperature and analyzed using the Imaging Analyzer. Positive cells were picked according to the fluorescent intensity of APC and the co-expressed mVenus fluorescent protein. The positive clones were then isolated, expanded and stocked.

2.4. *Preparation of primary murine and human mast cells*

Murine mast cells were prepared from the femurs of four- to six-week-old C57BL/6J mice. BM cells were cultured in RPMI1640 (Sigma-Adrich, St.Louis, US) supplemented with 10% (v/v) heat-inactivated FCS (SAFC Biosciences, Tokyo, Japan), and 4 ng/ml recombinant interleukin (IL)-3 (PeproTech, Rocky Hill, US). BM mast cells were used for experiments after they were cultured for six to eight weeks. We obtained approval of the ethical review boards to prepare primary human mast cells from CB-derived $CD34^+$ MNCs (RIKEN BioResource Center, Tsukuba, Japan). The $CD34^+$ cells were cultured in serum-free Iscove methylcellulose medium (Stem Cell Technologies Inc., Vancouver, BC, Canada) and Iscove modified Dulbecco medium containing SCF at 200 ng/mL, IL-6 at 50 ng/mL and IL-3 at 1 ng/mL as previously described (*23*). On day 42 of culture, methylcellulose was dissolved in phosphate-buffered saline (PBS) and the cells were resuspended and cultured in Iscove modified Dulbecco medium containing SCF at 100 ng/mL and IL-6 at 50 ng/mL with 2% FCS.

2.5. *Flow cytometry*

Cells were incubated with appropriately diluted, fluorescence-labeled primary Mab for 15 min at 4°C and washed with 1% (w/v) bovine serum albumin-containing PBS. In some cases, cells were re-incubated with labeled secondary antibody. The Mabs used were as follows: anti-mouse TER119-FITC (eBioscience, San Diego, CA), anti-swine CD45-FITC (clone # K252-1E4, AbD Serotec, Kidlington, UK), anti-swine CD3 (clone # 8E6, Monoclonal Antibody Center, WA, USA), anti-mouse CD117 (clone # 2B8, eBioscience) and anti-human CD117 (clone # YB5.B8, BD Bioscience), goat anti-mouse IgG1-RPE (Southern Biotech, Uden, Netherland) respectively. Cells were washed and further incubated with FITC-conjugated mouse anti-human IgE Mab (clone # BE5, eBioscience) on ice for 20 min. Stained cells were analyzed on FACS Calibur (Becton Dickinson, New Jersey, USA).

2.6. *Colony assay*

Newborn swine BM cells were washed and an aliquot was stained with 2A1 Mab as described above. After the staining with the Mab, cells were rewashed and sorted by employing a magnetic cell sorting system (AutoMACS, Miltenyi Biotec, Bergisch Gladbach, Germany) to separate $CD117^+$ cells from $CD117^-$ cells. The isolated cells were replated at 5×10^4/dish in 1 mL of methylcellulose-containing medium (StemCell technologies, Vancouver, Canada) in a 35 mm dish with mouse or human SCF (10 ng/mL), IL-3 (10 ng/mL), erythropoietin (2 U/mL) and granulocyte colony-stimulating factor (G-CSF) (10 ng/mL) and cultured at 37°C in a 5% CO_2 atmosphere. After 14 days of culture, the different types and numbers of hematopoietic colonies (colony-forming units (CFU)) were counted according to standard criteria. Samples from each animal were processed and assayed in triplicate with two different animals used for each of two separate experiments.

2.7. *Transplantation of swine hematopoietic cells into NOG mice*

$CD117^+$ cells were purified from newborn swine BMs by cell sorter as described above in section 2.6. Purity was more than 98% based on quantitation by flow cytometry. Nine-week-old NOG mice were irradiated with 2.5Gy X-ray prior to transplantation and swine cells were injected into mice intravenously (Suppl. Table 1, *http://www.biosciencetrends.com/docindex.php?year=2014&kanno=6*). Peripheral blood was collected *via* orbit under inhalation anesthesia at two and

four weeks after transplantation. MNCs were prepared and analyzed by flow cytomety.

2.8. *Transplantation of swine hematopoietic cells into NOG mice*

Student's *t*-test was performed, and data were expressed as mean ± S.D.

3. Results

3.1. *CD117 monoclonal antibody preparation*

The protocol used for CD117 monoclonal antibody preparation is shown in Suppl. Figure 1 (*http://www.biosciencetrends.com/docindex.php?year=2014&kanno=6*). First, swine CD117 cDNA was inserted into N576, an expression vector containing a monomer Venus yellow-green fluorescent protein (mVenus)-reporter gene, and the modified vector was transfected into the mouse lymphoma cell line A20 by electropolation. The expression of the mVenus gene was observed in more than 50% of the transfected cells 18-24 hr after transfection (Suppl. Figure 1A). Second, BALB/c mice were injected intraperitoneally initially with mitomycin C (MMC)-treated swine cord blood (CB) mononuclear cells (MNCs) and then with MMC treated N576-A20 cells as the booster immunizations (Suppl. Figure 1B). Third, the titer of the antiserum was checked against the CD117 expressed by the N576-HEK293 cells. The crossreactivity between N576-HEK293 and the antisera was confirmed by flow cytometry (Suppl. Figure 1C).

We selected a specific 2A1 subclone (Figure 1 and Suppl. Figure 2, *http://www.biosciencetrends.com/docindex.php?year=2014&kanno=6*) for further use because this clone secreted a Mab that reacted with the transfectants expressing CD117 and the mVenus fluorescent protein with similar or identical staining patterns (Figures 1B and 1C). All of the 2A1 subclones showed similar staining patterns, suggesting that they were stable expression products.

As CD117 is expressed on mast cells, we examined if the 2A1 Mab could also interact with the human and mouse CD117 molecules using cell lines derived from human or mouse primary mast cells. As shown in Figure 1D, neither human nor mouse mast cells were stained with 2A1. These results suggest that the 2A1 Mab is specific to swine CD117.

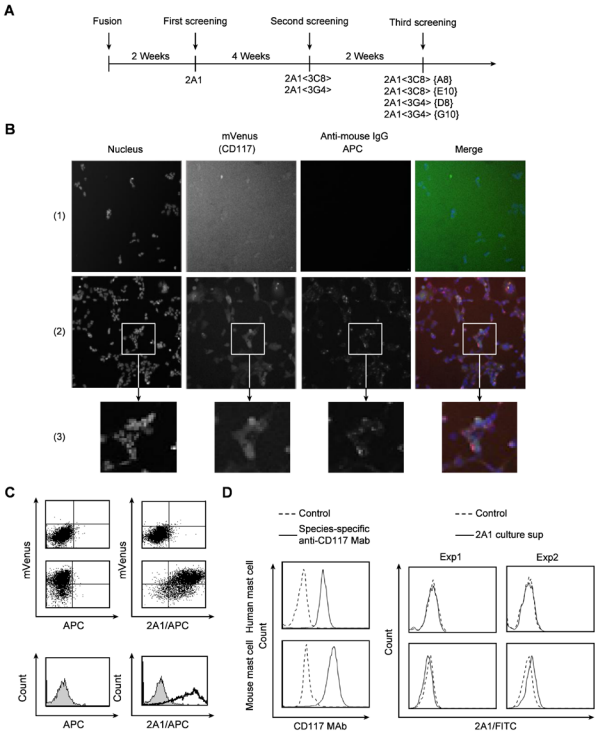

Figure 1. CD117-specific monoclonal antibody 2A1 specifically stains swine CD117. (A) Protocol for the cloning of swine CD117-specific Mab. Three screenings were performed after hybridoma fusion by limiting dilution of 2A1 hybridomas. **(B)** Imaging Analyzer image of the HEK293 parent cells **(1)** and CD117-HEK293 cells **(2)**. CD117 expression was monitored by mVenus expression. Screening of the hybridoma supernatants was performed by staining with the secondary antibody, anti-mouse IgG-APC. The encircled CD117-HEK293 cells in **(2)** are shown at a higher magnification (5×) in **(3)**. **(C)** The positive hybridoma supernatant submitted for the reactivity to the transfectant cells and analyzed by flow cytometry. The percentage of the cell numbers in the respective gates is shown in the quadrant panels. Control means the anti-mouse IgG-APC reactivity without the supernatants. **(D)** The reactivity of 2A1 Mab and species-specific anti-CD117 Mabs with human and mouse mast cells. As shown in the left panels, the human and mouse mast cells reacted with their respective species-specific anti-CD117 Mabs (anti-human CD117 or anti-mouse CD117 antibodies, respectively). Right panels; mast cells were stained with 2A1 and the dotted and solid curves are overlays of the control and 2A1 culture supernatants, respectively. Representative data of five independent assays are shown.

3.2. *CD117 expression in swine bone marrow (BM) cells*

To better clarify the existence of the swine CD117$^+$ cells in the lymphoid tissue, we examined their presence in the adult and newborn BMs, as hematopoietic stem/progenitor cells are abundant in the BM. Figure 2 shows that the newborn BM cells included a high level of 2A1-positive cells (ca.10%) compared to the ten fold lower levels (1.9%) in the adult BM cells. In addition, the ratio of CD117$^+$ cells is very low (0.5%) in the CB and no CD117$^+$ cells were detected in the spleen, lymph nodes and peripheral blood monocytes. These results suggest that CD117$^+$ cells and hematopoietic stem/progenitor cells exist in the swine bone marrow and other lymphoid tissues at a ratio that is comparable with human and mouse.

3.3. *Colony assay for the multipotency of CD117$^+$ cells*

To analyze the multipotency of CD117$^+$ BM cells *in vitro*, the swine BM MNCs were collected and stained

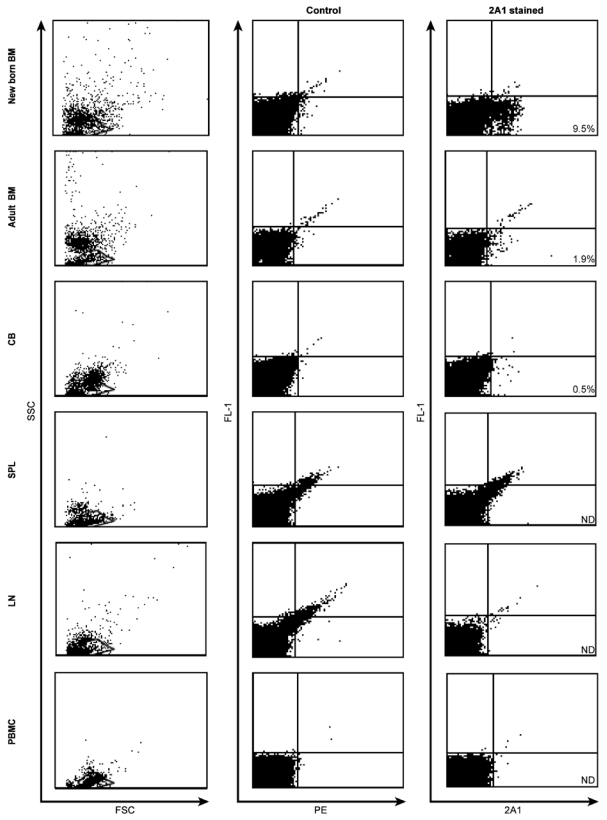

Figure 2. Abundance of swine CD117$^+$ cells in newborn BM relative to five other lymphoid tissue cells (adult BM, CB, SPL, LN and PBMC). Lymphoid tissue cells were stained with 2A1 Mabs. Control means the secondary antibody-stained cells. The percentage of 2A1 stained CD117$^+$ cells within the lymphoid-gate are shown in each panel. ND; not detected. Representative data of five independent assays are shown.

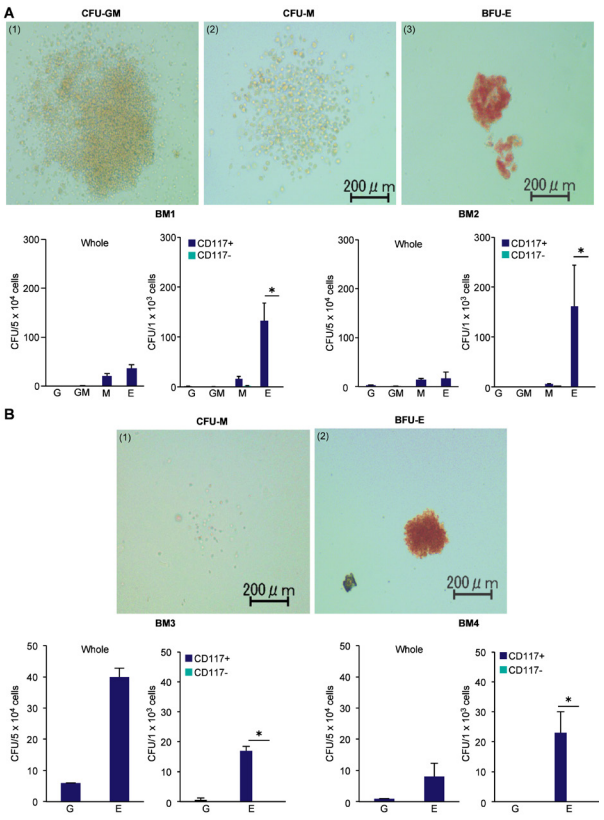

Figure 3. Swine CD117+ cells extensively develop into erythroid-lineage cells *in vitro*. BM cells were sorted as shown in Supplementary Figure 3 and the sorted cells were used in the colony assay. **(A)** Colony assay using the human cytokines SCF, IL-3, erythropoietin and G-CSF. **(1)** CFU-GM, **(2)** CFU-M, **(3)** BFU-E. (G; granulocyte, GM; granulocyte and monocyte, M; monocyte, E; erythrocyte). The data were obtained from two separate swine BM experiments, BM1 and BM2, for the human cytokine environment. Three independent cultures were performed for both of the two BMs and the colonies were counted and compared. The mark * represents the significant difference by *t*-test ($p < 0.05$). Two independent assays and representative photographs are shown here. **(B)** Colony assay using the mouse cytokines SCF, IL-3, erythropoietin and G-CSF. **(1)** CFU-G, **(2)** BFU-E. All pictures were taken by KEYENCE BIOREVO BZ-90000, Object lens: ×10 Plan Fluor NA 0.30 Ph1. The data were obtained from two separate swine BM experiments, BM3 and BM4, for the human cytokine environment. Three independent cultures were performed for both of the two BMs and the colonies were counted and compared. The mark * represents the significant difference by *t*-test ($p < 0.05$). Two independent assays and representative photographs are shown here.

with 2A1. The CD117$^+$ cells were purified as shown in Suppl. Figure 3 (*http://www.biosciencetrends.com/docindex.php?year=2014&kanno=6*). CD117$^+$ cells and CD117- cell fractions were partially purified by magnetic beads sorting at first and then to over 98% purity levels by additional sorting using a FACSaria (Suppl. Figure 3A). Both of the CD117 positive and negative cell fractions were then used in a colony assay by culturing the cells in the presence of the human cytokines, SCF, IL-3, erythropoietin and G-CSF. As a result of the cellular purifications and colony assays four types of cellular clones were identified in the BM cell cultures. These were granulocytes (G), granulocytes/monocytes (GM), monocytes (M) and erythrocytes (E). Notably, CD117$^+$ cells in the colony assay generated erythroid burst-forming units (BFU-E) with significantly higher efficiency than either the BM cells or CD117$^-$ cells. The generation of colony forming units (CFU) were also observed for G, M and GM, but at significantly lower levels for the CD117$^+$ cell fraction (Figure 3A). Similar results were obtained when the cells were cultured in the colony assay using the mouse instead of the human cytokines (Suppl. Figure 3B). In two of these experiments, the frequency of BFU-E in the CD117$^+$ cell fraction was significantly higher than in the CFU-M assay or in the CD117$^-$ cell fraction. The CFU of the other cell types, G and GM, were low or undetectable (Figure 3B and Suppl. Figure 3B). Compared to human cytokine conditions, the colony forming ability of BM cells was less effective with the mouse cytokines.

Overall, these results suggest that the swine CD117$^+$ BM cells have the potential to develop into erythroid-monocyte lineage *in vitro*.

3.3. *Development of swine hematopoietic cells in immunodeficient NOD/SCID/IL-2gc-null (NOG) mouse*

While mouse cytokines can support the development of swine erythroid cells and monocytes, other cell lineages

could not be detected by the *in vitro* colony assay. Therefore, we transplanted the swine hematopoietic cells into severely immunodeficient NOG mice to examine if lymphoid lineage cells could be developed from the CD117$^+$ cells *in vivo*. Swine CD117$^+$ cells were purified and transplanted into irradiated NOG mice and analysed by cytometry using different gate settings to detect erythroid cells, lymphoid cells and monocytes (Figure 4A). After 2 and 12 weeks post transplantation, lymphoid organs were collected and the presence of swine blood cells were examined by flow cytometry using the lymphoid gate setting. As a result,

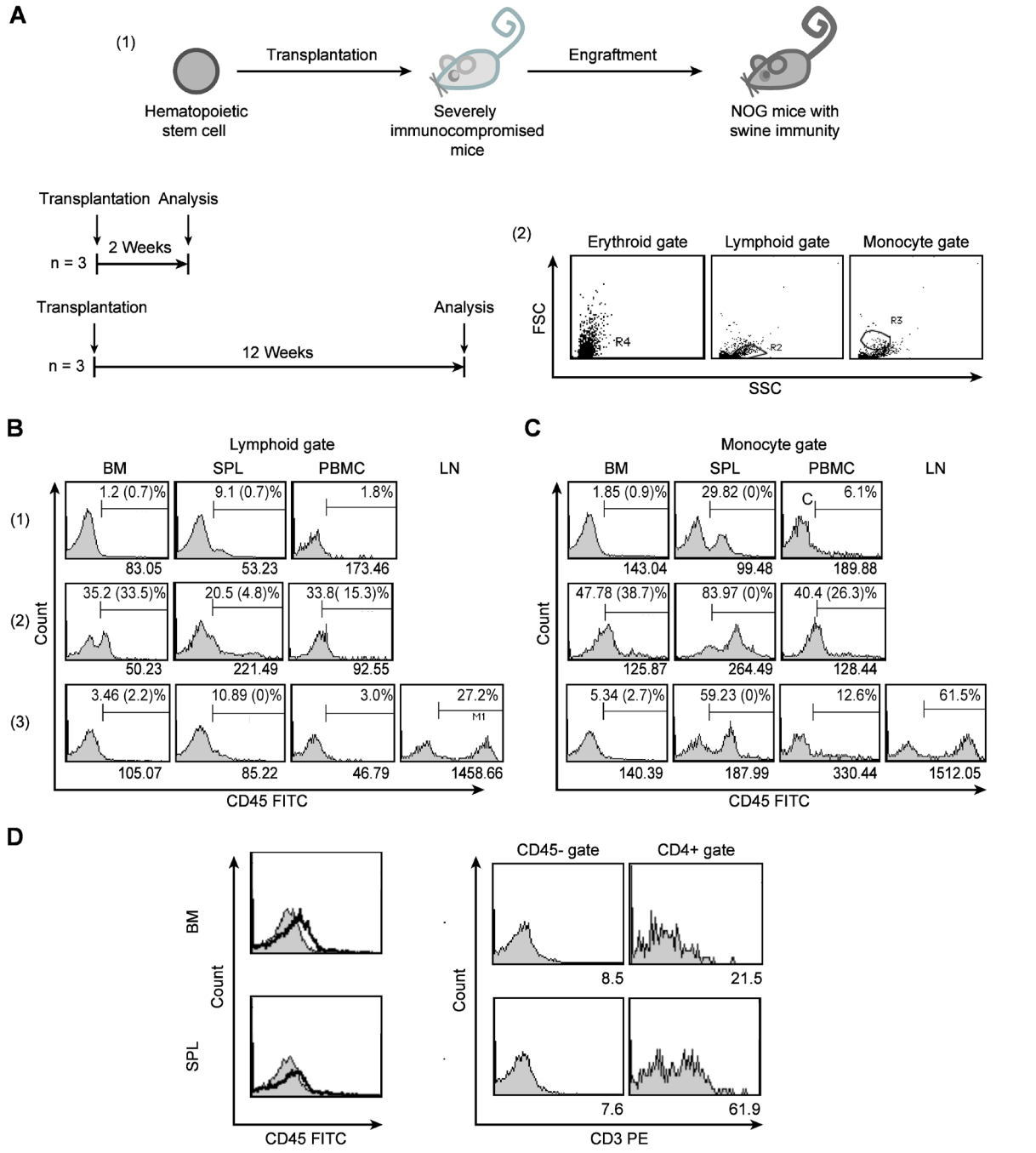

Figure 4. Repopulation of CD117$^+$ swine BM cells in immunodeficient NOG mice. (A) (1) Protocol for CD117$^+$ cell transplantation into NOG mice. In short term (2 w) and long term (12 w) analysis after the transplantation, lymphoid cells were analyzed for the swine cell engraftment either two weeks or twelve weeks after transplantation. **(2)** Flow cytometrical gates used for the analyses of erythroid (R4), lymphoid (R2) and monocyte (R3) cells were set by FSC and SSC. **B** and **C**. Flow cytometrical analysis of engrafted swine cells. Swine leukocytes were detected by swine CD45 expression using an anti-swine CD45-FITC antibody. Lymphoid-gated cells are shown in **B** and monocyte-gated cells in **C**. **(B) (1)** Non-transplanted control mice. **(2)** Two weeks after the transplantation. **(3)** Twelve weeks after the transplantation. Some of the SPL cells are stained with CD45-FITC. These are some non-specific binding of the antibodies to the cells as we analyzed by 2D-flow cytometry analysis (data not shown). The numbers show the shifted cell percentages compared to control mice without transplantation. In the brackets, shifted percentages of no-stain controls are shown. **(D)** Lymphoid-gated cells were analyzed for the expression of CD3. Swine CD45-FITC and CD3-PE double staining of the BM and SPL cells are shown in the panels. The mean fluorescent intensity (MFI) is shown below the panels. Representative data of three independent assays are shown.

swine CD45$^+$ cells were observed in BM, spleen (SPL) and the peripheral blood of NOG mice transplanted with CD117$^+$ cells 2 weeks after the transplantation (Figure 4B). Higher amounts of the CD45$^+$ cells were observed through the monocyte gate of the SPL cells 2 weeks after transplantation (Figure 4C). CD45$^+$ cells were also observed in the lymph node 12 weeks after transplantation. These results indicate that the engrafted swine white blood cells had developed successfully in the NOG mice. We used a TER119 antibody, which recognizes mouse erythrocyte to distinguish between the mouse and swine erythrocytes, and found that the NOG mice included TER119$^-$ cells in the erythrocyte gate, and that the swine CD117$^+$ cells might be differentiated into erythrocytes, which were TER119 (mouse erythroid marker) negative, *in vivo* (Suppl. Figure 4, *http://www.biosciencetrends.com/docindex.php?year=2014&kanno=6*).

The CD45$^+$ cells of the mice SPL were examined for the CD3 expression in lymphoid gate 12 weeks after the transplantation. As shown in Figure 4D, significant amount of CD3$^+$ cells were observed in the SPL.

These results show that the transplanted swine CD117$^+$ cells had developed into erythroid, myeloid and lymphoid cells in NOG mice and suggest that the swine CD117$^+$ cells are hematopoietic stem/progenitor cells that can be transplanted successfully to a different species under the right conditions of engraftment.

4. Discussion

CD117 is a cytokine receptor tyrosine kinase type III expressed on the surface of hematopoietic stem cells and when activated by the cytokine SCF can regulate the maintenance, proliferation, migration and differentiation of HSCs in the BM. In the swine, the stem cell activity of CD117$^+$ cells have been previously evaluated by using SCF to activate their stem cell potential to differentiate into various cellular lineages (*20,21*). Although a swine CD117 Mab has been developed and characterized (*24*), the species specificity of the Mab and xeno-transplantation of CD117$^+$ cells have not been reported. They checked *in vitro* development of erythroid and myeloid cells from Mab-enriched cells, but they could not detect lymphoid cell development. Swine SCF-reacting cells previously reported could not develop lymphoid cells, either (*25*). Because the species specificity of both tools was unclear, xeno-transplantation experiments using a species specific CD117 Mab might not be undertaken until we prepared our own highly species-specific anti-CD117 Mab clone. This Mab clone, 2A1, enabled us to evaluate the multipotency of swine CD117$^+$ cells *in vitro* and *in vivo*. The Mab reacted against the swine CD117 receptor expressed by a recombinant DNA vector N576 in HEK293 or A2 cells, was specific for the detection of CD117 in swine and did not cross react with the CD117 cells of mice or humans. This specificity allowed us to develop the *in vivo* xeno-transplantation system using NOG mice because the porcine specific CD117 antibody did not cross-react with other cells examined. In this *in vivo* system, we demonstrated that CD117$^+$ cells could develop into T cells, which indicate that the CD117$^+$ cells involve hematopoietic stem cells.

Consequently, on the basis of the specificity of Mab 2A1, we found that CD117$^+$ cells were abundant in the newborn swine BM, but not in CB or adult BM. Moreover, the CD117$^+$ cells from the newborn BM were found to develop into erythroid cells or monocytes using the *in vitro* colony assay and into lymphoid cells by the xeno-transplantation *in vivo* system. Thus, both the *in vitro* and the *in vivo* experiments confirmed that the CD117$^+$ cells from the newborn swine BM are hematopoietic stem/progenitor cells.

The similarity between our *in vitro* data for CD117$^+$ cells from the newborn BM and the data reported by Dor *et al*. (*25*) in the spleen or BM of young pigs less than 1 year old suggests a high efficiency of CD117$^+$ cell purification with SCF-binding affinity in their system. In our *in vitro* study, we also confirmed that the CD117$^+$ cells differentiated into the erythrocytes in the presence of mouse or human cytokines SCF, IL-3, erythropoietin and G-CSF. While the swine CD117$^+$ cells developed into erythroid colonies in our *in vitro* studies and those of others (24), we could not definitely conclude the potential of the CD117$^+$ cells to develop into erythroid cells in the mouse transplantation system because of the absence of a good erythrocyte monitoring system. We could only suggest that the TER119-negative erythroid gated cells were observed early after the CD117$^+$ cell transplantation. On the other hand, we found white blood cells including CD3$^+$ cells in the peripheral lymph organs of the transplanted NOG mice, suggesting that the CD117$^+$ cells had differentiated into the monocyte and lymphoid lineages. Human HSC that were transplanted into NOG mice developed into myeloid and lymphoid lineages, but not into erythroid lineage cells *in vivo* (*13,26*). The cytokine, erythropoietin, is a known requirement for the differentiation of CD117 stem cells into erythroid precursor cells and erythrocytes (*27*). The contrary results obtained in the *in vitro* and the *in vivo* systems respectively may be due to the presence of sufficient amount of erythropoietin in the *in vitro* system and its reduced amount in the *in vivo* system. Alternatively, other synergistic factors are missing or inhibitory factors are in play preventing the CD117 stem cells from developing into erythrocytes in the xeno-transplantation environment.

In conclusion, we produced a highly specific anti-swine CD117 Mab and used it to confirm that the swine CD117$^+$ stem cells have a multipotency that can differentiate into erythroid cells, monocytes and lymphoid cells depending on the *in vitro* or *in vivo* system chosen for analysis. The swine-NOG mouse transplantation system in conjunction with

specific detection reagents like the Mabs 2A1 shows an important experimental potential for the study of hematopoietic cells *in vivo*, especially for understanding the factors required in erythroid cell development from hematopoietic stem/progenitor cells.

Acknowledgements

This work was supported by JSPS KAKENHI Grant number 22380172 and MEXT-Supported Program for the Strategic Research Foundation at Privated Universities (2012-2016). We thank the members of Teaching and Research Support Center in Tokai University School of Medicine for their technical skills. We also thank Yumiko Nakagawa for her excellent animal care skills.

References

1. Smith KP, Luong MX, Stein GS. Pluripotency: Toward a gold standard for human ES and iPS cells. J Cell Physiol. 2009; 220:21-29.
2. Gokhale PJ, Andrews PW. The development of pluripotent stem cells. Curr Opin Genet Dev. 2012; 22:403-408.
3. Oberritter Z, Rolle U, Juhasz Z, Cserni T, Puri P. Altered expression of c-kit-positive cells in the ureterovesical junction after surgically created vesicoureteral reflux. Pediatr Surg Int. 2009; 25:1103-1107.
4. Leri A, Kajstura J, Anversa P. Role of cardiac stem cells in cardiac pathophysiology: A paradigm shift in human myocardial biology. Circ Res. 2011; 109:941-961.
5. Kawachi K, Iso Y, Sato T, Wakabayashi K, Kobayashi Y, Takeyama Y, Suzuki H. Effects of erythropoietin on angiogenesis after myocardial infarction in porcine. Heart Vessels. 2012; 27:79-88.
6. Rozemuller H, Prins H, Naaijkens B, Staal J, Bühring H, Martens A. Prospective isolation of mesenchymal stem cells from multiple mammalian species using cross-reacting anti-human monoclonal antibodies. Stem Cells Dev. 2010; 19:1911-1921.
7. Lunney JK. Advances in swine biomedical model genomics. Int J Biol Sci. 2007; 3:179-184.
8. d'Apice AJ, Cowan PJ. Xenotransplantation: The next generation of engineered animals. Transpl Immunol. 2009; 21:111-115.
9. Tseng YL, Sachs DH, Cooper DK. Porcine hematopoietic progenitor cell transplantation in nonhuman primates: A review of progress. Transplantation. 2005; 79:1-9.
10. He JQ, Vu DM, Hunt G, Chugh A, Bhatnagar A, Bolli R. Human cardiac stem cells isolated from atrial appendages stably express c-kit. PLoS One. 2011; 6:e27719.
11. Ezashi T, Telugu BP, Roberts RM. Induced pluripotent stem cells from pigs and other ungulate species: An alternative to embryonic stem cells? Reprod Domest Anim. 2012; 47 (Suppl 4):92-97.
12. Shultz LD, Brehm MA, Garcia-Martinez JV, Greiner DL. Humanized mice for immune system investigation: Progress, promise and challenges. Nat Rev Immunol. 2012; 12:786-798.
13. Ito M, Kobayashi K, Nakahata T. NOD/Shi-scid IL2rγ^{null} (NOG) mice more appropriate for humanized mouse models. Curr Top Microbiol Immunol. 2008; 324:53-76.
14. Suzuki M, Takahashi T, Katano I, Ito R, Ito M, Harigae H, Ishii N, Sugamura K. Induction of human humoral immune responses in a novel HLA-DR-expressing transgenic NOD/Shi-scid/γc^{null} mouse. Int Immunol. 2012; 24:243-252.
15. Sato Y, Nagata S, Takiguchi M. Effective elicitation of human effector CD8$^+$ T Cells in HLA-B*51:01 transgenic humanized mice after infection with HIV-1. PLoS One. 2012; 7:e42776.
16. Lennartsson J, Ronnstrand L. Stem cell factor receptor/c-Kit: From basic science to clinical implications. Physiol Rev. 2012; 92:1619-1649.
17. Saito Y, Kametani Y, Hozumi K, Mochida N, Ando K, Ito M, Nomura T, Tokuda Y, Makuuchi H, Tajima T, Habu S. The *in vivo* development of human T cells from CD34$^+$ cells in the murine thymic environment. Int Immunol. 2002; 14:1113-1124.
18. Kametani Y, Shiina M, Katano I, *et al*. Development of human-human hybridoma from anti-Her-2 peptide-producing B cells in immunized NOG mouse. Exp Hematol. 2006; 34:1240-1248.
19. Nunomura S, Shimada S, Kametani Y, *et al*. Double expression of CD34 and CD117 on bone marrow progenitors is a hallmark of the development of functional mast cell of Callithrix jacchus (common marmoset). Int Immunol. 2012; 24:593-603.
20. Le Guern AC, Giovino MA, Abe M, Theodore PR, Qi J, Down JD, Sachs DH, Sykes M, Yang YG. Stem cell activity of porcine c-kit$^+$ hematopoietic cells. Exp Hematol. 2003; 31:833-840.
21. Summerfield A, Horn M, Lozano G, Carrasco C, Atze K, McCullough K. C-kit positive porcine bone marrow progenitor cells identified and enriched using recombinant stem cell factor. J Immunol Methods. 2003; 280:113-123.
22. Mizutani A, Kikkawa E, Matsuno A, Shigenari A, Okinaga H, Murakami M, Ishida H, Tanaka M, Inoko H. Modified S/MAR episomal vectors for stably expressing fluorescent protein-tagged transgenes with small cell-to-cell fluctuations. Anal Biochem. 2013; 443:113-116.
23. Fukunaga M, Nunomura S, Nishida S, Endo K, Gon Y, Hashimoto S, Hashimoto Y, Okayama Y, Makishima M, Ra C. Mast cell death induced by 24(S),25-epoxycholesterol. Exp Cell Res. 2010; 316:3272-3281.
24. Perez C, Moreno S, Summerfield A, Domenech N, Alvarez B, Correa C, Alonso F, Ezquerra A, Dominguez J, Revilla C. Characterisation of porcine bone marrow progenitor cells identified by the anti-c-kit (CD117) monoclonal antibody 2B8/BM. J Immunol Methods. 2007; 321:70-79.
25. Dor FJ, Ramirez ML, Parmar K, Altman EL, Huang CA, Down JD, Cooper DK. Primitive hematopoietic cell populations reside in the spleen: Studies in the pig, baboon, and human. Exp Hematol. 2006; 34:1573-1582.
26. Ito M, Hiramatsu H, Kobayashi K, Suzue K, Kawahata M, Hioki K, Ueyama Y, Koyanagi Y, Sugamura K, Tsuji K, Heike T, Nakahata T. NOD/SCID/γ_c^{null} mouse: An excellent recipient mouse model for engagement of human cells. Blood. 2002; 100:3175-3182.
27. Agosti V, Karur V, Sathyanarayana P, Besmer P, Wojchowski DM. A KIT juxtamembrane PY567 -directed pathway provides nonredundant signals for erythroid progenitor cell development and stress erythropoiesis. Exp Hematol. 2009; 37:159-171.

(Received July 30, 2014; Revised November 11, 2014; Accepted December 13, 2014)

Original Article

DOI: 10.5582/bst.2014.01118

Detection methods for milk pathogenic bacteria by loop-mediated isothermal amplification

Wentao Yang, Xiaoning Song, Jingxin Wang, Zhen Li, Mingjiang Ji, Yufeng Li*

School of Bioengineering, Xihua University, Chengdu, Sichuan, China.

Summary **Milk is a common food, which is consumed all over the world. It is an important source of calcium. Meanwhile, it provides abundant protein, minerals and vitamins. However, pathogenic bacteria which exist in milk not only causes nutrition loss, but also produces toxins which may cause diarrhea, food poisoning, and even death. In order to control the microbial level of raw milk and eliminate the contamination of materials, this assay applied loop-mediated isothermal amplification to explore a new way to detect enterotoxigenic *Escherichia coli* (ETEC) in raw milk. The best reaction condition in detecting ETEC from raw milk was confirmed to be: 0.016 μM each of forward outer primer (primer F3) and backward outer primer (primer B3), 0.128 μM each of forward inner primer (primer FIP) and backward inner primer (primer BIP), 0.45 μM deoxy-ribonucleoside triphosphate (dNTPs), 2IU Bst DNA polymerase large fragment and template DNA were incubated at 63°C for 60 min. LAMP was proved to be specific, rapid and sensitive in detecting pathogenic bacteria which exist in milk.**

Keywords: Enterotoxigenic *Escherichia coli* (ETEC), loop-mediated isothermal amplification (LAMP), optimization of reaction condition, rapid detection, raw milk

1. Introduction

Food safety is a worldwide problem (*1*). Enterotoxigenic *Escherichia coli* (ETEC) is responsible for many large-scale foodborne disease outbreaks all over the world (*2,3*). Annually, ETEC is estimated to cause 200 million diarrheal episodes and approximately 380,000 deaths (*4,5*). The pathogenesis of ETEC-induced diarrhea is similar to that of cholera and includes the production of enterotoxins and colonization factors. The clinical symptoms of ETEC infection can range from mild diarrhea to a severe cholera-like syndrome (*6*).

Many methods have been developed to detect ETEC. Monoclonal-antibody method is time-consuming and requires specialized equipment (*7*). Rapid detection method Real-Time quantitative polymerase chain reaction (qPCR) has advantages of rapidity, sensitivity and specificity, but it requires expensive instruments: a qPCR system (*8*). Moreover, the wide range of inhibitors in biological samples(including organic and inorganic substances such as detergents, antibiotics, phenolic compounds, enzymes, polysaccharides, fats, proteins and salts) can inhibit amplification efficiency (*9,10*). It is essential, therefore, that sensitive, specific, rapid, cheap and simple diagnostic methods be developed for detection of ETEC. A novel nucleic acid amplification technology termed loop-mediated isothermal amplification (LAMP) has been developed to amplify nucleic acid rapidly (*11*). LAMP differs from PCR in that four to six primers and a strand-displacing Bst DNA polymerase recognize and amplify the target gene with high specificity at a constant temperature. Since it is isothermal, LAMP can be performed in a simple water bath, other than an expensive temperature cycling device. In addition, the LAMP assay is advantageous over Polymerase Chain Reaction (PCR) in that positive results can be directly detected through visual observation of turbidity changes, so sophisticated electrophoresis apparatus is not essential.

In the present study, extensive standardization of LAMP method was carried out for rapid detection of ETEC in raw milk. The purpose of this study is (*i*) To optimize the LAMP reaction in terms of temperature,

**Address correspondence to:*
Dr. Yufeng Li, School of Bioengineering, Xihua University, Road Jinzou, No.999, Chengdu, Sichuan Province, China.
E-mail: griffinyang123@yahoo.com

time and quantities of primers and Bst DNA polymerase fragment; (*ii*) To analyze the specificity and sensitivity of LAMP; and (*iii*) To establish an effective and low-cost method for detecting ETEC from raw milk.

2. Materials and Methods

2.1. *Bacterial strains and culture conditions*

Ten bacterial strains were used in the present study (Table 1). They were cultured for 24-48 h at 37°C in nutrient broth.

2.2. *Artificial contamination of raw milk*

Raw milk was purchased from retail shops in Chengdu City, Sichuan Province, China. The milk was divided into 25-mL test portions. Each test sample (25 mL) was then inoculated with 2 mL of ETEC cultures, resulting in a spiked level of between 10^8 and 10^9 cfu/mL.

2.3. *DNA extraction*

DNA from the pure culture of ten strains used in this study was extracted according to the manufacture's instruction of UNIQ-10 Spin Column Oligo DNA Purification Kit (Shanghai Bioengineering Co., Ltd., Shanghai, China). The DNA extracted was used as template in the later assay determining the optimum reaction conditions and analyzing the specificity of LAMP in detecting ETEC.

The contaminated raw milk was decimally diluted in buffer (20 mM Tris-HCl, pH 8.0; 2 mM EDTA, pH 8.0 and 1.2% Triton X-100). Then the DNA was extracted as follows: First, 1 mL of dilution was centrifuged for 1 min at 10,000× g (Tabletop refrigerated centrifuge, Thermo Fisher Scientific, Chengdu, Sichuan Province, China). After the supernatant was removed, the pellet was suspended in 200 μL of buffer (20 mM Tris-HCl, pH 8.0; 2 mM EDTA, pH 8.0, and 1.2% Triton X-100). Then the tubes were incubated at 56°C for 20 min (Constant temperature water bath, Jinchengguosheng Co.,Ltd, Jintan, Jiangsu Province, China). Finally, after vortex mixing (Essenscien, US) again, the tubes were centrifuged at 10,000× g for 2 min and the supernatant was used as DNA template in the assay comparing sensitivities of LAMP and PCR.

2.4. *LAMP primers*

In the present study, four sets of primers (Synthesized by Shanghai Sangon Biological Engineering Technology And Service Co., Ltd., China) *targeting the heat-labile enterotoxin A subunit and B subunit encoding gene* (Accession number in Genbank: S60731) were designed for the LAMP reaction (Table 2). Each set consisted of four primers: two inner primers (FIP and BIP) and two outer primers (F3 and B3).

2.5. *Optimization of reaction conditions of LAMP*

2.5.1. *Optimum temperature and time*

All the four sets of primers were tested to determine the set of LAMP primers that would give the clearest strips on 2.0% agarose gel(the assay was kept at 60°C for 60 min) (Electrophoresis equipment, Liuyi instrument factory, Beijing, China). Each reaction mixture consisted of 16 μM each of primer F3 and primer B3, 128 μM each of primer FIP and primer BIP, 4 μL of DNA template, 8 IU of Bst DNA polymerase large fragment, 0.45 μM of dNTPs, 5 μL betaine and 1× Thermopol Buffer (New England Biolabs (Beijing, Ltd.) in a total volume of 25 μL. To determine the optimum time and temperature for the reaction, the amplifications were carried out for different time periods (15 min, 30 min, 45 min, 60 min, and 75 min at 63°C) and temperatures (55, 58, 60, 63, and 65°C for 60 min). The reaction was terminated for 5 min at 80°C. LAMP products were subjected to electrophoresis on a 2.0% agarose gel and observed under UV light after staining with ethidium bromide (Gel imager, Bio-rad laboratories, Milan, Italy).

2.5.2. *Optimum quantities of reagents*

Optimum quantities of primers and Bst DNA polymerase large fragment to be added were also standardized at 60°C for 60 min. The following changes were attempted

Table 1. Bacterial strains used in the present study and their sources

No	Strain	Source
1	Enterotoxigenic *E.coli*: 44247	CMCC
2	Enteroinvasive *E.coli* ATCC44338	National vaccine and serum institute, PRC
3	*Proteus vulgaris* 1.1527	CGMCC
4	*Staphylococcus aureus subsp. aureus* 1.8721	CGMCC
5	*Shigella flexneri* 1.10599	CGMCC
6	*Salmonella enteritidis* 50040	CMCC
7	*Bacillus subtilis subsp. subtilis* 1.4255	CGMCC
8	*Sporosarcina sp.*1.192	CGMCC
9	*Bacillus sphaericus*	Microbiological Culture Collection Center of Xihua University
10	*Enterobacter aerogenes* 1.2571	CGMCC

CGMCC, China General Microbiological Culture Collection Center; CMCC, National Center for Medical Culture Collections.

Table 2. LAMP primers used in this study to detect ETEC by targeting *enterotoxin-encoding gene* (Accession Number in Genbank: S60731)

Primer name	Sequence
Primer set1-F3	5'-AGCGGCGCAACATTTCAG-3'
Primer set1-B3	5'-ATCAATTTTGGTCTCGGT-3'
Primer set1-F1P	5'-GCCATTGAAAGGATGAAGG-GATATGTGATTCTTAATGTG-3'
Primer set1-B1P	5'-ATATCTGAGGGTTTTTTT-CGAAGTCCCGGGCAGTCAAC-3'
Primer set2-F3	5'-CTATGTGCATACGGAGCT- 3′
Primer set2-B3	5'-CTCGGTAGATATGTGATTC- 3′
Primer set2-F1P	5'-CTTGTCATTTCG–GTCTATTACAGAACTATGTTCGGAATATAGCAAC- 3′
Primer set2-B1P	5'-CGAAGTCCCGGGC–CCTTCATCCTTTCAATGGCTTTTTTTTGGGAG- 3′
Primer set3-F3	5′-CCATTATATGCAAATGGCGA- 3′
Primer set3-B3	5′-GCTAAGTGAGCACTTCTCAA- 3′
Primer set3-F1P	5′-GGCATAAGACCTCCGGAAC-GAATTC- TTATACCGTGCTGACTCTAGAC- 3′
Primer set3-B1P	5′-TGATCACGCGAGAGGAACACAA-GAGAAGTGGAAACATATCCGTCA- 3′
Primer set4-F3	5′-ATTACATTTAAGAGCGGCGC-3′
Primer set4-B3	5′-GGTTCCTAGCATTAGACATGCTTT-3′
Primer set4-F1P	5′-GTATGGAATAATAAAACCCCTAAAGCAAACTAGTTTTCCA-3′
Primer set4-B1P	5′-TGTCCTTCATCCTTTCAATGGCAGGTCGAAGTCCCGGGCAGTC-3′

in the reaction to optimize the clearness of strips. Optimization of (*i*) amount of primers: the concentrations of primer B3 and primer F3 were increased progressively from 8 μM to 20 μM, *i.e*., 8 μM, 12 μM, 16 μM and 20 μM, and the concentration of primer BIP and primer FIP were increased from 64 μM to 160 μM, *i.e*., 64 μM, 96 μM, 128 μM, and 160 μM; (*ii*) amount of Bst DNA polymerase large fragment-five different amounts, *viz*., 2 IU, 4 IU, 6 IU, 8 IU, and 10 IU were tried.

2.6. *Detection of LAMP products*

The presence/absence of a whitish precipitate was analyzed visually. To confirm the amplification of DNA, 1.0 μL 10^{-2} diluted SYBR GreenI was added to the reaction mixture and the color change was observed. Meanwhile, LAMP products were subjected to electrophoresis on 2.0% agarose gel and observed under UV light after staining with ethidium bromide.

2.7. *Sensitivity of LAMP assay in detecting ETEC compared with PCR*

To compare the sensitivity of LAMP with PCR, 10-fold serial dilutions of the ETEC DNA extracted from raw milk were used as the template to detect the reaction limit. LAMP and PCR products were subjected to electrophoresis on 2.0% agarose gel and observed under UV light after staining with ethidium bromide.

2.8. *Specificity of LAMP assay in detecting ETEC*

All ten bacterial strains in Table 1 were used as templates to determine the specificity of LAMP reaction. The sample without template served as negative control. To exclude the false-positive result, the products of LAMP with DNA from ETEC as the template were digested by restriction endonuclease EcoRI (the reaction mixture consisted of 18 μL of ddH2O, 10 μL of products of LAMP, 2 μL of 10× NEBuffer and 2 μL restriction endonuclease EcoRI (New England Biolabs (Beijing, LTD) and was incubated at 37°C for 3 h). The products were subjected to electrophoresis on 2.0% agarose gel and observed under UV light after staining with ethidium bromide.

3. Results

3.1. *Determination of optimum conditions of LAMP reaction*

In this study, four sets of primers (primer set 1, primer set 2, primer set 3, and primer set 4) were designed targeting the *heat-labile enterotoxin A subunit and B subunit encoding gene* (Accession number in Genbank: S60731) and synthesized. ETEC could only be detected successfully by LAMP with primer set 3 (Figure 1A). The amplification of the target DNA could be observed under UV light. So in the next study, primer set 3 was chosen as the primer. The amplification of the template was successful with primer set 3 when the reactions were carried out at 63 and 65°C as observed by agarose gel electrophoresis, while the reaction at 55, 58, and 60°C couldn't produce any visible strips on gel electrophoresis (Figure 1B). The shortest time required for amplification by primer set 3 was proved to be 60 min (Figure 1C). Besides, the reaction lasted for 75 min (the other conditions *viz*., temperature, amounts of ingredients were consistent with the reaction that lasted for 60 min) didn't provide clearer strips. So it was concluded that a reaction time more than 1 h didn't provide a more reliable result. As a result, 60 min was proved to be the best reaction duration.

3.2. *Optimum quantities of reagents*

In this assay, amplification of the template DNA was induced only when the concentration of primers was

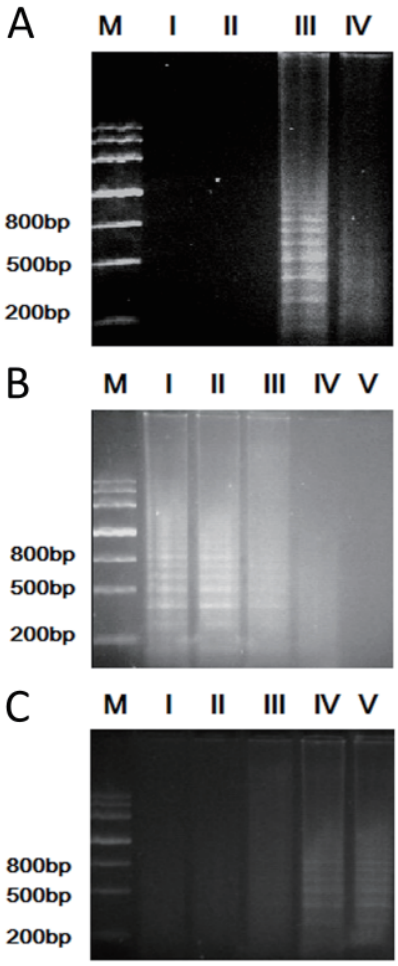

Figure 1. Determination of optimum primer set, temperature and time. (A) LAMP reaction with different primer set. M: DL2000 Plus DNA Marker, I: Primer set 1, II: Primer set 2, III: Primer set 3, IV: Primer set 4. **(B)** LAMP reaction at different temperatures. M: DL2000 Plus DNA Marker, I: 65°C, II: 63°C, III: 60°C, IV: 58°C, V: 55°C. **(C)** LAMP reaction lasted for different times. M: DL2000 Plus DNA Marker, I: 15 min, II: 30 min, III: 45 min, IV: 60 min, V: 75 min.

high enough (primer BIP and primer FIP higher than 128 μM, primer B3 and primer F3 higher than 16 μM) (Figure 2A). More primers led to clearer strips on agrose gel. ETEC could be successfully detected by LAMP with minimal Bst DNA polymerase large fragment (2 IU). It is obvious that reaction systems containing different amounts of Bst DNA polymerase large fragment produced the same results (Figure 2B). So we came to a conclusion that Bst DNA polymerase large fragment isn't the main influential factor.

3.3. *Sensitivity of LAMP assay*

Amplified DNA was observed at dilution 8 in LAMP, which corresponded to 547 cfu/mL, while amplification was observed only up to dilution 5 in PCR (Figure 3). So it was concluded that LAMP assay was 1,000 times more sensitive than PCR reaction in detecting ETEC from raw milk.

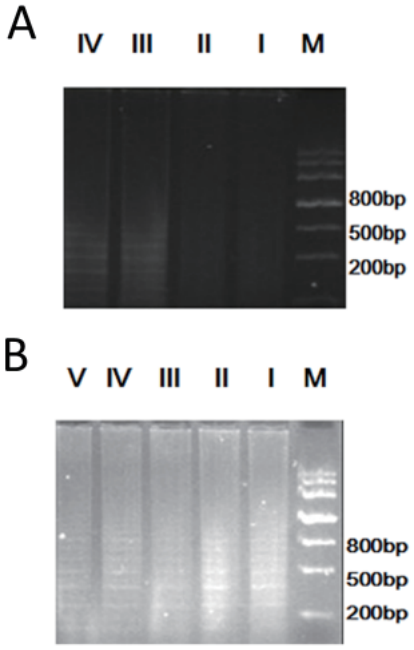

Figure 2. Determination of optimum quantities of reagents. (A) LAMP reaction with different amounts of primers. M: DL2000 Plus DNA Marker. I: primer B3 and primer F3: 8 μM, primer BIP and primer FIP: 64μM. II: primer B3 and primer F3: 12 μM, primer BIP and primer FIP: 96 μM. III: primer B3 and primer F3: 16 μM, primer BIP and primer FIP: 128 μM. IV: primer B3 and primer F3: 20 μM, primer BIP and primer FIP: 160 μM. **(B)** LAMP reaction with different amount of Bst DNA polymerase large fragment. M: DL2000 Plus DNA Marker, I: 2 IU, II: 4 IU, III: 6 IU, IV: 8 IU, V: 10 IU.

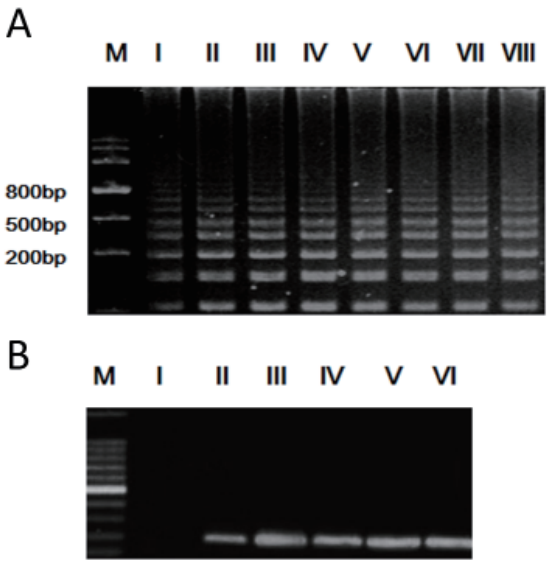

Figure 3. Comparative sensitivities of LAMP and PCR. (A) LAMP products with templates of different dilution rate. M: Marker, I: 10^{-8}, II: 10^{-7}, III: 10^{-6}, IV: 10^{-5}, V: 10^{-4}, VI: 10^{-3}, VII: 10^{-2}, VIII: 10^{-1}. **(B)** PCR products with templates of different dilution rate. I: 10^{-6}, II: 10^{-5}, III: 10^{-4}, IV: 10^{-3}, V: 10^{-2}, VI: 10^{-1}.

3.4. *Sensitivity of LAMP assay*

Among ten bacterial strains studied in this research (one ETEC, one EIEC and eight other bacterial strains), DNA from ETEC was amplified very specifically by

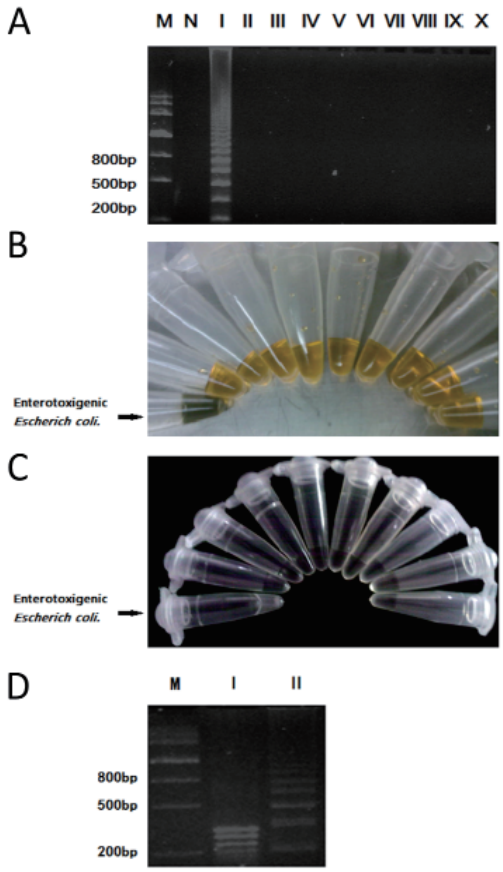

Figure 4. Specificity of the LAMP reaction for detection of ETEC. (A) M: DL2000 Plus DNA Marker. N: Negative control. I: Enterotoxigenic *Escherich coli*. II-X: Strains other than *E.coli*. **(B)** Visual detection using SYBR green 1. **(C)** Detection of whitish precipitate. **(D)** Identification of product of LAMP with template DNA from ETEC. M: DL2000 Plus DNA Marker 1: Fragment digested by restriction endonuclease EcoRI. 2: LAMP product undigested.

the LAMP reaction. The other nine bacterial strains did not provide any precipitate or strips on 2.0% agar gel, nor induce color reaction. After being digested by restriction endonuclease EcoRI, the Lamp product with DNA from ETEC as the template was cut into fragments. The electrophoresis result in Figure 4D proved that the lengths of fragments were consistent with the expected *viz*., 372, 285, 240, and 200 bp. This successfully proved the specificity of LAMP reaction in detecting ETEC.

4. Discussion

LAMP has been widely used as a tool in disease diagnosis (*12,13*), detection of food-borne Pathogenic microorganisms (*14*) and rapid authentication of ingredients (*15*). In the present study, the LAMP method developed was specific for ETEC strain and had no amplified product for 9 non-*E.coli* strains. We reasonably considered that primer set 3 had high specificity for ETEC. Six independent sequences recognized the target gene in the initial stage, and four independent sequences amplified the target sequence in the later stage of LAMP reaction (*16*), while the PCR reaction only had a pair of primers to amplify the target gene. Considering the high sensitivity of LAMP might lead to false-positive strips, we digested the LAMP product with restriction endonuclease EcoRI. The lengths of the fragment digested were consistent with the expected result. This proved the amplification of ETEC DNA, other than background amplification.

The figures presented in this study suggest that the LAMP assay is 1,000 times more sensitive than PCR for detection of ETEC from raw milk. Most studies using the LAMP reaction for detection have found sensitivity to be equal to or 10 times more than conventional PCR/ RT-PCR (*17-20*).

In the present study, it was established that the LAMP reaction for the detection of ETEC works well at both 63 and 65°C (*21*). The present study demonstrated the minimum time for formation of electrophoresis strips at 60 min. This was similar to earlier studies (*21,22*). Following the standardization of temperature and time, optimization of the LAMP assay was also carried out with regard to the effect of the amount of primers and Bst DNA polymerase large fragment on formation of electrophoresis strips on agrose. The electrophoresis strips were found to form with at least 16 μM each of outer primers and 128 μM each of inner primers. In the LAMP reaction, there was no increase of amplification with increasing amounts of Bst DNA polymerase large fragment used. This is an advantage of LAMP assay, which could lower detection cost.

In conclusion, LAMP is a rapid (about 60 min), sensitive (1,000 times more sensitive than conventional PCR assay), cheap (the reaction can be carried out in an isothermal water bath, other than an expensive isothermal-cycling device), convenient (the result could be observed by naked eye, so tedious electrophoresis is not essential), exclusive and inclusive (no false-positive and specific) detection tool for detection of ETEC from raw milk. LAMP technology is friendly for farmers as the detection can be carried out in any simple field laboratory without any professional knowledge. Visualization of the result is convincing to the farmer. It is suitable as a routine diagnostic tool in private clinics and field laboratories.

Acknowledgements

This work was supported by a grant (Supporting program of science and technology, Chengdu, Sichuan Province, China. No.: 14205413). We thank Dr. Mingliang He of The Chinese University of Hong Kong for his useful suggestions and ideas.

References

1. Todd EC. Epidemiology of foodborne diseases: A worldwide review. World Health Stat Q. 1997; 50:30-50.

2. Harada T, Itoh K, Yamaguchi Y, Hirai Y, Kanki M, Kawatsu K, Seto K, Taguchi M, Kumeda Y. A foodborne outbreak of gastrointestinal illness caused by enterotoxigenic *Escherichia coli* serotype O169:H41 in Osaka, Japan. Jpn J Infec Dis. 2013; 66:530-533.
3. Cho SH, Kim J, Oh KH, Hu JK, Seo J, Oh SS, Hur MJ, Choi YH, Youn SK, Chung GT, Choe YJ. Outbreak of enterotoxigenic *Escherichia coli* O169 enteritis in school children associated with consumption of Kimchi, Republic of Korea, 2012. Epidemiol Infec. 2014; 142:616-623.
4. Steffen R, Castelli F, Nothdurft HD, Rombo L, Zuckerman AN. Vaccination against enterotoxigenic *Escherichia coli*, a cause of travelers' diarrhea. J Travel Med. 2005; 12:102-107.
5. Wenneras C, Erling VA. Prevalence of enterotoxigenic *Escherichia coli*-associated diarrhoea and carrier state in the developing world. J Health Popul Nutr. 2004; 22:370-382.
6. Qadri F, Svennerholm AM, Faruque ASG, Sack RB. Enterotoxigenic *Escherichia coli* in developing countries: Epidemiology, microbiology, clinical features, treatment, and prevention. Clin Microbiol Rev. 2005; 18:465-483.
7. Trevanich S, Miyamoto T, Harada Y, Honjoh K, Hatano S. Rapid detection of enterotoxigenic *Escherichia coli* O6 in water by using monoclonal antibody and a photon-counting television camera. J Food Prot. 2000; 63:534-538.
8. Grant MA, Hu JX, Jinneman, KC. Multiplex real-time PCR detection of heat-labile and heat-stable toxin genes in enterotoxigenic *Escherichia coli*. J Food Prot. 2006; 69:412-416.
9. Wilson IG. Inhibition and facilitation of nucleic acid amplification. Appl Environ Microbiol. 1997; 63:3741-3751.
10. Abu Al-Soud W, Radstrom P. Capacity of nine thermostable DNA polymerases to mediate DNA amplification in the presence of PCR-inhibiting samples. Appl Environ Microbiol. 1998; 64:3748-3753.
11. Notomi T, Okayama H, Masubuchi H, Yonekawa T, Watanabe K, Amino N, Hase T. Loop-mediated isothermal amplification of DNA. Nucleic Acids Res. 2000; 28:E63.
12. Chaouch M, Mhadhbi M, Adams ER, Schoone GJ, Limam S, Gharbi Z, Darghouth MA, Guizani I, BenAbderrazak S. Development and evaluation of a loop-mediated isothermal amplification assay for rapid detection of Leishmania infantum in canine leishmaniasis based on cysteine crotease B genes. Vet Parasitol. 2013; 198:78-84.
13. Ge Z, Qing Y, Zicheng S, Shiying S. Rapid and sensitive diagnosis of Acanthamoeba keratitis by loop-mediated isothermal amplification. Clin Microbiol Infec. 2013; 19:1042-1048.
14. Niessen L, Luo J, Denschlag C, Vogel RF. The application of loop-mediated isothermal amplification (LAMP) in food testing for bacterial pathogens and fungal contaminants. Food Microbiol. 2013; 36:191-206.
15. Li M, Wong YL, Jiang LL, Wong KL, Wong YT, Lau CBS, Shaw PC. Application of novel loop-mediated isothermal amplification (LAMP) for rapid authentication of the herbal tea ingredient *Hedyotis diffusa* Willd. Food Chem. 2013; 141:2522-2525.
16. Nagamine K, Kuzuhara Y, Notomi T. Isolation of single-strand DNA from loop-mediated isothermal amplification products. Biochem Biophys Res Commun. 2012; 290:1195-1198.
17. Gunimaladevi I, Kono T, Venugopal MN, Sakai M. Detection of koi herpesvirus in common carp, Cyprinus carpio L., by loop-mediated isothermal amplification. J Fish Dis. 2004; 27:583-589.
18. Caipang CMA, Haraguchi I, Ohira T, Hirono I, Aoki T. Rapid detection of a fish iridovirus using loop-mediated isothermal amplification (LAMP). J Virol Methods. 2004; 121:155-161.
19. Kono T, Savan R, Sakai M, Itami T. Detection of white spot syndrome virus in shrimp by loop-mediated isothermal amplification. J Virol Methods. 2004; 115:59-65.
20. Saleh M, Soliman H, El-Matbouli M. Loop-mediated isothermal amplification (LAMP) for rapid detection of Renibacterium salmoninarum, the causative agent of bacterial kidney disease. Dis of Aquat Organ. 2008; 81:143-151.
21. Pillai D, Bonami JR, Widada JS. Rapid detection of Macrobrachium rosenbergii nodavirus (MrNV) and extra small virus (XSV), the pathogenic agent of white tail disease of Macrobrachium rosenbergii (De Man), by loop-mediated isothermal amplification. J Fish Dis. 2006; 29:275-283.
22. Thai HTC, Le MQ, Vuong CD, Parida M, Minekawa H, Notomi T, Hasebe F, Morita K. Development and evolution of a novel loop-mediated isothermal amplification method for rapid detection of severe acute respiratory syndrome corona virus. J Clin Microbiol. 2004; 42:1956-1961.

(Received November 3, 2014; Revised December 20, 2014; Accepted December 21, 2014)

Original Article

DOI: 10.5582/bst.2014.01092

Osteoprotegerin is up-regulated in pancreatic cancers and correlates with cancer-associated new-onset diabetes

Wanchun Shi[1], Wei Qiu[1], Wenhua Wang[1], Xiaohui Zhou[1], Xiaojing Zhong[1], Gang Tian[2,*], Anmei Deng[3,*]

[1] *Department of Endocrinology, Huzhou Central Hospital, Zhejiang, China;*
[2] *Department of Stomatology, Changhai Hospital, the Second Military Medical University, Shanghai, China;*
[3] *Department of Laboratory Diagnostic, Changhai Hospital, Second Military Medical University, Shanghai, China.*

Summary **New-onset diabetes might help to yield biomarkers for the early diagnosis of pancreatic cancer (PaC). In this study, we computationally predicted and experimentally validated osteoprotegerin (OPG) being associated with pancreatic cancer related new-onset diabetes. We first performed a meta-analysis on microarray datasets to search for genes specifically highly expressed in PaC, and then filtered for cytokines involved in islet dysfunction. The expression of OPG in PaC and normal pancreas were validated by immunohistochemistry. Serum OPG levels in healthy controls, non-cancerous diabetes and PaC patients with or without diabetes were detected by enzyme-linked immunosorbent assay (ELISA). *In silico* assay found that OPG up-regulated in PaC tissues in comparison to normal pancreas. Immunohistochemical data further confirmed that OPG was overexpressed in PaC samples. Furthermore, increased expression of OPG in PaC tissues correlated to the occurrence of new-onset diabetes, and adversely affected the patients' overall survival in both univariate and multivariate analysis. In addition, the serum levels of OPG were significantly higher in pancreatic cancer patients with new-onset diabetes than other groups including pancreatic patients without diabetes, new-onset type 2 diabetes and healthy controls. In conclusion, there is a close association between OPG and pancreatic cancer related new-onset diabetes, and OPG might serve as a potential biomarker for the early diagnosis of pancreatic cancer from populations with new-onset diabetes.**

Keywords: Pancreatic cancer, diabetes, OPG, immunohistochemistry, serum

1. Introduction

Pancreatic cancer (PaC) ranks as the fourth or fifth leading cause of cancer death in the world (*1*). At diagnosis, more than 85% of patients with PaC are at an advanced stage and unresectable, with an extremely poor survival. Therefore, there is an urgent need to identify novel early biomarkers for PaC.

New-onset diabetes pancreatic cancer (PaC-DM) frequently occurs within about 2 years prior to cancer diagnosis (*2*). Therefore, new-onset diabetes may be a useful clue to screen early PaC patients (*3-5*). However, although several putative biomarkers such as S100-A8 have been proposed, currently, it is still difficult to clinically distinguish cancerous and non-cancerous new-onset diabetes (*6*).

Accumulating evidence suggests that some circulating proteins or cytokines secreted by the tumor cells may exert a para-neoplastic effect on islets, and cause insulin resistance and β-cell dysfunction, which results in new-onset diabetes in patients with PaC (*7*).

In this study, in searching for the publicly available gene expression microarray datasets, we identified osteoprotegerin (OPG), a potential diabetes-related

**Address correspondence to:*
Dr. Gang Tian, Department of Stomatology, Changhai Hospital, the Second Military Medical University, Shanghai 200433, China.
E-mail: gangtianch@163.com

Dr. Anmei Deng, Department of Laboratory Diagnostic, Changhai Hospital, Second Military Medical University, Shanghai 200433, China.
E-mail: anmeideng@aliyun.com

cytokine, selectively upregulated in PC tissues. We further investigated the clinical and pathological significance of OPG in a pancreatic cancer cohort, and its utility as a serum biomarker to distinguish cancerous and non-cancerous new-onset diabetes was also evaluated.

2. Materials and Methods

2.1. *Data mining*

The Oncomine database (*https://www.oncomine.org*) was used to interrogate 7 publicly available datasets for mining cytokine gene expression in human pancreatic carcinomas as described previously (*8*). We first identified a p-value below 0.05 and a fold-change of 1.5 for differently expressed genes in pancreatic cancer tissues compared to control. The gene ranks across 7 datasets were compared, and then a concept filter "cytokines" was used to identify known diabetes-related factors up-regulated in pancreatic cancer tissues at the mRNA level.

2.2. *Immunohistochemical expression of OPG in pancreatic cancer tissues*

For immunohistochemical analysis, 83 stage I-II pancreatic cancer tumors and paired normal adjacent pancreas from patients who underwent primary surgical resection between September 2004 and December 2008 were analyzed. Forty patients were determined to be in stage I, and 43 in stage II. No patients received previous radiotherapy and/or chemotherapy before surgical resections. Clinicopathological information for each subject, including gender, age, TNM classification, history of diabetes, perineural invasion status, and overall survival, was collected retrospectively and is summarized in Table 1.

Each pathological section was subjected to immunohistochemical staining with an avidin-biotin-peroxidase complex system. Briefly, after deparaffinization and rehydration, epitope retrieval was carried out in 10 mmol/L citrate buffer (pH = 6.0) for 15 min. The activity of endogenous peroxidases was blocked with 3% hydrogen peroxide for 10 min at room temperature. The sections were then incubated with anti-OPG antibody (Santa Cruz Biotechnology, Inc, Santa Cruz, CA, USA) at a dilution of 1:100 overnight at 4°C, followed by incubation with an HRP-conjugated secondary antibody for 30 minutes at room temperature. 3,3'-Diaminobenzidine (DAB) was used as a chromogenic substrate. The positivity index was expressed as the percentage of moderate or strong staining cancer cells in each lesion. The cases with an index more than the median value were defined as high-OPG expression level, and the others as low-OPG expression level.

2.3. *Evaluation of serum OPG levels*

After excluding poor quality samples, we measured fasting serum OPG levels in 24 healthy subjects with normal fasting glucose levels, 23 non-cancer patients with new-onset type 2 diabetes, 20 pancreatic cancer cases with normal fasting glucose levels, and 25 pancreatic cancer patients with new-onset diabetes. All these four groups were age and sex matched. Among the patients with pancreatic cancer, 27 cases were at early-stage (I/II) and 18 were at late-stage (III/IV). The TNM stage of two pancreatic cancer groups were not significantly different. The levels of serum OPG were quantified using a commercial enzyme-linked immunosorbent assay (ELISA) kit according to the manufacturer's instructions (R&D Systems Inc. Minneapolis, Minnesota, USA).

2.4. *Statistics*

The correlation between OPG expression levels and clinicopathological characteristics was analyzed using the Pearson χ^2 test. The Kaplan-Meier method was used for survival analysis in terms of OPG expression, and evaluated by the log-rank test. Multivariate analysis was performed using a Cox proportional hazard model. Statistical comparisons of serum OPG levels between groups were performed using *t* tests. Differences were considered statistically significant at *p* value less than 0.05.

3. Results

3.1. *In silico assay identified OPG up-regulated in PaC tissues in comparison with normal pancreas.*

We performed a meta-analysis on 7 gene expression microarray datasets from the Oncomine database to identify up-regulated pancreatic cancer-related genes, then filtered for cytokines with known involvement in diabetes. Among the top 20 up-regulated cytokines in pancreatic cancers, OPG has been validated to inhibit islet function using multiple lines of evidence. Therefore, OPG may be a candidate cancer-derived mediator for pancreatic cancer-related diabetes. Our *in silico* results indicated that a significant increase in OPG mRNA level was observed in pancreatic cancer samples compared to adjacent non-tumor or normal tissues in 5 (including the largest two cohorts) out of 7 databases.

3.2. *Immunohistochemical results of OPG expression*

To further evaluate the potential clinical implication of OPG in pancreatic cancer progression, we next analyzed its expression by immunohistochemistry in 83 pairs of pancreatic cancer specimens at early stages. As

seen in Figure 1, normal adjacent and normal pancreas showed weak OPG immunostaining, while prominent staining was observed in the tumor samples compared to that in the normal tissues. The positive staining is diffuse, cytoplasmic/nuclear in cancer cells, but occasionally in stromal cells.

3.3. *Association between OPG expression levels in pancreatic cancer tissues with clinicopathological characteristics and survival*

In tumor samples, high OPG expression level was more frequently observed in patients with new-onset diabetes compared with patients without new-onset diabetes (40.9% *vs*. 66.7%, $p = 0.0311$) (Table 1). Except for diabetes history, no significant association was been identified between OPG expression levels compared to other clinicopathological characteristics (Table 1). Furthermore, increased OPG adversely affected survival in univariate analysis, and remained a strong independent prognostic factor for patients with pancreatic cancers in multivariate analysis (Table 2).

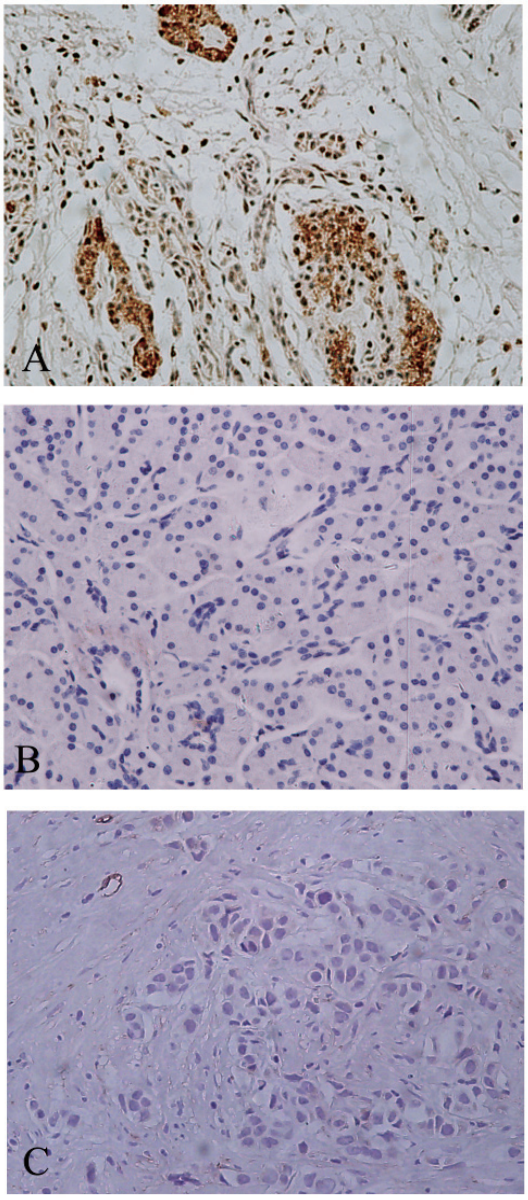

Figure 1. Representative images of osteoprotegerin immunostaining. Positive staining in pancreatic cancer tissues **(A)**; negative staining in normal adjacent pancreas tissues **(B)** and pancreatic cancer tissues **(C)**.

3.4. *Serum OPG levels in PaC-DM patients compared with other groups*

A Box-and-whisker plot of OPG serum levels in two non-cancer subject groups (with and without new-onset diabetes) and two cancer subject groups (with and without new-onset diabetes) is shown in Figure 2. *PaC-DM* patients had the highest level of serum OPG. In particular, the receiver operating characteristic curve (ROC) revealed that serum OPG had an Area under the ROC curve (AUC) of 0.737 ($P = 0.0012$) with a sensitivity of 68.0% and a specificity of 73.9% to distinguish *PaC-DM* cases from new-onset DM patients.

4. Discussion

Identification of the mediators to distinguish new-onset PaC-DM from the more common type 2 diabetes mellitus could serve as an important tool for screening for PaC at an asymptomatic time. Recent studies have

Table 1. ACorrelation of the expression of OPG expression with clinicopathological characteristics in 83 pancreatic cancers

Variable	No.	OPG Expression		*p* value
		Low ($n = 41$)	High ($n = 42$)	
Age (years)				
<65	49	20	29	0.2590
≥65	34	19	15	
Gender				
Male	52	25	27	0.9760
Female	31	14	17	
Grade				
1-2	60	31	29	0.2569
3	23	8	15	
Tumor size				
T1	5	1	4	
T2	65	33	32	0.3305
T3	13	5	8	
Lymph node metastasis				
Negative	48	24	24	0.6736
Positive	35	15	20	
TNM stage				
I	40	22	18	0.2338
II	43	17	26	
Neural invasion				
Negative	35	18	17	0.6387
Positive	48	21	27	
Diabetes history				
No	44	26	18	0.0311
New-onset	33	11	22	
Type 2	6	2	4	

Table 2. Univariate and multivariate Cox regression analysis for overall survival based on OPG expression and clinicopathological characteristics

	Univariate survival analyses			Multivariate survival analysis		
Variable	*P* value	HR	95% CI of HR	*P* value	HR	95% CI of HR
Age	0.9750	0.9911	0.5682 to 1.7288			
Gender	0.0639	0.5665	0.3115 to 1.0302			
Grade	0.0098	2.1415	1.2047 to 3.8067	0.0283	1.9344	1.0759 to 3.4780
Tumor size	0.7694	0.9111	0.4903 to 1.6930			
Lymph node metastasis	0.0133	1.9977	1.1583 to 3.4453	0.7801	1.1504	0.4323 to 3.0612
TNM stage	0.0122	2.0501	1.1725 to 3.5847	0.4240	1.5007	0.5576 to 4.0394
Neural invasion	0.0197	1.9991	1.1199 to 3.5685	0.2198	1.4894	0.7908 to 2.8051
Diabetes history	0.7464	0.9334	0.6160 to 1.4144			
OPG expression	0.0041	2.3272	1.3116 to 4.1293	0.0189	2.0314	1.1277 to 3.6591

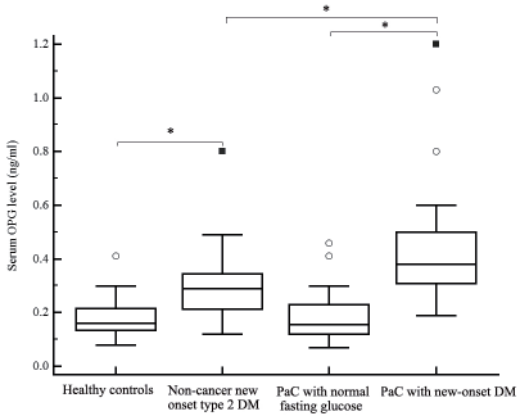

Figure 2. OPG is a potential candidate biomarker for PaC-DM. New-onset diabetes pancreatic cancer patients had the highest level of serum OPG. DM means diabetes mellitus.

found several diabetogenic secretory products of pancreatic cancer, such as adrenomedullin, macrophage migration inhibitory factor (*9-11*).

Osteoprotegerin (OPG) is a soluble decoy receptor for tumor necrosis factor (TNF)-related apoptosis inducing ligand (TRAIL), and belongs to the tumor necrosis factor receptor superfamily (TNFRSF) (*12,13*). In this study, for the first time, we discovered several lines of evidence supporting that OPG may serve as a novel diabetogenic cytokine of pancreatic cancer. First, OPG expression was significantly increased in PaC tissues compared with normal pancreas. Second, in PaC tumors, OPG overexpression is associated with new-onset PaC-DM. Third, Patients with new-onset PaC-DM had a higher serum OPG level than those without diabetes mellitus. Toffoli *et al*. (*14*) found that OPG induces morphological alterations and reduction of islet function in mouse pancreatic islets, and islet RAS overactivity represents one possible mechanism responsible for this effect. Together with our findings, we suggest that at least in part of PaC tissues, islet cells would face high OPG stress, and thus be more susceptible to damage than normal human islets. This study also provides the rationale to consider OPG as a candidate target for new approaches to retard the development of PaC-DM.

Moreover, this study further found that over-expression of OPG predicts poor prognosis for PaC, and acts as an independent prognostic factor. These findings strongly indicated that except as a diabetogenic factor, OPG may play a critical role in PaC development and progression, and recent evidence also support that OPG acts as key modulator on a metastasis-promoting effect and resistance to TRAIL-induced apoptosis in cancers including PaC (*15*).

Serum OPG levels increased in both patients with diabetes and patients with pancreatic cancer (*16-18*). Our results are consistent with the previous findings, and further demonstrated that PaC-DM had a higher serum OPG level than the new onset common diabetes mellitus and PaC without DM. Interestingly, serum OPG levels could distinguish patients with PaC-DM from those with new-onset type 2 DM, suggesting the potential utility of OPG as a candidate serum biomarker of new-onset PaC-DM.

In conclusion, this present study indicates OPG is a candidate diabetogenic cytokine for new-onset PaC-DM, and may also serve as a novel prognostic factor for PaC and a new serum biomarker for patients with early PaC. Further experimental and clinical studies are required to investigate the exact role of OPG in PaC as well as its utility in the screening of PaC-DM among subjects with new-onset diabetes mellitus.

Acknowledgements

This work was supported by the "1255" Subject Construction and Scientific Innovation Program of Changhai Hospital (No. CH125541800) and the General Program of Health Bureau of Shanghai (2012, No. 146).

References

1. Van Cutsem E, Vervenne W L, Bennouna J, Humblet Y, Gill S, Van Laethem J L, Verslype C, Scheithauer W, Shang A, Cosaert J, Moore MJ. Phase III trial of

bevacizumab in combination with gemcitabine and erlotinib in patients with metastatic pancreatic cancer. J Clin Oncol. 2009; 27:2231-2237.
2. Pannala R, Basu A, Petersen GM, Chari ST. New-onset diabetes: A potential clue to the early diagnosis of pancreatic cancer. Lancet Oncol. 2009; 10:88-95.
3. Pannala R, Leirness JB, Bamlet WR, Basu A, Petersen GM, Chari ST. Prevalence and clinical profile of pancreatic cancer-associated diabetes mellitus. Gastroenterology. 2008; 134:981-987.
4. Lai SW, Liao KF. New-onset diabetic patients need pancreatic cancer screening. J Clin Gastroenterol. 2013; 47:372.
5. Mizuno S, Nakai Y, Isayama H, *et al*. Diabetes is a useful diagnostic clue to improve the prognosis of pancreatic cancer. Pancreatology. 2013; 13:285-289.
6. Basso D, Greco E, Fogar P, Pucci P, Flagiello A, Baldo G, Giunco S, Valerio A, Navaglia F, Zambon CF, Falda A, Pedrazzoli S, Plebani M. Pancreatic cancer-derived S-100A8 N-terminal peptide: A diabetes cause? Clin Chim Acta. 2006; 372:120-128.
7. Sah RP, Nagpal SJ, Mukhopadhyay D, Chari ST. New insights into pancreatic cancer-induced paraneoplastic diabetes. Nat Rev Gastroenterol Hepatol. 2013; 10:423-433.
8. Rhodes DR, Kalyana-Sundaram S, Mahavisno V, Varambally R, Yu J, Briggs BB, Barrette TR, Anstet MJ, Kincead-Beal C, Kulkarni P, Varambally S, Ghosh D, Chinnaiyan AM. Oncomine 3.0: Genes, pathways, and networks in a collection of 18,000 cancer gene expression profiles. Neoplasia. 2007; 9:166-180.
9. Aggarwal G, Ramachandran V, Javeed N, *et al*. Adrenomedullin is up-regulated in patients with pancreatic cancer and causes insulin resistance in beta cells and mice. Gastroenterology. 2012; 143:1510-1517 e1511.
10. Tan L, Ye X, Zhou Y, Yu M, Fu Z, Chen R, Zhuang B, Zeng B, Ye H, Gao W, Lin Q, Li Z, Zhou Q. Macrophage migration inhibitory factor is overexpressed in pancreatic cancer tissues and impairs insulin secretion function of beta-cell. J Transl Med. 2014; 12:92.
11. Sharaf RN, Butte AJ, Montgomery KD, Pai R, Dudley JT, Pasricha PJ. Computational prediction and experimental validation associating FABP-1 and pancreatic adenocarcinoma with diabetes. BMC Gastroenterol. 2011; 11:5.
12. Malyankar UM, Scatena M, Suchland KL, Yun TJ, Clark EA, Giachelli CM. Osteoprotegerin is an alpha vbeta 3-induced, NF-kappa B-dependent survival factor for endothelial cells. J Biol Chem. 2000; 275:20959-20962.
13. Takeda K, Smyth MJ, Cretney E, Hayakawa Y, Kayagaki N, Yagita H, Okumura K. Critical role for tumor necrosis factor-related apoptosis-inducing ligand in immune surveillance against tumor development. J Exp Med. 2002; 195:161-169.
14. Toffoli B, Bernardi S, Candido R, Sabato N, Carretta R, Corallini F, Secchiero P, Zauli G, Fabris B. Osteoprotegerin induces morphological and functional alterations in mouse pancreatic islets. Mol Cell Endocrinol. 2011; 331:136-142.
15. Kanzaki H, Ohtaki A, Merchant FK, Greene MI, Murali R. Mutations in K-Ras linked to levels of osteoprotegerin and sensitivity to TRAIL-induced cell death in pancreatic ductal adenocarcinoma cells. Exp Mol Pathol. 2013; 94:372-379.
16. Secchiero P, Corallini F, Pandolfi A, Consoli A, Candido R, Fabris B, Celeghini C, Capitani S, Zauli G. An increased osteoprotegerin serum release characterizes the early onset of diabetes mellitus and may contribute to endothelial cell dysfunction. Am J Pathol. 2006; 169:2236-2244.
17. Rasmussen LM, Tarnow L, Hansen TK, Parving HH, Flyvbjerg A. Plasma osteoprotegerin levels are associated with glycaemic status, systolic blood pressure, kidney function and cardiovascular morbidity in type 1 diabetic patients. Eur J Endocrinol. 2006; 154:75-81.
18. Lipton A, Ali SM, Leitzel K, Chinchilli V, Witters L, Engle L, Holloway D, Bekker P, Dunstan CR. Serum osteoprotegerin levels in healthy controls and cancer patients. Clin Cancer Res. 2002; 8:2306-2310.

(Received August 27, 2014; Revised November 12, 2014; Accepted December 10, 2014)

Original Article

DOI: 10.5582/bst.2014.01070

The use of ventriculoperitoneal shunts for uncontrollable intracranial hypertension in patients with HIV-associated cryptococcal meningitis with or without hydrocephalus

Li Liu[1], Renfang Zhang[1], Yang Tang[1], Hongzhou Lu[1,2,3,*]

[1] *Key Laboratory of Medical Molecular Virology of MOE/MOH, Department of Infectious Disease, Shanghai Public Health Clinical Center, Shanghai, China;*
[2] *Department of Infectious Disease, Huashan Hospital affiliated with Fudan University, Shanghai, China;*
[3] *Department of Internal Medicine, Shanghai Medical College, Fudan University, Shanghai, China.*

Summary **Extremely elevated intracranial pressure (ICP) in patients with HIV and cryptococcal meningitis is a poor prognostic predictor of death during initial therapy. The risks associated with implanting a cerebrospinal fluid (CSF) shunt into immunocompromised patients with ongoing CSF infection have historically discouraged surgeons from implanting CSF shunts in patients with HIV and cryptococcal meningitis. An unanswered question is whether ventriculoperitoneal (VP) shunts can effectively provide long-term treatment for patients with intracranial hypertension and HIV-associated cryptococcal meningitis in China. Outcomes for 9 patients with HIV-associated cryptococcal meningitis who were given VP shunts for increased ICP were retrospectively analyzed. Each patient's age, sex, clinical manifestations, CD4+ lymphocyte count, HIV viral load, neurological status, CSF features, image findings, anad other opportunistic infections were recorded for analysis. All patients had signs and symptoms of increased ICP, including headaches, nausea, and vomiting. Seven patients (77.78%) had visual loss due to persistent papilledema. The median time from diagnosis of cryptococcal meningitis to VP shunting in the 9 patients was 5 months (range 0.5-12.5 months). Seven patients (77.78%) had good outcomes, with recovery from 1 month to 48 months. Two patients had poor outcomes; one died six months after shunting due to severe adverse reactions to antiretroviral drugs, and the other died two weeks after surgery. Patients with intracranial hypertension and HIV-associated cryptococcal meningitis who cannot tolerate cessation of external lumbar CSF drainage or frequent lumbar punctures may be eligible for VP shunt placement, despite severe immunosuppression and persistent CSF cryptococcal infection.**

Keywords: Intracranial pressure, ventriculoperitoneal shunts, HIV, cryptococcal meningitis

1. Introduction

Cryptococcal meningitis is the most common life threatening fungal infection and the most common neurological complication in patients with HIV (*1,2*). After *Pneumocystis jirovecii* pneumonia (PCP) and tuberculosis, cryptococcal meningitis is the third leading cause of death in patients with HIV in Shanghai. Despite the advent of new antifungal drugs and modern imaging techniques, the mortality and morbidity of HIV-associated cryptococcal meningitis remain high. Persistently increased intracranial pressure (ICP) is the most accurate predictor of poor prognosis in patients with HIV-associated cryptococcal meningitis (*3-5*), which can cause deterioration of neurological status and mental acuity and impairment of vision (*6*). Although serial high-volume lumbar puncture remains the standard of care for *Cryptococcus*-associated intracranial hypertension, some patients cannot tolerate intermittent cerebrospinal fluid (CSF) drainage. Additionally, the risk

**Address correspondence to:*
Dr. Hongzhou Lu, Department of Infectious Diseases, Shanghai Public Health Clinical Center, No. 2901 Caolang Road, Shanghai 201508, China.
E-mail: luhongzhou@fudan.edu.cn

of brain herniation caused by frequent lumbar punctures for elevated ICP has been a major concern among clinicians (*7*). Cerebrospinal fluid shunts may allow patients with HIV who have intracranial hypertension to leave the hospital with sustained alleviation of symptoms. The risk of shunt infection in the context of severe immune-suppression, shunt obstruction by elevated CSF protein, and peritoneal *Cryptococcus* seeding from direct transport of infected fluid has historically discouraged surgeons from implanting CSF shunts in patients with HIV and cryptococcal meningitis. However, several cases of ventriculoperitoneal (VP) shunt placement in HIV-infected patients with elevated ICP and cryptococcal meningitis have been reported (*8*), and most of these cases succeeded in long-term symptomatic improvement (*9*). However, no such cases have been reported in China. The question remains whether VP shunts can effectively provide long-term treatment for patients with intracranial hypertension and HIV-associated cryptococcal meningitis in China.

Reported here are 9 HIV-infected patients with extremely elevated ICP and active cryptococcal meningitis who were successfully treated with VP shunts. One patient has been treated for almost 4 years without complications. In contrast, two patients died after surgery. Nonetheless, the key task is to determine the effectiveness and safety of VP shunts in HIV-infected patients with cryptococcal meningitis.

2. Patients and Methods

2.1. *Patients*

During a period of 5 years (2009-2013), 90 HIV-infected patients with cryptococcal meningitis were identified at Shanghai Public Health Clinical Center. Of these patients, 9 were treated with VP shunts.

HIV infection was defined as a positive result on a screening test and confirmation of the presence of antibodies to HIV. Cryptococcal meningitis was defined as isolation of *Cryptococcus neoformans* from ≥ 1 CSF culture, a positive CSF cryptococcal antigen titer, or positive results of CSF India ink studies. Hydrocephalus was diagnosed based on the presence of a dilated temporal horn of the lateral ventricle, without obvious brain atrophy on the initial and/or follow-up CT or MRI. To avoid interference in statistical results, the exclusion criteria for this study were as follows: (*i*) evidence of concomitant acute meningitis not due to *C. neoformans*, (*ii*) lack of follow-up data on antifungal treatment, (*iii*) presence of recurrence of cryptococcal meningitis, and (*iv*) neurological deficits due to previous head injury, cerebral infarction, or intracranial hemorrhage.

2.2. *Data collection*

This retrospective study was approved by the ethics committee of Shanghai Public Health Clinical Center. All patient records were anonymous and a de-identified ID number was used prior to analysis.

For each patient, the age, sex, clinical manifestations, CD4+ lymphocyte count, HIV viral load, neurological status, CSF features, image findings, and presence of other opportunistic infections were all recorded for analysis.

2.3. *CSF opening pressure*

The CSF opening pressure measured *via* a lumbar puncture was recorded.

2.4. *CSF analysis*

Samples of CSF obtained *via* a lumbar puncture were sent to the laboratory for cell analysis and determination of glucose and protein levels before and after VP shunting.

2.5. *Treatment*

Antifungal regimens including amphotericin B plus flucytosine and voriconazole were added in the first 2 weeks of treatment. Patients with increased ICP were given intravenous mannitol or underwent repeated lumbar punctures. If there was further deterioration of neurological status, decreased mental acuity, or impaired vision due to increased pressure, the patient was transferred to Neurosurgery for surgery. Eight patients were treated with a VP shunt (Medtronic system). All patients underwent antiretroviral therapy (ART) after 2 to 4 weeks of antifungal treatment. Only one patient was ART- naïve when undergoing VP shunting.

2.6. *Therapeutic outcome*

Therapeutic outcomes 1, 3, 6, and 12 months after placement of the VP shunt were determined based on the results of CSF analysis and relief of clinical symptoms. Asymptomatic status, mild disability, and moderate disability were considered to be favorable outcomes. Major disability, vegetative status, and death were considered to be poor outcomes. Some patients were followed-up in the Outpatient department after discharge from hospital, and others were interviewed by telephone to determine their neurological outcomes.

3. Results

The general characteristics of the 9 patients after admittance to the hospital are shown in Table 1. All patients were in the late stage of AIDS with very low CD4+ T lymphocyte levels and a very high plasma HIV viral load. When cryptococcal meningitis was

Table 1. Clinical characteristics of patients upon admission

Patient	Age/sex	CD4 count (cells/μL)	HIV viral load (copies/mL)	CSF pressure (cm H_2O)	CSF protein (mg/L)	CSF glucose (mmol/L)	Symptom	CT/MRI scan findings	Anti-fung. therapy
1	31/M	2	ND	> 400	171	3.5	FE, HA, N/V	No	Amph B,5-FC,Fluc
2	38/M	1	581000	> 400	228	3.64	FE, HA, N/V	No	Amph B,5-FC,Fluc
3	23/M	11	110000	> 400	85	2.33	HA, N/V, CO	No	Amph B,5-FC,Fluc
4	30/M	9	62700	> 400	57	3.36	HA	No	Amph B,5-FC,Fluc
5	35/M	15	30800	> 400	342	2.6	HA, N/V, LOC	No	Amph B,5-FC,Fluc
6	28/M	4	251000	> 400	86	2.89	HA, VL, CO, DEM	No	Amph B,5-FC,Fluc
7	34/M	32	98300	> 400	257	2.09	HA, VL	No	Amph B,5-FC,Fluc
8	43/M	12	969000	> 400	114	2.47	HA, N/V, LOC	No	Amph B,5-FC,Fluc
9	28/M	7	1310000	> 400	257	3	HA, N/V	No	Amph B,5-FC,Fluc

LOC indicates loss of consciousness; FE, fever; HA, headaches; N/V, nausea and vomiting; VL, visual loss; CO, convulsions; DEM, impaired eye movement; Amph B, amphotericin B; 5FC, 5-flucytosine; Fluc, fluconazole; ND, not done.

diagnosed, patients received antifungal treatment. All patients had headaches and vomiting, and some presented with other neurological symptoms including visual loss, convulsions, and impaired eye movement (Table 1).

The general characteristics of these patients who underwent shunting and various outcomes are shown in Table 2. After effective treatment, the CSF cultures of 7 patients (7 of 9, 77.78%) tested negative for *Cryptococcus neoformans* when they underwent shunting (Table 2). The other two patients tested positive for *Cryptococcus neoformans* at the time of surgery. Eight patients had received ART before VP shunting, and the median time from ART to surgery was 4.5 months (range 0.5-12.5 months). Notably, 6 of these patients had complete viral suppression (HIV viral load below the test limit, Table 2) when they underwent surgery. The CD4+ lymphocyte count in these patients increased after ART but remained below 100 cells/μL. Two patients had a high HIV viral load at the time of surgery - one was ART-naïve and the other had undergone 0.5 months of ART.

All patients underwent VP shunting because of deteriorating neurological status or loss of consciousness, decreased mental acuity, or vision loss associated with persistently increased ICP. All patients had signs and symptoms of increased ICP including headaches, nausea, and vomiting. Seven patients (77.78%) had visual loss due to persistent papilledema. One of these 7 patients presented with deafness, another with ptosis, and another with impaired eye movement. Five patients (55.56%) had convulsions or a loss of consciousness due to greatly increased ICP. Only 3 patients (33.33%) had hydrocephalus with ventricular dilatation according to brain CT or MRI scans. The median time from diagnosis of cryptococcal meningitis to VP shunting in these 9 patients was 5 months (range 0.5-12.5months).

Two patients underwent anti-tuberculosis therapy at the time of surgery. One patient had been on anti-TB therapy for 5 months and the other for 2 months. Sputum TB cultures for both patients were negative before surgery. One of these two patients died two weeks after surgery.

All patients (100%) had an increased CSF opening pressure (> 400 mm H_2O) over a prolonged period. The cell count, protein levels, and glucose levels of the CSF were all within the normal ranges. The CSF opening pressure returned to normal after shunting in all patients. CSF protein levels were elevated in 5 patients (55.56%), with levels in 4 between 1,000 and 2,000 mg/L. Only one patient had a CSF protein level over 3,000 mg/L, and this patient died two weeks after shunt placement.

Of the 9 patients, 7 (77.78%) had good outcomes with recovery from 1 month to 48 months. The first patient has been treated with VP shunting for almost 4 years without complication. Only two patients had poor outcomes. One died half a year after shunt placement due to severe adverse reactions to antiretroviral drugs, and the other died two weeks after surgery. The CSF protein levels in this patient increased to 3,770 mg/L after surgery. These levels increased again to 13,000 mg/L 2 days later and the cell count was 260 cell/L. The patient experienced a loss of consciousness 7 days after shunt placement and a CT scan revealed hypodense lesions in the basal ganglia and periventricular areas on the left. Infection was clinically diagnosed, so the patient was treated with both antibiotics and anti-TB drugs because the pathogen could not be identified. The shunt became obstructed, and eventually the patient died.

4. Discussion

CSF shunts have been used to manage increased ICP after cryptococcal meningitis in patients with and without HIV (*6,10*). The presumed increase in risk of shunt infection resulting from immunosuppression, shunt obstruction from elevated CSF protein, and peritoneal *Cryptococcus* seeding from direct transport of infected fluid has traditionally discouraged the placement of CSF shunts in patients with HIV and cryptococcal meningitis (*9*). In addition, the historically

Table 2. Clinical characteristics of and outcomes for patients receiving VP shunts for elevated ICP and HIV-associated cryptococcal meningitis with long-term follow-up over 12 months

Patient	Duration of ART before VP shunt (mo)	CD4 count (cells/μL)	HIV viral load (copies/mL)	CSF pressure (cm H_2O)	CSF culture of *Cryptococcus neoformans*	Neuro-deficit	CT/MRI scan findings	Medication for other OI	Time (mo) from diagnosis/ treatment to shunt	Outcome, 1 mo	Outcome, 3 mos	Outcome, 6 mos	Outcome, 12 mos
1	12	90	< 40	> 400	Neg	HA, N/V, LOC, VL, CO	Ventriculomegaly	No	12.5	Recover	Recover	Recover	Recover
2	9	40	< 40	> 400	Neg	HA, N/V, LOC, CO	Ventriculomegaly	No	9.5	Recover	Recover	Recover	*
3	4	27	ND	> 400	Neg	HA, N/V, LOC, VL, CO	Ventriculomegaly	No	5	Recover	Recover	Recover	Recover
4	3	26	< 40	> 400	Neg	HA, N/V, ptosis, CO	NO	No	3.5	Recover	Recover	Recover	Recover
5	3	29	< 40	> 400	Neg	HA, N/V, LOC, VL, deafness	NO	No	3.5	Recover	Recover	Recover	Recover
6	0	4	251000	> 400	Pos	HA, VL, CO, DEM	NO	No	0.5	Recover	Recover	--	--
7	12	76	< 40	> 400	Neg	HA, VL	NO	No	12.5	Recover	Recover	--	--
8	0.5	12	969000	> 400	Pos	HA, N/V, LOC, VL	NO	No	2	**	--	--	--
9	5	27	< 40	> 400	Neg	HA, N/V, VL	NO	No	6.5	Recover	Recover	--	--

LOC indicates loss of consciousness; HC, hydrocephalus; CC, cryptococcoma; HA, headaches; N/V, nausea and vomiting; VL, visual loss; CO, convulsions; DEM, impaired eye movement; Neg, negative; Pos, positive; TB, tuberculosis. * died half a year after shunt placement due to severe adverse reactions to antiretroviral drugs. ** died two weeks after surgery.

poor life expectancy of patients with end-stage HIV/AIDS has caused further questioning of the long-term benefits of VP shunting. Reported here are outcomes for 9 patients with elevated ICP secondary to HIV-associated cryptococcal meningitis. Eight patients were successfully treated with VP shunts for several months without complication, and only one patient died two weeks after surgery. Although 4 patients had CSF protein levels between 1,000 and 2,000 mg/L, and shunt obstruction did not occur. Shunt infection did not occur as a complication despite severely compromised immune function (median CD4 count: 27 cells/μL). Two patients died. One died half a year after shunt placement; death was due to severe adverse reactions to antiretroviral drugs and unrelated to VP shunting. The other patient died two weeks after the surgery because of a severe central nervous system infection. The patient had significantly increased CSF protein levels and an elevated cell count, suggesting infection. The pathogen of infection was unclear. Eventually, the patients died despite receiving antibiotics and anti-TB medications. The cause of death could not be verified because the patient's relatives refused an autopsy. Because the patient was also infected with tuberculosis, tuberculosis was assumed to have disseminated to the central nervous system after surgery because of poor control. The use of VP shunts in patients co-infected with other uncontrolled opportunistic infections should be carefully evaluated.

Among the 7 patients who had good outcomes, 6 had complete HIV viral suppression. One ART-naïve patient who underwent VP shunting only 0.5 month after diagnosis with a very high HIV viral load but also had a very good outcome. No studies have examined whether a high HIV viral load is a factor related to the prognosis for VP shunting in such patients. The suppression of HIV could promote immune reconstitution, protecting patients from other infections after surgery and providing surgeons with protection from HIV infection after possible exposure. The limited sample in the current study precluded determination of whether a high viral load affects prognosis.

VP shunting resolved symptoms for a number of months after surgery. The first patient has been treated with VP shunting for almost 4 years without complication. The median time from diagnosis of cryptococcal meningitis to VP shunting in these 9 patients was 5 months (range: 0.5-12.5 months). The symptoms of decreased mental acuity and impaired vision due to persistently increased ICP resolved soon after VP shunting. Ptosis eventually disappeared, and vision was gradually restored. Woodworth *et a*l. (*9*) reported two patients with intracranial hypertension and HIV-associated cryptococcal meningitis who underwent VP shunting but who were unable to tolerate cessation of external lumbar CSF drainage or frequent lumbar punctures. In these two patients, the time from

when cryptococcal meningitis was diagnosed to when VP shunting was performed was 5 and 0.5 months, respectively. These patients remained asymptomatic for 12 and 16 months after surgery without evidence of shunt infection or malfunction. Two of the current patients underwent surgery with no control of *Cryptococcus neoformans* infection. One had a good outcome, and the other died of infection after surgery. The duration of anti-cryptococcal treatment is not a key factor when choosing VP shunting.

Several factors contributed to the decision to place a VP shunt. Patients had a typical presentation of HIV-associated cryptococcal meningitis with substantially increased opening pressures along with severe headaches, nausea and vomiting, loss of consciousness, marked visual changes, ptosis, or ataxia. Patients responded favorably to removal of a large volume of CSF *via* a lumbar puncture but required continuous lumbar CSF drainage to remain neurologically asymptomatic. However, continuous papilledema can cause vision loss in some patients, severely impacting their daily lives. Of the 9 current patients, 7 (77.78%) had visual loss due to persistent papilledema. In addition, the inability to tolerate cessation of continuous CSF drainage, due to acute symptom recurrence despite maximal antifungal therapy, suggested the need for VP shunting. VP shunting should be given priority when vision loss appears despite continuous lumbar punctures. Only three patients (33.33%) had hydrocephalus with ventricular dilatation according to brain CT or MRI scans. In fact, extremely increased ICP without hydrocephalus associated with cryptococcal meningitis can also be resolved using VP shunting (*11*).

External lumbar drainage *via* daily lumbar puncture, insertion of a lumbar drain, or placement of a VP shunt is recommended if focal neurologic signs and altered consciousness are not noted and radiographic images reveal no space-occupying lesions (*3*). However, frequent lumbar punctures and large-volume drainage in the face of elevated ICP have raised concerns among clinicians about the risk of brain herniation (*7*). Lumbar shunts in patients with HIV-associated cryptococcal meningitis have been described with slightly greater frequency. However, Woodworth *et al*. (*9*) suggested that these shunts are more prone to failure compared to VP shunts. Fessler *et al*. (*12*) studied the role of lumbar peritoneal shunts in the treatment of 8 patients with HIV-associated cryptococcal meningitis. They found that nearly half of the lumbar shunts failed. One of these patients responded favorably after a switch to VP shunting and the patient benefited from long-term shunting. In another study of cryptococcal meningitis in HIV-infected patients, Stevens *et al*. (*8*) suggested that managing elevated ICP with a VP shunt in this patient population may result in better long-term outcomes. The current findings corroborate these observations because most of the current patients have had a satisfactory course several months after VP shunt placement.

The current findings suggest that VP shunts remove a large amount of CSF and lower ICP, thereby significantly improving outcomes for patients with HIV-associated cryptococcal meningitis and persistently increased ICP. The benefits of placing VP shunts (long-term symptom control, elimination of the use of a percutaneous spinal catheter and the associated risk of infection, ability to provide care outside a hospital setting) in this patient population may outweigh the risks of potential infection, cryptococcal dissemination, and shunt obstruction. The limited sample in the current report implies that larger prospective studies are needed to better assess the potential utility of VP shunts in these patients. However, the placement of VP shunts in this patient population may be a reasonable and effective treatment modality with potentially beneficial outcomes.

Acknowledgements

This work was supported by a grant from the 12th Five-year Plan (grant no. 2012ZX10001003).

References

1. Jackson A, van der Horst C. New insights in the prevention, diagnosis, and treatment of cryptococcal meningitis.Curr HIV/AIDS Rep. 2012; 9:267-277.
2. Roy M, Chiller T. Preventing deaths from cryptococcal meningitis: From bench to bedside. Expert Rev Anti Infect Ther. 2011; 9:715-717.
3. Graybill JR, Sobel J, Saag M, *et al*. Diagnosis and management of increased intracranial pressure in patients with AIDS and cryptococcal meningitis. Clin Infect Dis. 2000; 30:47-54.
4. York J, Bodi I, Reeves I, Riordan-Eva P, Easterbrook PJ. Raised intracranial pressure complicating cryptococcal meningitis: Immune reconstitution inflammatory syndrome or recurrent cryptococcal disease? J Infect. 2005; 51:165-171.
5. Sun HY, Hung CC, Chang SC. Management of cryptococcal meningitis with extremely high intracranial pressure in HIV-infected patients. Clin Infect Dis. 2004; 38:1790-1792.
6. Denning DW, Armstrong RW, Lewis BH, Stevens DA. Elevated cerebrospinal fluid pressures in patients with cryptococcal meningitis and acquired immunodeficiency syndrome. Am J Med. 1998; 91:267-272.
7. Antinori S, Ridolfo AL, Gianelli E, Piazza M, Gervasoni C, Monforte AA. The role of lumbar puncture in the management of elevated intracranial pressure in patients with AIDS-associated cryptococcal meningitis. Clin Infect Dis. 2000; 31:1309-1310.
8. Stevens DA, Denning DW, Shatsky S, Armstrong RW, Adler JD, Lewis BH. Cryptococcal meningitis in the immunocompromised host: Intracranial hypertension and other complications. Mycopathologia. 1999; 146:1-8.
9. Woodworth GF, McGirt MJ, Williams MA, Rigamonti D. The use of ventriculoperitoneal shunts for uncontrollable

intracranial hypertension without ventriculomegally secondary to HIV-associated cryptococcal meningitis. Surg Neurol. 2005; 63:529-531.
10. Bach MC, Tally PW, Godofsky EW. Use of cerebrospinal fluid shunts in patients having acquired immunodeficiency syndrome with cryptococcal meningitis and uncontrollable intracranial hypertension. Neurosurgery. 1997; 41:1280-1283.
11. Liliang PC, Liang CL, Chang WN, Lu K, Lu CH. Cryptococcal meningitis with uncontrollable intracranial hypertension in HIV-negative patients: Use of ventriculoperitoneal shunts in patients without hydrocephalus. Clin Infect Dis. 2002; 34:e64-68.
12. Fessler RD, Sobel J, Guyot L, Crane L, Vazquez J, Szuba MJ, Diaz FJ. Management of elevated intracranial pressure in patients with cryptococcal meningitis. J Acquir Immune Defic Syndr. 1998; 17:132-142.

(Received June 24, 2014 ; Revised November 11, 2014 ; Accepted December 13, 2014)

Original Article

DOI: 10.5582/bst.2014.01120

Adjuvant sorafenib reduced mortality and prolonged overall survival and post-recurrence survival in hepatocellular carcinoma patients after curative resection: A single-center experience

Wei Zhang*, Gang Zhao*, Kai Wei*, Qingxiang Zhang, Weiwei Ma, Tianqiang Song, Qiang Wu, Ti Zhang, Dalu Kong, Qiang Li**

Department of Hepatobiliary Cancer, Tianjin Medical University Cancer Institute and Hospital, National Clinical Research Center for Cancer and Key Laboratory of Cancer Prevention and Therapy, Tianjin

Summary **Adjuvant therapy after resection of hepatocellular carcinoma (HCC) is limited. Here, we evaluated the effects of postoperative sorafenib on recurrence and survival in HCC patients. Recurrence-free survival and overall survival were analyzed as the main endpoint, recurrence rate, and mortality rate were analyzed as second endpoint. Furthermore, post-recurrence survival was also analyzed. Clinicopathological factors were compared between sorafenib and control groups. Seventy-eight patients were eligible for final data analysis (46 in control group; 32 in sorafenib group). Sorafenib did not significantly prolong recurrence-free survival (11.0 months in the control group *vs*. 11.7 months in the sorafenib group, $p = 0.702$), but significantly prolonged overall survival (32.4 *vs*. 25.0 months, $p = 0.046$). Sorafenib did not reduce recurrence rate (67.7% *vs*. 78.3%, $p = 0.737$), but significantly reduced mortality rate (28.1% *vs*. 60.9%, $p = 0.004$). The increased post-recurrence survival (22.2 *vs*. 4.4 months, $p = 0.003$) may have contributed to the survival benefit after recurrence in the sorafenib group. Adjuvant sorafenib did not decrease tumor recurrence, but significantly reduced mortality and prolonged overall survival of HCC patients after curative resection, probably by inhibiting tumor growth after tumor recurrence.**

Keywords: Hepatocellular carcinoma, resection, sorafenib

1. Introduction

Hepatocellular carcinoma (HCC) is a leading cause of cancer-related death worldwide and the most deadly cancer in China (*1*), and its incidence continues to increase, especially in North America (*2,3*). Surgery, tumor ablation, and liver transplantation are the main potentially curative treatments for HCC. However, tumor recurrence rate is very high after liver resection and tumor ablation, which is a major problem affecting long term survival (*4,5*). Various postoperative interventions, such as adjuvant therapy with interferon, Vitamin E or K2, or I^{131}, are used to reduce the incidence of tumor recurrence after curative treatment (*6,7*). The adjuvant application of interferon (*7-10*) and antiviral treatment (*11,12*) seems promising but should be confirmed in further multi-center phase III clinical trials.

Sorafenib is an oral, multitargeted inhibitor of tyrosine kinases (such as the vascular endothelial growth factor receptor, Raf kinase, and the platelet-derived growth factor receptor), and it has been shown to inhibit tumor angiogenesis and to induce apoptosis of HCC tumor cells (*13*). Two independent randomized Phase III clinical trials showed that sorafenib was the only effective systemic drug to improve survival in patients with advanced HCC (*14,15*). Furthermore, sorafenib is reported to be well tolerated and safe in patients who received liver transplantation and is associated with a survival benefit (*16-18*). In a

*These authors contributed equally to this works.
***Address correspondence to:*
Dr. Tianqiang Song, Department of Hepatobiliary Surgery, Tianjin Medical University Cancer Institute and Hospital, National Clinical Research Center for Cancer, Key Laboratory of Cancer Prevention and Therapy, 24 Bin Shui Road, Hexi District, Tianjin 300060, China.
E-mail: tjchi@hotmail.com

randomised controlled phase III clinical trial (STORM), sorafenib was administrated to patients with a median-high risk of recurrence, the clinical trial is still ongoing and waiting for final results (*19*). Recently, a retrospective study with 31 patients using sorafenib as an adjuvant therapy after liver resection for HCC showed that time to recurrence in the sorafenib arm was significantly prolonged (by 8 months) compared to that in the control arm (*20*). However, because of the small sample size in this study, the effects of sorafenib in the adjuvant setting remain unclear.

Here, we describe our preliminary results regarding the efficacy of adjuvant sorafenib after liver resection for patients with hepatocellular carcinoma.

2. Materials and Methods

2.1. *Patients and follow-up*

This study was a single-institutional retrospective analysis of the effects of sorafenib in patients with HCC after curative resection. Between August 1, 2009, and December 31, 2011, 248 cases of HCC received liver resection. HCC was diagnosed by two independent pathologists (Cao WF and Zhan ZL). Curative resection was defined as complete removal of tumor without residual tumor by microscopy and free of tumor within one month after operation. One hundred and sixty-two patients without microvessel invasion were regarded as low-risk for recurrence and were excluded; and 8 patients with tumor thrombosis in the main trunk of the portal vein were regarded as un-curative resection and were also excluded. Among 78 patients who were eligible for the final analysis, 32 patients received sorafenib treatment after hepatectomy within one month after hepatectomy and 46 patients who did not receive adjuvant sorafenib treatment were included in the control group. The protocol for adjuvant sorafenib treatment has been approved by the Ethics Committee of Tianjin Medical University Cancer Hospital.

Relevant clinical data, including medical history, demographic data, laboratory results, tumor characteristics, and follow-up data were recorded prospectively. The primary end points were recurrence-free survival (RFS) and overall survival (OS); the secondary end points were recurrence rate and mortality rate; and another end point was post-recurrence survival. After operation, patients were followed up in our clinic every 1-2 months for routine blood tests, liver function tests, tumor markers including AFP and ultrasound for the first year, and every 3 months one year after operation. If recurrence was suspected, enhanced magnetic resonance imaging or computed tomography scan was performed immediately. If recurrence was confirmed, surgical resection, radiofrequency ablation or trans-arterial remobilization were given to the patients accordingly.

2.2. *Clinicopathological factors*

Clinicopathological factors in this study were selected for their potential relationship to the prognosis on the basis of the previous studies, including age (< 54 or ≥ 54 years, mean age = 54 years), gender (male or female), tumor size (< 5 cm or ≥ 5 cm), number of tumor nodules (single or multiple), microvascular invasion (yes or no), intrahepatic metastasis (yes or no), tumor differentiation (Edmondson's classification I or II was classified into the high-differentiation group, and classification III or IV was classified into the low-differentiation group), portal vein thrombosis (PVTT) is defined as direct invasion of a second branch of portal vein. Invasion of main portal vein or main trunks of portal vein were excluded.

2.3. *Sorafenib treatment and evaluation*

All the patients in the sorafenib (Bayer Healthcare, Leverkusen, Germany) group received an initial dosage of 400 mg twice daily continuously, except in cases in which the drug was discontinued owing to death, tumor progression, or adverse effects such as deterioration of liver function. Blood pressure, coagulation function, hematological parameters and CT scan were monitored every month. If adverse events classified as CTCAE-3 or higher occurred, the dosage of sorafenib was reduced or administration of sorafenib was withdrawn.

2.4. *Statistical analysis*

Survival analysis was computed by the Kaplan-Meier method and the log-rank test for univariate analysis, and Cox regression was used for multivariate analysis. Overall survival (OS) was calculated from the date of surgery to the date of death or the last follow-up. Recurrence-free survival (RFS) was calculated from the date of surgery to the date of recurrence or the last follow-up. Post-recurrence survival was calculated from the date of first recurrence to the date of death or the last follow-up. The χ^2 test, Fisher's exact probability, and Student's *t* test were used for comparisons between groups. Statistical analyses were performed with SPSS 16.0 for Windows (SPSS Inc., Chicago, IL). Two-tailed $p < 0.05$ was considered to indicate a statistically significant difference.

3. Results

3.1. *Patient demographics and tumor characteristics*

Table 1 shows the demographic data and tumor characteristics for all the patients. Median age was 54 years (range 21 to 81 years), and the age of patients in the sorafenib group were similar to that of patients in the control group (54.5 ± 1.6 *vs*. 51.7 ± 1.4, $p = 0.224$).

The male/female ratio was 42:4 in the control group versus 25:7 in the sorafenib group. All the patients had good Eastern Cooperative Oncology Group performance status scores (0-1) before commencement of sorafenib therapy, and the liver function of all the patients was classified as Child-Pugh A. Patients in the sorafenib group have similar tumor size compared to than of patients in the control group (5.7 ± 0.6 cm *vs*. 7.7 ± 0.8, $p = 0.064$). Multiple tumors were present in 18 of 46 patients in the control group and in 11 of 32 patients in the sorafenib group ($p = 0.669$). Portal vein thrombosis was present in 12 of 46 patents in the control group, whereas 8 of 32 patients in the sorafenib group had portal vein thrombosis ($p = 0.914$). Tumor differentiation was low (Edmondson III or IV) in 16 patients in the control group and 7 patients in the sorafenib group ($p = 0.536$) (Table 1). Major resection (≥ 3 segments) was performed in 16 of 46 patients in control group and in 11 of 32 patients in sorafenib group (34.8% *vs*. 34.4%, $p = 0.97$).

Table 1. Patient demographics and tumor characteristics at baseline

Demographic or characteristic	Control ($n = 46$)	Sorafenib ($n = 32$)	p-value
Gender (male/female)	42/4	25/7	0.100
Age, years (mean ± S.D.)	54.5 ± 1.6	51.7 ± 1.4	0.224
Age (< 54 years/ ≥ 54 years)	21/25	15/17	0.915
Hepatitis status (HBV/non-HBV)	38/8	28/4	0.912
Tumor size (cm, mean ± S.D.)	7.7 ± 0.8	5.7 ± 0.6	0.064
Tumor size (< 5 cm/ ≥ 5 cm)	17/29	15/17	0.381
AFP (< 20/ ≥ 20 ng/mL)	22/24	16/16	0.850
No. of tumors (single/multiple)	28/18	21/11	0.669
Portal vein thrombosis (yes/no)	12/34	8/24	0.914
Tumor differentiation (high/low)	30/16	25/7	0.536
Intrahepatic metastasis (yes/no)	26/20	17/15	0.767
TNM stage (II/III)	26/20	22/10	0.275
Recurrence (yes/no)	36/10	24/8	0.737
Death (yes/no)	28/18	9/23	0.004

Abbreviations: HBV, hepatitis B virus; SD, standard deviation; TNM, tumor-node-metastasis.

3.2. *Treatment efficacy*

Sorafenib significantly prolonged OS: the 1-, 2-, and 3-year OS rates were 79.8%, 68.1%, and 45.4% for the sorafenib group and 60.9%, 52.2%, and 38.0% for the control group. Median OS was 25.0 months (95% CI: 7.3-42.7 months) in the control group and 32.4 months (95% CI: 24.3-40.5 months) in the sorafenib group, and the difference was statistically significant ($p = 0.046$, Figure 1A).

Sorafenib did not prolong RFS: the 1-, 2-, and 3-year RFS percentages were 46.9%, 25.2%, and 18.9% for the

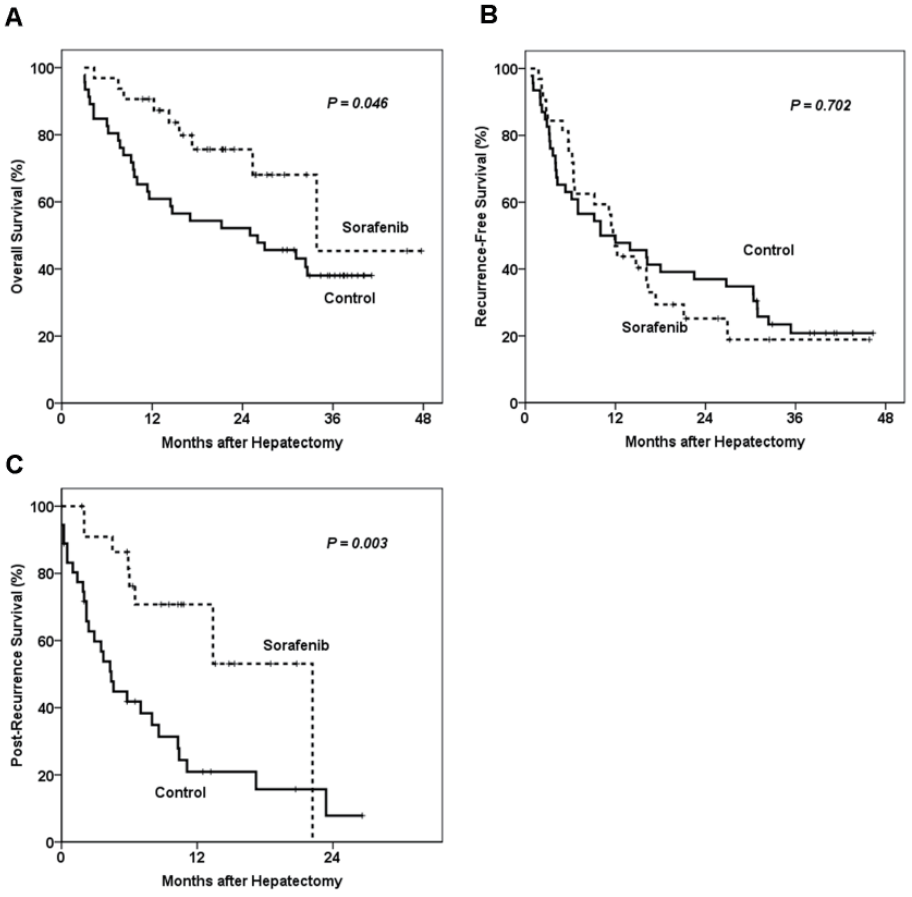

Figure 1. The effects of adjuvant sorafenib on RFS, OS and post-recurrence survival. (A) Overall survival, **(B)** Recurrence-free survival, and **(C)** Post-Recurrence Survival of HCC patients treated with adjuvant sorafenib after curative resection.

Table 2. Univariate and multivariate analysis for Overall Survival (OS) and Recurrence-Free Survival (RFS)

Factors	OS				RFS			
	Univariate *p*	Multivariate			Univariate *p*	Multivariate		
		HR	95% CI	*p*		HR	95% CI	*p*
Sorafenib	0.046	0.490	0.224-1.071	0.074*	0.702			
Gender (male/female)	0.432				0.816			
Age (< 54 years/ ≥ 54 years)	0.722				0.823			
Tumor size (< 5 cm/ > 5 cm)	0.576				0.734			
AFP (< 20 *vs*. ≥ 20)	0.631				0.604			
No. of tumors (single/multiple)	0.173	1.358	0.637-2.893	0.428	0.063	1.871	1.045-3.349	0.035
Portal vein thrombosis (yes/no)	0.106	1.533	0.561-4.193	0.405	0.022	2.601	1.119-6.049	0.026
Tumor differentiation (high/low)	0.284				0.628			
Intrahepatic metastasis (yes/no)	0.071	1.550	0.761-3.154	0.227	0.209			
TNM stage (II/III)	0.051	1.037	0.371-2.895	0.945	0.155	0.655	0.287-1.492	0.314

HR, hazard ratio; TNM, tumor-node-metastasis; CI, confidence interval; *, $p = 0.040$ if forward stepwise (likelihood ration) is used in the COX analysis.

sorafenib group and 47.8%, 37.0%, and 20.8% for the control group. Median RFS was 11.0 months (95% CI: 1.5-20.1 months) in the control group and 11.7 months (95% CI: 10.1-13.2 months) in the sorafenib group ($p = 0.702$, Figure 1B).

Tumor recurrence occurred in 36 patients (78.3%) in the control group and 24 patients (67.7%) in the sorafenib group ($p = 0.737$); 28 patients (60.9%) died in the control group, compared to 9 patients (28.1%) in the sorafenib group ($p = 0.004$) (Table 1). Recurrent tumor was not significantly different in location, for liver recurrence occurred in 33 of 46 in control group and 22 of 32 in the sorafenib group (71.7% *vs*. 68.8%, $p > 0.05$), and lung metastasis occurred in 3 of 46 in control group and 2 of 32 in sorafenib group (28.3% *vs*. 31.2%, $p > 0.05$).

Post-recurrence survival was significantly longer in the sorafenib group than that in the control group; in the control group, the median post-recurrence survival was 4.4 months (95% CI: 2.9-5.9 months), and in the sorafenib group, the median post-recurrence survival was 22.2 months (95% CI: not reached) ($p = 0.003$, Figure 1C).

Univariate analysis showed that adjuvant sorafenib, multiple tumors, portal vein thrombosis, intrahepatic metastasis and TNM stage III were risk factors for OS, while only adjuvant sorafenib was an independent risk factor of overall survival (HR: 0.490, 95% CI: 0.224-1.071, $p = 0.040$). As for Recurrence Free Survival, univariate analysis showed that multiple tumors, portal vein thrombosis and TNM stage III were risk factors, however, only multiple tumors (HR = 1.871, 96% CI: 1.045-3.349, $p = 0.035$) and portal vein thrombosis (HR = 2.601, 95% CI: 1.119-6.049, $p = 0.026$) were independent risk factors (Table 2).

3.3. *Patients' adherence and tolerability for sorafenib treatment*

All the patients had good adherence in both the sorafenib group and control group. Grade 3 adverse effects occurred in 6 patients with sorafenib treatment but with a reduction to half dosage, all the patients recovered and 4 patients received full dose again. None of the patients withdrew sorafenib treatment

4. Discussion

The results of the current study showed that sorafenib neither reduced recurrence rate nor prolonged RFS. However, sorafenib reduced mortality rate and prolonged overall survival; furthermore, sorafenib prolonged post-recurrence survival, perhaps because the recurrent tumors that developed after sorafenib treatment progressed more slowly.

Sorafenib has two main types of effects: an anti-angiogenic and a direct antitumoral effect (*13*). Tumor angiogenesis occurs only after a tumor grows to a certain minimum size (*e.g.*, 1 cm) (*21*), and anti-angiogenic agents are mostly tumor-static agents, that is, they retard tumor growth rather than reduce tumor size (*22*). Therefore, the anti-angiogenic effect of sorafenib can be expected to play a role only when a tumor is sufficiently large, and sorafenib is unlikely to decrease tumor growth before tumor recurrence. It has been reported that sorafenib delays the progression of recurrent tumors following liver transplantation, and this delay is associated with a survival benefit (*6*). Wang *et al*. found that in two cohorts of patients ($n = 39$ patients, 24 of whom received best supportive care and 15 of whom received sorafenib) who presented with HCC recurrence after liver transplantation, patients' outcome in the sorafenib group was significantly better than that in the other group, with a median survival from recurrence of 21.3 vs. 11.8 months (HR = 5.2, $p = 0.0009$), and a median survival from untreatable presentation/progression of 10.6 vs. 2.2 months (HR = 21.1, $p < 0.0001$).

Resistance to anti-angiogenic therapy is common, and some tumors possess intrinsic mechanisms of resistance to sorafenib (*23*). Despite the success of sorafenib in the treatment of some patients with

advanced HCC (*24*), most such patients do not respond to sorafenib, and some patients who initially respond subsequently develop resistance and experience tumor progression (*25*). Sorafenib also directly targets tumor cells, but perhaps only tumor cells with a specific activated signaling pathway and the drug may thus exert its direct effects only in patients whose tumors exhibit that specific molecular pathway. Molecular markers may be useful for predicting the efficacy of sorafenib. Specifically, mitogen-activated protein kinase and signal transducer and activator of transcription 3 are known targets of sorafenib in HCC (*26*), but the prognostic value of these markers has not yet been confirmed. Results obtained in a mouse model indicate that the efficacy of sorafenib against HCC may depend on the level of expression of HIV-1 Tat interactive protein 2 (HTATIP2) in tumors (*27*).

Meanwhile, factors in the tumor and host microenvironment should also have been considered in the resistance of sorafenib, for studies have shown that progression-free survival under sorafenib treatment is significantly shorter in patients with high levels of angiogenin-2 (Ang-2) and granulocyte colony-stimulating factor (G-CSF), and that as the number of cytokines present at high concentrations increases, the treatment response deteriorates (*28*). Short-term and high-dose sorafenib treatment is associated with decreased survival in multiple preclinical animal models (*29,30*). Thus, molecular markers in serum and in tumor tissue will be of prognostic value and may permit prediction of the efficacy of sorafenib.

The current study has several limitations. First, it was a retrospective study, and the cases included in the control and treatment groups were not randomized. Second, the sample size was small. Randomized controlled clinical trials should be carried out to confirm the present findings in a larger population. Finally, molecular prediction of efficacy of sorafenib should be emphasized, and a molecular classification of HCC based on genome-wide investigations and identification of patient subclasses according to drug responsiveness will lead to a more personalized medicine.

In conclusion, adjuvant sorafenib did not decrease tumor recurrence, but significantly reduced mortality and prolonged overall survival of HCC patients after curative resection, probably by inhibiting tumor growth and prolonging post-recurrence survival after tumor recurrence. Randomized controlled clinical trials with specific emphasis on molecular markers are needed for selecting optimal candidates for sorafenib treatment and prediction of its efficacy.

Acknowledgements

This project was supported by a grant from the National Natural Science Foundation of China (No. 81101871 & No.81372635), a grant from Tianjin Municipal Science and Technology Commission (TSTC, No.14JCYBJC25200), and by a grant from Major Program of National Natural Science Foundation of Tianjin (No. 11JCZDJC18800). Program for New Century Excellent Talents of Tianjin Medical University Cancer Hospital.

References

1. Zeng H, Zheng R, Guo Y, *et al*. Cancer survival in China, 2003-2005: A population-based study. Int J Cancer. 2014. doi:10.1002/ijc.29227
2. Jemal A, Bray F, Center MM, Ferlay J, Ward E, Forman D. Global cancer statistics. CA Cancer J Clin. 2011; 61:69-90.
3. Siegel R, Ma J, Zou Z, Jemal A. Cancer statistics, 2014. CA Cancer J Clin. 2014; 64:9-29.
4. Tang ZY. Hepatocellular carcinoma surgery--review of the past and prospects for the 21st century. J Surg Oncol. 2005; 91:95-96.
5. Fan ST, Mau Lo C, Poon RT, Yeung C, Leung Liu C, Yuen WK, Ming Lam C, Ng KK, Ching Chan S. Continuous improvement of survival outcomes of resection of hepatocellular carcinoma: A 20-year experience. Ann Surg. 2011; 253:745-758.
6. Zhong JH, Li H, Li LQ, You XM, Zhang Y, Zhao YN, Liu JY, Xiang BD, Wu GB. Adjuvant therapy options following curative treatment of hepatocellular carcinoma: A systematic review of randomized trials. Eur J Surg Oncol. 2012; 38:286-295.
7. Sun HC, Tang ZY, Wang L, Qin LX, Ma ZC, Ye QH, Zhang BH, Qian YB, Wu ZQ, Fan J, Zhou XD, Zhou J, Qiu SJ, Shen YF. Postoperative interferon α treatment postponed recurrence and improved overall survival in patients after curative resection of HBV-related hepatocellular carcinoma: A randomized clinical trial. J Cancer Res Clin Oncol. 2006; 132:458-465.
8. Lo CM, Liu CL, Chan SC, Lam CM, Poon RT, Ng IO, Fan ST, Wong J. A randomized, controlled trial of postoperative adjuvant interferon therapy after resection of hepatocellular carcinoma. Ann Surg. 2007; 245:831-842.
9. Chen LT, Chen MF, Li LA, *et al*. Long-term results of a randomized, observation-controlled, phase III trial of adjuvant interferon Alfa-2b in hepatocellular carcinoma after curative resection. Ann Surg. 2012; 255:8-17.
10. Clavien PA. Interferon: The magic bullet to prevent hepatocellular carcinoma recurrence after resection? Ann Surg. 2007; 245:843-845.
11. Huang G, Lau WY, Wang ZG, Pan ZY, Yuan SX, Shen F, Zhou WP, Wu MC. Antiviral therapy improves postoperative survival in patients with hepatocellular carcinoma: A randomized controlled trial. Ann Surg. 2014. PMID:25072444.
12. Sun HC, Zhang W, Qin LX, Zhang BH, Ye QH, Wang L, Ren N, Zhuang PY, Zhu XD, Fan J, Tang ZY. Positive serum hepatitis B e antigen is associated with higher risk of early recurrence and poorer survival in patients after curative resection of hepatitis B-related hepatocellular carcinoma. J Hepatol. 2007; 47:684-690.
13. Liu L, Cao Y, Chen C, Zhang X, McNabola A, Wilkie D, Wilhelm S, Lynch M, Carter C. Sorafenib blocks the RAF/MEK/ERK pathway, inhibits tumor angiogenesis,

and induces tumor cell apoptosis in hepatocellular carcinoma model PLC/PRF/5. Cancer Res. 2006; 66:11851-11858.
14. Cheng AL, Kang YK, Chen Z, *et al*. Efficacy and safety of sorafenib in patients in the Asia-Pacific region with advanced hepatocellular carcinoma: A phase III randomised, double-blind, placebo-controlled trial. Lancet Oncol. 2009; 10:25-34.
15. Llovet JM, Ricci S, Mazzaferro V, *et al*. Sorafenib in advanced hepatocellular carcinoma. N Engl J Med. 2008; 359:378-390.
16. Waghray A, Balci B, El-Gazzaz G, Kim R, Pelley R, Narayanan Menon KV, Estfan B, Romero-Marrero C, Aucejo F. Safety and efficacy of sorafenib for the treatment of recurrent hepatocellular carcinoma after liver transplantation. Clin Transplant. 2013; 27:555-561.
17. Saab S, McTigue M, Finn RS, Busuttil RW. Sorafenib as adjuvant therapy for high-risk hepatocellular carcinoma in liver transplant recipients: Feasibility and efficacy. Exp Clin Transplant. 2010; 8:307-313.
18. Shetty K, Dash C, Laurin J. Use of adjuvant sorafenib in liver transplant recipients with high-risk hepatocellular carcinoma. J Transplant. 2014; 2014:913634.
19. Printz C. Clinical trials of note. Sorafenib as adjuvant treatment in the prevention of disease recurrence in patients with hepatocellular carcinoma (HCC) (STORM). Cancer. 2009; 115:4646.
20. Wang SN, Chuang SC, Lee KT. Efficacy of sorafenib as adjuvant therapy to prevent early recurrence of hepatocellular carcinoma after curative surgery: A pilot study. Hepatol Res. 2014; 44:523-531.
21. Folkman J. Tumor angiogenesis and tissue factor. Nat Med. 1996; 2:167-168.
22. Lencioni R, Llovet JM. Modified RECIST (mRECIST) assessment for hepatocellular carcinoma. Semin Liver Dis. 2010; 30:52-60.
23. Bergers G, Hanahan D. Modes of resistance to anti-angiogenic therapy. Nat Rev Cancer. 2008; 8:592-603.
24. Bruix J, Raoul JL, Sherman M, *et al*. Efficacy and safety of sorafenib in patients with advanced hepatocellular carcinoma: Sub-analyses of a phase III trial. J Hepatol. 2012; 57:821-829.
25. Villanueva A, Llovet JM. Targeted therapies for hepatocellular carcinoma. Gastroenterology. 2011; 140:1410-1426.
26. Tai WT, Cheng AL, Shiau CW, Huang HP, Huang JW, Chen PJ, Chen KF. Signal transducer and activator of transcription 3 is a major kinase-independent target of sorafenib in hepatocellular carcinoma. J Hepatol. 2011; 55:1041-1048.
27. Zhang W, Sun HC, Wang WQ, Zhang QB, Zhuang PY, Xiong YQ, Zhu XD, Xu HX, Kong LQ, Wu WZ, Wang L, Song TQ, Li Q, Tang ZY. Sorafenib down-regulates expression of HTATIP2 to promote invasiveness and metastasis of orthotopic hepatocellular carcinoma tumors in mice. Gastroenterology. 2012; 143:1641-1649 e5.
28. Llovet JM, Bruix J. Molecular targeted therapies in hepatocellular carcinoma. Hepatology. 2008; 48:1312-1327.
29. Ebos JM, Mastri M, Lee CR, Tracz A, Hudson JM, Attwood K, Cruz-Munoz WR, Jedeszko C, Burns P, Kerbel RS. Neoadjuvant antiangiogenic therapy reveals contrasts in primary and metastatic tumor efficacy. EMBO Mol Med. 2014; 6:1561-1576.
30. Ebos JM, Kerbel RS. Antiangiogenic therapy: Impact on invasion, disease progression, and metastasis. Nat Rev Clin Oncol. 2014; 8:210-221.

(Received November 4, 2014; Revised November 8, 2014; Accepted December 17, 2014)

Original Article

DOI: 10.5582/bst.2014.01101

Telaprevir-based triple therapy for hepatitis C null responders among living donor liver transplant recipients

Junichi Kaneko[1], Yasuhiko Sugawara[1,*], Takamune Yamaguchi[1], Nobuhiro Harada[1], Nobuhisa Akamatsu[1], Takeaki Ishizawa[1], Taku Aoki[1], Yoshihiro Sakamoto[1], Kiyoshi Hasegawa[1], Sumihito Tamura[1], Tomohiro Tanaka[2], Norihiro Kokudo[1]

[1] *Division of Artificial Organ and Transplantation, Department of Surgery, The University of Tokyo, Tokyo, Japan;*
[2] *Organ Transplantation Service, The University of Tokyo, Tokyo, Japan.*

Summary **Telaprevir (TVR), a direct -acting protease inhibitor, was recently reported to improve treatment efficacy when used in combination with peg-interferon (PEG-IFN) and ribavirin (RBV) as triple therapy for HCV in non-transplant patients. The aim of the present study was to investigate the feasibility of TVR-based triple therapy among Japanese living donor liver transplant (LDLT) recipients who had been resistant to dual treatment with PEG-IFN and RBV. Among 133 HCV-positive LDLT recipients, 8 null responders during or after dual treatment with PEG-IFN and RBV were finally indicated for TVR-based triple therapy after treatment. All 8 patients had been resistant to dual treatment with PEG-IFN and RBV. While the cyclosporine trough level was well controlled with an 80% dose reduction during TVR administration, the end - of - treatment response rate was only 25% (2/8), with 63% (5/8) of patients developing anemia that required a blood transfusion and 50% (4/8) of patients developing leukopenia that required filgrastim. Dose reduction or treatment discontinuation was required in all cases. Based on the poor efficacy and the unacceptable high rate of cytopenic events, TVR-based triple therapy is not indicated for those resistant to dual treatment with PEG-IFN and RBV.**

Keywords: Hepatitis C, Telaprevir, living donor liver transplantation, Japanese, null responder

1. Introduction

Hepatitis C virus (HCV) infection is the leading indication for liver transplantation in both Western countries and Japan. Unfortunately, liver transplantation does not cure HCV-infected recipients, and re-infection of HCV universally occurs with accelerated disease progression compared with that in the nontransplant population, resulting in poor outcomes for HCV-infected recipients. Graft and patient survival could be improved with successful antiviral treatment, but the efficacy of the standard antiviral treatment with peginterferon (PEG-IFN) and ribavirin (RBV) is unsatisfactory and poorly tolerated for recurrent hepatitis C in the posttransplant setting compared with nontransplant patients, with sustained virologic response (SVR) rates ranging from 0% to 56% (median: 33%) (*1*).

Telaprevir (TVR), a direct acting protease inhibitor, was recently approved for clinical use, and the administration of TVR in combination with PEG-IFN/RBV substantially improves SVR rates in comparison with standard treatment using PEG-IFN/RBV in nontransplant HCV-positive patients, including treatment-naïve patients, null-responders to previous treatment, and even relapsers after previous treatment. Triple combination therapy with TVR/PEG-IFN/RBV is now a standard treatment for patients with genotype 1 chronic hepatitis C (HCV) (*2*).

Validation of the triple therapy for recurrent hepatitis C after liver transplantation is urgently needed, but there are significant concerns regarding the safety and efficacy of TVR administration for posttransplant

**Address correspondence to:*
Dr. Yasuhiko Sugawara, Artificial Organ and Transplantation Division, Department of Surgery, Graduate School of Medicine, University of Tokyo, 7-3-1 Hongo, Bunkyo-ku, Tokyo 113-8655, Japan.
E-mail: yasusugatky@yahoo.co.jp

recipients due to the severe side effects and potentially strong drug-drug interaction with calcineurin inhibitors (CNI). Several preliminary reports regarding triple therapy for deceased donor liver transplantation (DDLT) in Western countries were recently published (*3,4*). However, efficacy and safety was not well describe in a living donor liver transplant (LDLT) setting in an Japanese population (*5*). Here we report the preliminary experience of TVR-based triple therapy in Japanese living donor liver transplant recipients who had been resistant to dual treatment with PEG-IFN and RBV.

2. Patients and Methods

Between January 1996 and July 2013, 133 adult-to-adult LDLTs were performed for HCV-positive recipients at the University of Tokyo Hospital. The transplantation procedures, including donor selection criteria, surgical procedures, and postoperative management, are described elsewhere (*6*). As previously reported (*7*), preemptive PEG-IFN /RBV treatment was administered for 119 of our 133 HCV-positive LDLT recipients, excluding cases of early death (within 3 months) after LDLT ($n = 4$), cases with spontaneous SVR ($n = 5$), and cases without antiviral treatment due to clinical decision ($n = 5$). Briefly, preemptive treatment was initiated just after the recipient's condition stabilized (approximately 1 month after LDLT) with low-dose IFN alpha 2b and RBV (400 mg/day), followed by escalation to PEG-IFN (1.5 μg/kg per week) and RBV (800 mg/day) depending on the patient's tolerance. The treatment duration was not predetermined, and continued for 12 months more after the serum HCV-RNA became negative. The response was considered to be SVR if the serologic results were negative for another 6 months after therapy was discontinued. That is, a continuous peg-IFN/RBV approach was applied for null-responders. SVR was achieved in 42 patients, and 27 patients discontinued preemptive treatment due to patient death, clinical reasons, intolerance, or refusal of treatment.

2.1. *Patient selection for triple therapy*

Inclusion criteria for TVR-based triple therapy in this study were null responders during or after the preemptive treatment described above. Consequently, candidates for triple therapy had already undergone our preemptive antiviral treatment regimen for at least 12 months, except for 2 patients: 1 with early recurrent hepatitis C and high aspartate transaminase and alanine transaminase levels during preemptive treatment at 5 months after liver transplantation, and the other with fibrosing cholestatic hepatitis during preemptive treatment at 2 months after liver transplantation. Patient selection is shown in the flowchart in Figure 1. A total of 8 patients (6 men, 2 women) were enrolled in this study. The study protocol was approved by the

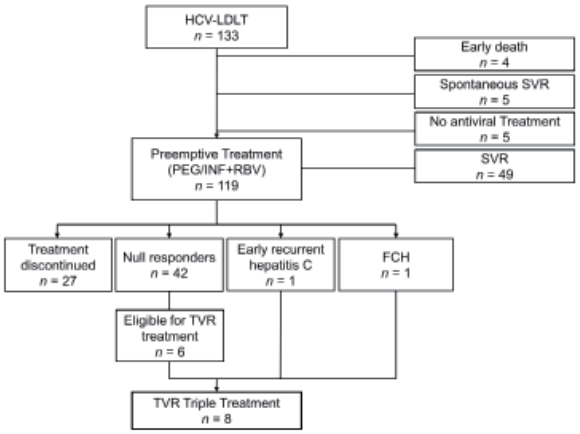

Figure 1. Flow diagram of the patients enrolled in the Telaprevir (TVR)-based triple therapy. Abbreviations: HCV-LDLT, living donor liver transplantation for hepatitis C; SVR, sustained virological response; PEG/INF, peginterferon; RBV, ribavirin; FCH, fibrosing cholestatic hepatitis.

University of Tokyo Ethics Committee (No. 2140) and registered in the UMIN-clinical trials registry (UMIN000013628, *https://center.umin.ac.jp/ctr/index.htm*). Informed consent was obtained from all patients. The follow-up period was 13 month in all participants.

2.2. *The triple therapy regimen and immunosuppression*

The protocol for TVR-based triple therapy comprised TVR (Telaprevir, Mitsubishi Tanabe Pharma Corp. Osaka, Japan), PEG-IFN (Pegintron, peginterferon Alfa-2b, MSD K.K., Tokyo, Japan), and RBV (Rebetol, MSD K.K.) for 12 weeks without a lead-in phase. After triple therapy for 12 months, treatment with PEG-IFN/RBV was continued for at least 36 weeks more, and even further in cases without viral eradication. TVR was administered orally at 1,000 to 1,500 mg/day, PEG-IFN was administered subcutaneously at 0.8 to 1.7 μg/kg/week, and RBV was administered orally at 200 mg/day. Dose adjustments were made based on patient tolerance, side effects, and laboratory results.

Our regimen for postoperative immunosuppression is described in detail elsewhere (*8*). Basically, dual immunosuppression with tacrolimus and methylprednisolone was used, and conversion from tacrolimus to cyclosporine (CsA) was performed without delay if patients developed adverse events due to tacrolimus (*9*). Considering the strong drug-drug interaction between TVR and CNI (*10*), especially tacrolimus, tacrolimus was converted to CsA before initiating the triple therapy in all cases, and all patients were admitted to the hospital for 7 to 14 days to measure blood trough levels of CsA and to adjust the CsA dose. On the first day of triple therapy, the CsA dose was reduced to 20% of the original daily dose, and adjusted according to therapeutic monitoring. Close monitoring with daily measurement of the trough levels of CsA was performed during hospitalization, and once a week for

12 weeks at the outpatient clinic. After the completion of TVR, the original daily dose of CsA was resumed.

2.3. *Monitoring for hepatitis C virus and adverse events*

The HCV genotype was determined before liver transplantation. The nucleotide sequences of the core and non-structural 5A (NS5A) regions of genotype 1b were determined using a direct sequencing method, as described previously (*11*). The interleukin 28B (IL28B) genotype was examined using the Invader assay (Third Wave Technologies, Madison, WI, USA) (*12*). Liver biopsy was performed before initiating the triple therapy and evaluated by a pathologist according to the Ishak score for assessing the stage of fibrosis and the degree of necroinflammatory activity (*13*). HCV-RNA was measured by reverse-transcriptase polymerase chain reaction (TaqMan HCV; Roche Diagnostics Japan K.K., Tokyo, Japan) before starting the treatment and monthly after that. Serum HCV-RNA was considered negative when the results were below the lower limit of quantification (15 IU/mL).

After initiating the triple therapy, blood counts, and liver and renal function were examined every day during admission, and once a week for 12 weeks until the end of TVR administration. Thereafter, these were measured every 4 weeks. The estimated glomerular filtration rate (eGFR; mL/min/1.73 m^2) was calculated using the following formula: 194 × serum creatinine (– 1.094) × age (– 0.287) × 0.739 (if female), Japanese equation (equation 4) (*14*).

Filgrastim (75 μg; Gran, Kyowa Hakko Kirin Co., Ltd., Tokyo, Japan) was administered subcutaneously to patients with neutrophil counts below 1,000/mm^3. Packed red blood cell transfusion was performed when the hemoglobin level dropped below 8 g/dL.

2.4. *Ethics statement*

All LDLTs were performed after individually obtaining informed consent from recipients and donors. LDLT program at The University of Tokyo Hospital has been approved by it's Institutional Review Board, and all aspects of the procedures have been conducted according to the principles expressed in the Declaration of Helsinki. The current human subject research was approved as project number G3515 by Graduate School of Medicine and Faculty of Medicine, the University of Tokyo Research Ethics Committee and Human Genome, Gene Analysis Research Ethics Committee. All subjects have been properly instructed and participated by signing the appropriate informed consent paperwork. In the preparation of this manuscript, all efforts have been made to protect patient privacy and anonymity.

2.5. *Statistical analysis*

CsA levels and eGFR before initiating therapy were compared with those at 1 week after initiating the triple therapy by Student's *t* test using GraphPad Prism 5 (GraphPad Software, San Diego, CA, USA). Data are expressed as mean and ± standard deviation (S.D.). A p value less than 0.05 was considered statistically significant.

3. Results

The patient characteristics of the eight recipients are summarized in Table 1. The time from LDLT to initiation of the triple therapy was 4.4 ± 3.6 y. Mean recipient age was 59 ± 5.3 y. The HCV genotype was 1b in all patients except for one with a 2a genotype. All eight patients were null-responders to preemptive treatment. Among them, two patients with early recurrent hepatitis C and fibrosing cholestatic hepatitis were switched to triple therapy during preemptive treatment with conventional dual drugs.

3.1. *Immunosuppressant modification*

Among the eight patients, six had already been converted to CsA before the induction of triple therapy. Consequently, two patients were newly changed from tacrolimus to CsA as a maintenance immunosuppressant before initiating TVR. The CsA trough levels before (81 ± 45 ng/mL) and 1 week after (82 ± 30 ng/mL) initiating the triple treatment did not differ significantly ($p = 0.54$; Table 2). The maintenance dose of CsA after

Table 1. Patient characteristics

Patient No.	Sex	Age	Weight	Time from LT (Y)	Previous treatment	HCV genotype	NS5A	IL-28B polymorphism	Liver biopsy
1	M	56	65	9.5	NR	1b	intermediate	T/C	A2F3
2	M	64	52	7.8	NR	1b	wild	T/C	-
3	F	55	46	0.4	NR	1b	wild	T/C	A1F1
4	M	66	63	6.3	NR	1b	NA	C/C	A1F1
5	M	61	60	4.0	NR	1b	intermediate	T/C	A2F0
6	M	60	59	6.2	NR	1b	NA	T/T	A1F1
7	M	50	63	0.6	NR	1b	mutant	T/T	A1F1
8	F	63	36	0.2	NR	2a	mutant	T/T	A2F0

Abbreviations: LT, liver transplantation; NR, null responder, HCV, hepatitis C virus; NS5A, non-structural 5A; IL-28B, interleukin 28B.

Table 2. Characteristics of the 8 patients during treatment

Patient No.	Pretreatment CsA dose (mg/day)	CsA dose during study (mg/day)	CsA trough level (ng/mL)		MP (mg/d)	MMF (mg/d)	TVR (mg/d)	RBV (mg/d)	PEG-IFN (μg/kg/w)	BT	Filgrastim use	Therapy Discontinue	Infection	eGFR (mL/min/ 1.73 m^2)	eGFR (mL/min/ 1.73 m^2)	HCV-RNA (Log10 IU/mL)			Outcome
			Pre	1w after										pre	end of study	0w	12w	48w	
1	60	10	36	50	-	1500	1500	200	0.8	+	-	13 w	-	32	6	5.3	0.0	6.8	NR
2	60	10	33	49	2	1500	1500	200	1	+	+	13 w	-	42	37	5.5	0.0	7.5	NR
3	100	20	141	116	6	-	1500	200	1.7	+	+	-	-	68	79	6.6	0.0	5.7	NR
4	100	10	74	104	2	-	1500	200	0.8	-	+	-	-	48	52	6.4	1.2	7.0	NR
5	50	10	30	40	3	1500	1000	200	1.4	+	-	6 w	CMV	43	44	6.8	1.2	6.9	NR
6	100	10	92	89	2	1000	1500	200	1.5	-	-	-	pneumonia	44	45	5.4	0.0	0.0	ETR
7	120	20	138	110	6	-	1500	200	1.5	-	-	-	-	62	89	2.7	0.0	7.1	NR
8	120	30	104	94	8	-	1000	200	1.5	+	+	-	CMV	87	28	7.8	3.2	0.0	ETR

Abbreviations: CsA, cyclosporine A; MP, methylprednisolone; MMF, mycophenolate mofetil; TVR, Telaprevir; RBV, ribavirin ; BT, packed red blood cell transfusion; CMV, cytomegalovirus; eGFR, estimated glomerular filtration rate; NR, null responder; ETR, end of treatment response.

the adjustment was 17% (range 10-25%) of the original daily dose (Table 2).

3.2. *Efficacy of the triple treatment*

At 4 weeks after initiating TVR-based triple therapy, all 8 patients had HCV-RNA levels under 200 IU/mL, and HCV-RNA was undetectable in 50% (4/8) of patients showing a rapid virologic response (undetectable serum HCV at 4 weeks after treatment). At the end of the treatment period (48 weeks), 38% (3/8) of patients showed a partial response (> 2 log HCV decrease) and 25% (2/8) of patients had become HCV-negative, achieving the end-of-treatment response, but re-elevation of HCV-RNA titer occurred in 50% (4/8) of the patients during the subsequent dual therapy period. Changes in the HCV-RNA levels in all patients treated with TVR-based triple therapy are shown in Figure 2.

One patient who did not achieve negative-HCV status at all through the treatment period had a C/C IL-28B polymorphism.

One patient (Patient No.8) developed fibrosing cholestatic hepatitis 2.4 months after liver transplantation. The total bilirubin level was 2.6 mg/dl. Liver biopsy revealed no acute rejection, but A2/F0 was noted. After initiating TVR-based triple therapy for this patient, aspartate transaminase, alanine transaminase, and total bilirubin levels returned to the normal range.

3.3. *Tolerance to the treatment and adverse events*

TVR-based triple therapy was discontinued in one patient at 6 weeks due to cytomegalovirus infection. TVR was temporally discontinued in another two patients at 4 and 10 weeks, respectively, due to elevated transaminase levels, and subsequently resumed. PEG-IFN and RBV were discontinued in two patients at 13 weeks due to severe fatigue with anemia. Other adverse events were as follows: requiring PEG-IFN dose reduction, 50% (4/8); leukopenia with filgrastim use, 50% (4/8); anemia with packed red blood cell transfusion, 63% (5/8); symptomatic skin rashes, 13% (1/6); and infectious complications, 38% (3/8).

Figure 2. Changes in HCV-RNA level in all patients treated with the TVR-based triple therapy. Each solid gray to black line represents an individual patient. The dotted line represents the lower limit of quantification (15 IU/mL).

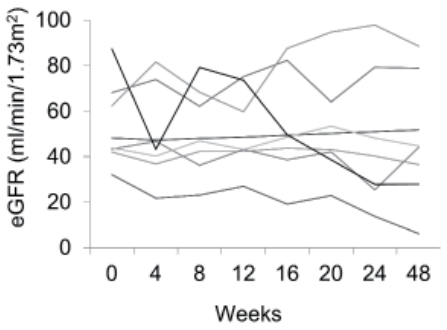

Figure 3. Changes in the estimated glomerular filtration rate (eGFR; mL/min/1.73 m^2) during TVR-based triple therapy. Each solid gray to black line represents an individual patient.

In contrast, we observed no acute rejection, hepatic decompensation, or treatment - related mortality among the eight recipients.

3.4. *Renal function*

In 63% (5/8) of patients, eGFR decreased during the initial 4 weeks, but there was no significant difference between the eGFR level before (53 ± 18 mL/min/1.73 m^2) and at the end (47 ± 27 mL/min/1.73 m^2) of the treatment (p = 0.53). One patient developed end-stage renal disease at end of the study, eventually requiring hemodialysis. Changes in the eGFR during TVR-based triple therapy in each patient are shown in Figure 3.

4. Discussion

The present report describes our initial experience treating recurrent hepatitis C with TVR-based triple therapy in Japanese LDLT recipients. In contrast to several Western reports of the triple therapy demonstrating moderate success for genotype 1 recurrent hepatitis C after DDLT (*3,15,16*), the present results were discouraging, with an end-of-treatment response rate of only 25% (2/8). It is important to note, however, that all eight recipients indicated for the triple therapy in our study had been resistant to standard dual treatment with PEG-IFN and RBV. In the aforementioned Western reports (**3,15,16**), triple therapy was used as the initial antiviral treatment for recurrent disease after liver transplantation. Unlike this report, Ikegami and colleagues reported that 82% of patients achieved SVR after LDLT, however, 18% (2/11) of patients did not have previous IFN treatment history (*5*). Thus, based on the present study: 1) TVR-based triple therapy provided disappointing results for HCV-positive recipients who did not respond to standard dual therapy, 2) TVR-based triple therapy could be performed safely in Japanese LDLT recipients but requires meticulous CNI management and will result in a high incidence of cytopenic events.

Previous reports in a DDLT setting demonstrated the efficacy of TVR-based triple therapy against HCV recurrence after liver transplantation. Pungpapong and colleagues (*15*) reported that 67% (14/21) of patients receiving TVR-based triple therapy achieved undetectable HCV-RNA levels at 24 weeks after finishing treatment without viral breakthrough. Another study described an SVR rate of 56% (5/9) (*17*). Coilly and colleagues (*16*) reported that a complete virologic response was obtained after 12 weeks of TVR-based triple therapy in 58% of patients treated with TVR. The end-of-treatment virologic response rate was 40% (4/10) and 20% (1/5) of the patients achieved an SVR. In the present study, however, only 25% (2/8) of patients achieved HCV-negative status at the end of therapy. Accumulating reports from Western countries in a DDLT setting suggest the efficacy of triple therapy for recurrent hepatitis C with genotype 1b (*3,15,16*), but the present results demonstrated dismal results for non-responders to standard dual therapy. Documented drug-drug interactions with protease inhibitors have raised concerns about the safety of protease inhibitors in the post-transplant setting. In a previous study, TVR increased the area under the blood concentration time-curve of cyclosporine by 4.6-fold, while tacrolimus led to a 70-fold increase (*10*). Hence, we, as other institutions, used cyclosporine rather than tacrolimus because of the relatively fewer drug-drug interactions. A key finding of the present study is that Japanese LDLT recipients could safely be managed with an initial 80% reduction of the CsA dose in adjusting the trough level of CsA during TVR administration. The dose reduction necessary to maintain the same trough level of CsA seems comparable to that recommended in Western DDLT populations (*15*).

As emphasized in other studies using TVR in the treatment of recurrent HCV after liver transplantation (*3,15,16*), the high frequency of hematologic adverse events is a major concern of TVR-based triple therapy, and is higher than that in the non-transplant population and more severe than that in the standard dual treatment among transplant recipients. In our study, 63% (5/8) of patients developed anemia requiring a blood transfusion and 50% (4/8) of patients developed leukopenia requiring filgrastim. The RBV dose was minimized (200 mg/day) from the beginning of the treatment in our protocol. Pungpapong and colleagues (*15*) similarly described that 46% (16/35) of patients required a packed red blood cell transfusion, 77% (27/35) required an erythropoiesis-stimulating agent for anemia, and 17% (6/34) required filgrastim for leukopenia. Accumulating preliminary reports (*15*) confirmed that the dose reductions of PEG- IFN and RBV are universal in triple therapy for posttransplant recipients. Although recent data suggest that the RBV dose can be lowered in nontransplant patients treated with TVR-based triple therapy without a loss of efficacy (*18*), the optimal doses of RBV and PEG- IFN for transplant recipients

under triple therapy requires further study.

Another concern regarding antiviral treatment with TVR is its impact on renal function. Liver transplant recipients have impaired renal function, mainly due to long-term use of CNIs. In this study, the recipients showed impaired renal function with a mean eGFR of 53 mL/min/1.73 m^2 at the beginning of the triple therapy. After initiating TVR-based triple therapy, the eGFR decreased in 63% (5/8) of patients within the first 4 weeks with a mean eGFR of 47 mL/min/1.73 m^2. The pretreatment eGFR and that at the end of TVR-based triple therapy, however, were not significantly different from each other. Similar reversible renal dysfunction during the TVR-based triple therapy was reported by Pungpapong and colleagues (*15*). Because TVR has never been reported to be nephrotoxic in non-transplant setting trials, the renal impairment could be due to changes in CNI pharmacokinetics during triple therapy, despite strict CNI trough level monitoring and dose adjustment.

There are several limitations to our report. First, the main limitation is that treatment was arbitrarily performed for a small number of cases, which makes the data inadequate to support the findings. Second, in addition to the high rate of treatment discontinuation, the dose of TVR and RBV were unacceptably reduced to appropriately assess the efficacy of TVR. Third, none of the patients were naïve for antiviral treatment after transplant but were resistant to the standard dual treatment, making it difficult to compare the findings with those from other studies. In conclusion, we report our preliminary experience of triple therapy with TVR and PEG- IFN /RBV to treat recurrent HCV resistant to the standard dual treatment among Japanese LDLT recipients. The efficacy of TVR-based triple therapy was disappointing, and associated with difficulty controlling CNI trough levels and an unacceptable high rate of cytopenic events. Therefore, we conclude that TVR-based triple therapy is not indicated for those resistant to standard PEG/ IFN and RBV treatment. Recently, simeprevir, a new direct - acting protease inhibitor, was approved for clinical use in both the United States and in Japan. Preliminary reports indicate that simeprevir, when used in association with PEG-IFN /RBV among nontransplant patients, has a more potent effect for achieving SVR with fewer adverse events (*19,20*), and has no drug-drug interaction with CNIs (*21*). Triple therapy for recurrent HCV with simeprevir is currently under investigation in our institution.

References

1. Akamatsu N, Sugawara Y. Liver transplantation and hepatitis C. Int J Hepatol. 2012; 2012:686135.
2. Ghany MG, Nelson DR, Strader DB, Thomas DL, Seeff LB. An update on treatment of genotype 1 chronic hepatitis C virus infection: 2011 practice guideline by the American Association for the Study of Liver Diseases. Hepatology. 2011; 54:1433-1444.
3. Werner CR, Egetemeyr DP, Lauer UM, Nadalin S, Konigsrainer A, Malek NP, Berg CP. Telaprevir-based triple therapy in liver transplant patients with hepatitis C virus: a 12-week pilot study providing safety and efficacy data. Liver Transpl. 2012; 18:1464-1470.
4. Reddy KR, Everson GT. Treatment of chronic hepatitis C with protease inhibitor-based therapy after liver transplantation. Hepatology. 2013; 58:1181-1184.
5. Ikegami T, Yoshizumi T, Kato M, Yamamoto S, Fukuhara T, Matsuura Y, Nakamura S, Itoh S, Shirabe K, Maehara Y. Reduced-Dose Telaprevir-Based Triple Antiviral Therapy for Recurrent Hepatitis C After Living Donor Liver Transplantation. Transplantation. 2014.
6. Sugawara Y, Makuuchi M, Kaneko J, Ohkubo T, Matsui Y, Imamura H, Kokudo N. Living-donor liver transplantation in adults: Tokyo University experience. J Hepatobiliary Pancreat Surg. 2003; 10:1-4.
7. Tamura S, Sugawara Y, Yamashiki N, Kaneko J, Kokudo N, Makuuchi M. Pre-emptive antiviral therapy in living donor liver transplantation for hepatitis C: observation based on a single-center experience. Transplant international : official journal of the European Society for Organ Transplantation. 2010; 23:580-588.
8. Kaneko J, Sugawara Y, Tamura S, Aoki T, Sakamoto Y, Hasegawa K, Yamashiki N, Kokudo N. De novo malignancies after adult-to-adult living-donor liver transplantation with a malignancy surveillance program: comparison with a Japanese population-based study. Transplantation. 2013; 95:1142-1147.
9. Tamura S, Sugawara Y, Kishi Y, Akamatsu N, Kaneko J, Murai N, Makuuchi M. Conversion to cyclosporine provides valuable rescue therapy for living donor adult liver transplant patients intolerant to tacrolimus: A single-center experience at the University of Tokyo. Transplant Proc. 2004; 36:3242-3244.
10. Garg V, van Heeswijk R, Lee JE, Alves K, Nadkarni P, Luo X. Effect of telaprevir on the pharmacokinetics of cyclosporine and tacrolimus. Hepatology. 2011; 54:20-27.
11. Enomoto N, Sakuma I, Asahina Y, Kurosaki M, Murakami T, Yamamoto C, Ogura Y, Izumi N, Marumo F, Sato C. Mutations in the nonstructural protein 5A gene and response to interferon in patients with chronic hepatitis C virus 1b infection. N Engl J Med. 1996; 334:77-81.
12. Suppiah V, Moldovan M, Ahlenstiel G, *et al*. IL28B is associated with response to chronic hepatitis C interferon-alpha and ribavirin therapy. Nature genetics. 2009; 41:1100-1104.
13. Desmet VJ. Knodell RG, Ishak KG, Black WC, Chen TS, Craig R, Kaplowitz N, Kiernan TW, Wollman J. Formulation and application of a numerical scoring system for assessing histological activity in asymptomatic chronic active hepatitis [Hepatology 1981;1:431-435]. J Hepatol. 2003; 38:382-386.
14. Matsuo S, Imai E, Horio M, Yasuda Y, Tomita K, Nitta K, Yamagata K, Tomino Y, Yokoyama H, Hishida A. Revised equations for estimated GFR from serum creatinine in Japan. American journal of kidney diseases : the official journal of the National Kidney Foundation. 2009; 53:982-992.
15. Pungpapong S, Aqel BA, Koning L, Murphy JL, Henry TM, Ryland KL, Yataco ML, Satyanarayana R, Rosser

BG, Vargas HE, Charlton MR, Keaveny AP. Multicenter experience using telaprevir or boceprevir with peginterferon and ribavirin to treat hepatitis C genotype 1 after liver transplantation. Liver Transpl. 2013; 19:690-700.
16. Coilly A, Roche B, Dumortier J, Leroy V, Botta-Fridlund D, Radenne S, Pageaux GP, Si-Ahmed SN, Guillaud O, Antonini TM, Haim-Boukobza S, Roque-Afonso AM, Samuel D, Duclos-Vallee JC. Safety and efficacy of protease inhibitors to treat hepatitis C after liver transplantation: A multicenter experience. J Hepatol. 2014; 60:78-86.
17. Werner CR, Egetemeyr DP, Lauer UM, Nadalin S, Konigsrainer A, Malek NP, Berg CP. Feasibility of Telaprevir-Based Triple Therapy in Liver Transplant Patients with Hepatitis C Virus: SVR 24 Results. PloS one. 2013; 8:e80528.
18. Sulkowski M, Roberts SK, Afdhal NH, Andreone P, Diago M, Pol S, Poordad F, Zeuzem S, Bengtsson L, Luo D, Witek J, Adda N. 594 Ribavirin Dose Modification in Treatment-NaïVE and Previously Treated Patients Who Received Telaprevir Combination Treatment: No Impact on Sustained Virologic Response in Phase 3 Studies. Gastroenterology. 2012; 142:S-919.
19. Zeuzem S, Berg T, Gane E, *et al*. Simeprevir Increases Rate of Sustained Virologic Response Among Treatment-Experienced Patients With HCV Genotype-1 Infection: A Phase IIb Trial. Gastroenterology. 2013.
20. Fried MW, Buti M, Dore GJ, *et a*l. Once-daily simeprevir (TMC435) with pegylated interferon and ribavirin in treatment-naive genotype 1 hepatitis C: The randomized PILLAR study. Hepatology. 2013; 58:1918-1929.
21. Mahadevan S, Simion A, Mortier S, Peeters M, Beumont M. No clinically significant interaction between the investigational HCV protease inhibitor TMC435 and the immunosuppressives cyclosporine and tacrolimus. Hepatology. 2012; 56:231A.

(Received September 22, 2014; Revised November 18, 2014; Accepted December 14, 2014)

Commentary

DOI: 10.5582/bst.2014.01132

Health problems associated with international travel: A case of cutaneous myiasis in China due to *Cordylobia anthropophaga* imported from Uganda

Wei Ruan, Yan Feng, Lingling Zhang, Jimin Sun, Linong Yao*

Zhejiang Provincial Center for Disease Control and Prevention, Hangzhou, China.

Summary **More affordable international travel, global trade and commerce, and the exporting of labor have all contributed to international population mobility. Furthermore, population migration leads to the incidence or recurrence of once-controlled diseases. Evidence shows that the popularity of travel can impact health through imported infections and illness. Imported cutaneous myiasis, a type of skin lesion, has attracted the attention of the current authors. This condition often occurs among travelers and it has been reported in several non-endemic countries. However, diagnosis of myiasis and identification of the larvae are difficult. Advances in molecular detection techniques could provide a new way to identify larvae. This study used sequencing of the 28S rRNA gene and morphology to identify the larva infesting the upper arm of a Chinese woman returning from Uganda. The larva was identified as *Cordylobia anthropophaga* (*C. anthropophaga*) and the sequences were submitted to GenBank (accession number: KM506761). As foreign interaction increases, imported health problems may become more common in China. Knowledge about various pathogens needs to be increased and molecular methods need to be used to accurately identify those pathogens.**

Keywords: Larva, imported, molecular identification, morphology

1. Introduction

More affordable international travel, the development of global trade and commerce, and the exporting of labor have all contributed to international population mobility. Migration is a major factor that has led to changes in infectious diseases, such as the reappearance of controlled malaria (*1*) and an increasing number of dengue outbreaks (*2*).

Every year, 20%-70% of travelers from the industrialized world to the developing world report travel-associated illness, including fever, diarrhea, dermatologic conditions (*3*). According to the China National Tourism Administration, more than 9.8 million Chinese traveled internationally in 2013, representing an increase of 18% from the figure in 2012. This indicates massive migration. The popularity of international travel is overshadowed by threats to travelers' health from imported infections and illness such as malaria, Chagas disease, African trypanosomiasis, leishmaniasis, toxoplasmosis, and babesiosis (*4*). According to the Canadian Travel Medicine Network, 90.3% of travelers in Canada acquired a travel-related arthropod bite, giardiasis, malaria, or strongyloidiasis from 2009 to 2011 (*5*). Herbinger *et al*. also reported that travelers in sub-Saharan Africa had the highest relative risk of acquiring skin disorders (*6*).

In recent years, cutaneous myiasis, a type of skin lesion, often occurring among travelers, has garnered attention. This condition has been reported in several countries, including Spain (*7*), Japan (*8*), the UK (*9*), and the US (*10*). Twenty-nine cases of cutaneous myiasis were reported in China from

**Address correspondence to:*
Dr. Linong Yao, Division of Parasite Disease Intervention, Department of Communicable Disease Control and Prevention, Zhejiang Provincial Center for Disease Control and Prevention, Hangzhou 310051, China.
E-mail: ylinong@163.com

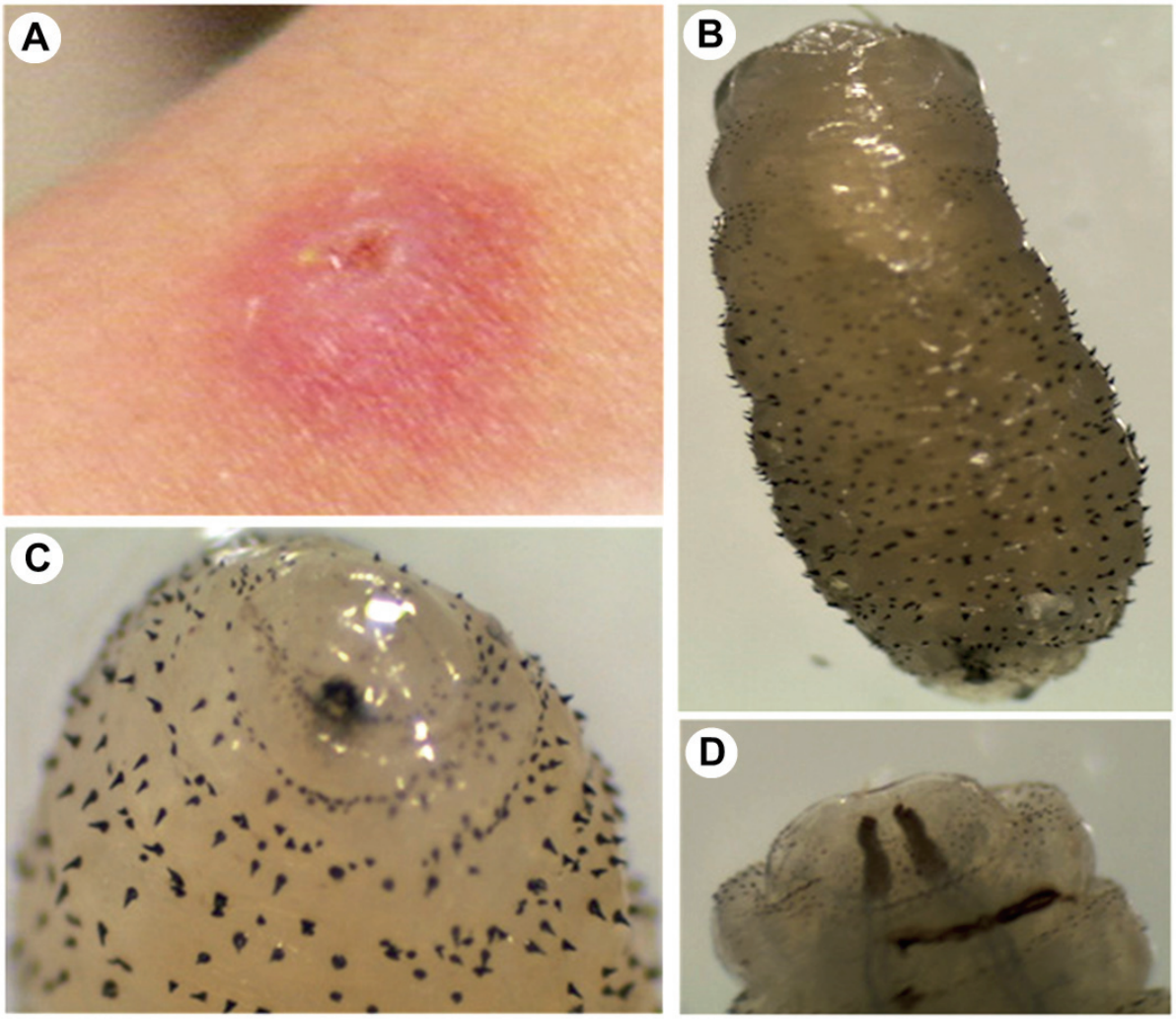

Figure 1. Characteristics of a larva. (A) A furuncular lesion on the upper arm after the larva was removed; **(B)** Intact larva under the anatomical lens; **(C)** The larva's two black-toothed hooks; **(D)** Posterior spiracles under a light microscope.

1995-2001, occurring frequently in nomadic areas and most involved *Hypoderma bovis*, *H. lineatum*, or *Gastrophilus nigricornis* (*11*). Cutaneous myiasis caused by other species has seldom been reported in China.

Currently, methods for diagnosis of myiasis and identification of the larvae are limited to clinical manifestations, an epidemiological history, and morphology of the larvae or identification of the adult fly when the larvae mature. Nevertheless, identification could be indeterminate if a clear picture is unavailable. Advances in molecular detection techniques may provide a new way to identify larvae, particularly when the larvae are dead or only partially intact. The 28S rRNA gene has been used as a genetic marker for molecular identification of larvae in Japan and Nigeria (*8,12*) but its use in China has never been reported. The current study used a new method of molecular identification to identify an ivory white worm from the upper arm of a Chinese woman who returned from Uganda.

2. Case presentation

2.1. *General information*

A 26-year old woman from Zhejiang Province, China travelled to Uganda for 10 days at the end of July 2014. During her time in Uganda, the woman claimed to have suffered mosquito bites. When she returned to China, she noted swelling, slight itching, and pain from a bite on her left upper arm. A lesion appeared and then developed into a nodule approximately 2-3 cm in diameter. In order to drain the nodule, the patient pressed hard on the lesion and she removed an ivory white worm. Swelling partially subsided the next day and the woman sent the worm to the Provincial Center for Disease Control and Prevention. A physical examination of the woman revealed a hard red nodule covered with a thin scab on the left upper arm (Figure 1A). The woman was in good condition overall with no fever or lymphadenectasis. The patient was advised to dab iodine and erythromycin ointment onto the skin

A

Primer	Sequence
28S rRNA F1	GGGAGGAAAAGAAACTAACAAGGA
28S rRNA R1	CTGTTTCGGTCTTCCATCAGGG
28S rRNA F2	CTTAGTAGCGGCGAGCGAAAA
28S rRNA R2	TTCCCCTGACTTCAACCTGATC

B

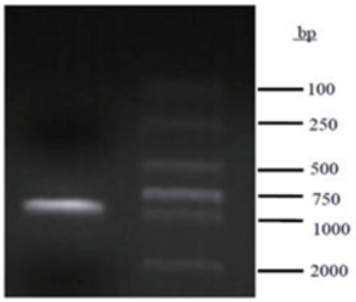

Figure 2. PCR amplification of the 28S rRNA gene. (A) Primers for PCR identification; **(B)** Agarose gel electrophoresis of the PCR product.

lesion. Three days later, the lesion scabbed and the swelling subsided. Ten days later, the nodule gradually disappeared. The patient developed no additional skin lesions.

2.2. *Identification of the larva*

2.2.1. *Morphological identification*

The larva was kept in normal saline so that it would remain alive when placed on a glass slide for morphological identification. The larva had a cylindrical body about 5 mm in length that was ivory white in color. Light microscopy revealed that the body of the larva had 10 segments and each segment had a number of black mucrones arranged uniformly in transverse rows (Figure 1B). In addition, a pair of black-toothed hooks was noted near the mouth (Figure 1C). Distinctive posterior spiracles with two linear slits on each side were noted on the caudal region of the larva (Figure 1D).

2.2.2. *Molecular identification*

DNA was gradually extracted from the larva with a QlAamp DNA Mini kit (Qiagen, Germany) in accordance with the manufacturer's instructions. Nested PCR amplification of the 28S rRNA gene was performed with uniquely designed primers (Figure 2A). Two successive runs of nested PCR were both carried out under the following conditions: initial denaturation at 94°C for 5 min, 30 cycles of denaturation at 94°C for 30 sec, annealing at 60°C for 30 sec, and elongation at 72°C for 2 min, followed by a final elongation step at 72°C for 5 min. Amplified target fragments were verified using 1.5% agarose gel electrophoresis (Figure 2B). The PCR product was purified and bi-directionally sequenced by BGI, China. The sequences had 99% (918/919) similarity to partial 28S rRNA gene sequences from *C. anthropophaga* in the GenBank database (isolated by Yaounde in 1999, accession number: AJ551432) according to the Basic Local Alignment Search Tool (BLAST). The current sequences were subsequently submitted to GenBank and given the accession number KM506761.

3. How does infestation with *C. anthropophaga* happen?

Myiasis was first described by Hope in 1840 and refers to the infestation of human and vertebrate animal tissue by the larvae of *Diptera* (adult flies with two wings). Myiasis usually occurs in tropical and subtropical areas including Central America, South America, Africa, and the Caribbean Islands (*13,14*). Based on the site of infestation, myiasis is classified as cutaneous, enteric, ophthalmic, nasopharyngeal, auricular, oral, or urogenital (*15*).

Depending on the species of larvae responsible, cutaneous myiasis presents clinically in three main forms: furuncular, migratory, and wound myiasis (*16*). Furuncular myiasis is commonly caused by the larvae of *Dermatobia hominis*, *Cordylobia anthropophaga* (*C. anthropophaga*), *Cuterebra* spp., *Wohlfahrtia vigil*, and *W. opaca* (*14*). The geographic location of these larvae varies. As an example, *Dermatobia hominis* is common in Central and South America while *C. anthropophaga* is common in Tropical Africa (*14,17*).

The *Cordylobia* genus, which falls under the family *Calliphoridae*, includes three species: *C. anthropophaga*, *C. ruandae*, and *C. rhodhaini*. All three of these species can cause furuncular myiasis but *C. anthropophaga* is the most common cause. *C. anthropophaga* is commonly known as the tumbu fly (*14*) and it infests a variety of different hosts but particularly rodents and dogs (*17*). The adult female *C. anthropophaga* lays batches of 100-300 eggs in sandy soil and damp clothing that are often contaminated with urine or feces. Humans are readily susceptible to the tumbu fly during the rainy season (*17*). When the host lays in sand or comes in contact with contaminated clothing, the larvae can approach and penetrate the skin unnoticed in 60 sec (*17*). In the current case, the larva may have penetrated the tissue via a lesion caused by a

mosquito bite. The larval infestation causes a protruding lesion below the skin and the host may feel pain of varying degrees. If the host is not treated, the mature larva will emerge from the skin, fall to the ground, and pupate in 8-12 days (*18*).

4. Challenges in identification

Outside endemic regions, diagnosis of imported illness is challenging and requires experienced specialists. Identification of larvae is also demanding and requires specialists in parasitology and entomology. When travelers with symptoms seek care after they return from endemic areas, their travel history can easily be overlooked by both doctors and patients. Moreover, a lack of knowledge and experience on diagnosing imported illness of part of doctors often results in failure to identify the parasite responsible. However, molecular identification requires few specific skills related to morphology and can easily be performed by most hospitals in China.

This study described a typical case of furuncular myiasis caused by *C. anthropophaga*. To the extent known, few studies in China have described the identification of myiasis based on molecular methods and morphology. Sequencing of the 28S rRNA gene of the larva provides a simpler method of diagnosis and provides better evidence than morphology.

Given the potential for an increase in imported health problems in China, both doctors and CDC personnel should pay more attention to these rare microorganisms and parasites. Knowledge about various pathogens needs to be increased and accurate methods of molecular identification need to be used to identify these pathogens. These steps should help patients receive adequate and timely treatment and result in a good prognosis.

Acknowledgements

This work was supported by grants from the Zhejiang Provincial Medicine and Health Technology Project (No.2013KYA041) and the Laboratory of Parasite and Vector Biology, MOPH (WSBKTKT201306).

References

1. Shkurti K, Vyshka G, Velo E, Bocari A, Kokici M, Kraja D. Imported malaria in Albania and the risk factors that could allow its reappearance. Malar J. 2013; 12:197.
2. Grange L, Simon-Loriere E, Sakuntabhai A, Gresh L, Paul R, Harris E. Epidemiological risk factors associated with high global frequency of inapparent dengue virus infections. Front Immunol. 2014; 5:280.
3. Ryan ET, Wilson ME, Kain KC. Illness after international travel. N Engl J Med. 2002; 347:505-516.
4. Pereira BI, Nazareth C, Malcata L, Alves H, Fernandez JR, Sargento C, da Cunha S. [Transfusion-transmitted protozoal infections: What is the risk in non-endemic countries?]. Acta Med Port. 2011; 24 Suppl 4:897-906.
5. Boggild AK, Geduld J, Libman M, Ward BJ, McCarthy AE, Doyle PW, Ghesquiere W, Vincelette J, Kuhn S, Freedman DO, Kain KC. Travel-acquired infections and illnesses in Canadians: Surveillance report from CanTravNet surveillance data, 2009-2011. Open Med. 2014; 8:e20-32.
6. Herbinger KH, Siess C, Nothdurft HD, von Sonnenburg F, Loscher T. Skin disorders among travellers returning from tropical and non-tropical countries consulting a travel medicine clinic. Trop Med Int Health. 2011; 16:1457-1464.
7. Kovaleva A, Climent PC, Becares CV, Martin Azana MJ, Irishina N, Goy EI. Urogenital myiasis by *Cordylobia anthropophaga*. J Pediatr Adolesc Gynecol. 2013; 26:e123-125.
8. Fujisaki R, Makimura K, Hayashi T, Yamamura M, Yamaoka T, Shiraishi K, Ishibashi S, Kawakami S, Kurihara T, Nishiya H. Exotic myiasis caused by 19 larvae of *Cordylobia anthropophaga* in Namibia and identified using molecular methods in Japan. Trans R Soc Trop Med Hyg. 2008; 102:599-601.
9. Pepper WC, Benaragama SK, Kalsi JS, Karim O. Cutaneous myiasis of *Cordylobia anthropophaga*. Urology. 2008; 72:65.
10. Wangia M, Glenn C, Mitchell C, Fisher S. Florid *Cordylobia anthropophaga* furuncular myiasis from travel in Nigeria. J Dermatol. 2012; 39:1099-1100.
11. Jiang C. A collective analysis on 54 cases of human myiasis in China from 1995-2001. Chin Med J (Engl). 2002; 115:1445-1447.
12. Ogo NI, Onovoh E, Okubanjo OO, Galindo RC, De la Lastra JM, De la Fuente J. Molecular identification of *Cordylobia anthropophaga* Blanchard (*Diptera*: *Calliphoridae*) larvae collected from dogs (Canis familiaris) in Jos South, Plateau State, Nigeria. Onderstepoort J Vet Res. 2012; 79:E1-4.
13. CDC. Parasites - Myiasis. http://www.cdc.gov/parasites/myiasis/ (September 16, 2014).
14. McGraw TA, Turiansky GW. Cutaneous myiasis. J Am Acad Dermatol. 2008; 58:907-926; quiz 927-909.
15. Magnarelli LA, Andreadis TG. Human cases of furuncular, traumatic, and nasal myiasis in Connecticut. Am J Trop Med Hyg. 1981; 30:894-896.
16. Hall M, Wall R. Myiasis of humans and domestic animals. Adv Parasitol. 1995; 35:257-334.
17. Robbins K, Khachemoune A. Cutaneous myiasis: A review of the common types of myiasis. Int J Dermatol. 2010; 49:1092-1098.
18. Ockenhouse CF, Samlaska CP, Benson PM, Roberts LW, Eliasson A, Malane S, Menich MD. Cutaneous myiasis caused by the African tumbu fly (*Cordylobia anthropophaga*). Arch Dermatol. 1990; 126:199-202.

(Received November 27, 2014; Revised December 13, 2014; Accepted December 18, 2014)

Commentary

DOI: 10.5582/bst.2014.01119

Medical emergency rescue in disaster: The international emergency response to the Haiyan typhoon in Philippines

Feng Ling[1], Zhen Ye[2,*], Wenwei Cai[3], Ye Lu[1], Shichang Xia[1], Zhiping Chen[1], Enfu Chen[1], Xiaofeng Wang[1], Zhen Wang[1], Huakun Lv[1], Zhenyu Gong[1,*]

[1] *Zhejiang Provincial Center for Disease Control and Prevention, Hangzhou, China;*
[2] *Zhejiang Health and Family Planning Commission, Hangzhou, China;*
[3] *The Emergency Department of Zhejiang Provincial People's Hospital, Hangzhou, China.*

Summary **Following Typhoon Haiyan, the World Health Organization (WHO) has been supporting the Government of the Philippines in coordinating the incoming relief supplies from more than 30 international humanitarian health or¬ganizations. During the 10 days in Abuyong, Philippines, the Chinese medical rescue team consisting of 50 experts specialized in clinical medicine and disease prevention and control action was taken including, medical treatment, environmental disinfection and health education. A total of 1,831 cases and 2,144 outpatients were treated, blood tests, B-ultrasound, electrocardiogram (ECG) and other laboratory examinations were carried out for more than 615 patients; a cumulative 90,000 square meters in external environment were disinfected, and more than 500 health education materials were handed out. Besides, measures of purifying drinking water, and rebuilding the local hospital have also been carried out. The international emergency response to the Haiyan typhoon in Philippines contributed to reconstruct the local disaster health system by the activities from international medical emergency rescue. To improve the capacity of international medical emergency rescue in disaster, the special project of foreign medical emergency rescue should be set in countries' medical emergency rescue, and disaster emergency medical rescue should be reserved as a conventional capacity.**

Keywords: Medical emergency rescue, typhoon, disaster, emergency response

1. Introduction

The typhoon stroked the Philippines on November 8, 2013, which was the strongest in local history, causing massive destruction and 25 million people were affected. More than 5,000 people were confirmed dead, and many others had lost their homes (*1*). Health facilities were damaged or completely destroyed across large swathes of the affected regions, and, as a result of the breadth and severity of the storm, health services in the worst affected areas have ceased to exist or have been severely stretched, with medi¬cal supplies in very short supply.

Following Typhoon Haiyan, the World Health Organization (WHO) has been supporting the Government of the Philippines in coordinating the incoming relief supplies from more than 30 international humanitarian health organizations.

After the disaster, a national medical rescue team consisting of 50 experts specialized in clinical medicine and disease prevention and control was organized by Chinese government, which arrived in Abuyong, Philippines to provide medical rescue to the hospitals in Abuyong, where the local medical system has been paralyzed, and the only local hospital does not have the ability to admit patients after Haiyan. During the 10 days in Abuyong, measures of medical treatment, environmental disinfection and health education,

**Address correspondence to:*
Dr. Zhenyu Gong, Zhejiang Provincial Center for Disease Control and Prevention, 3399 Bin Sheng Road, Binjiang District, 310051 Hangzhou, China.
E-mail: zhygong@cdc.zj.cn

Dr. Zhen Ye, Zhejiang Health and Family Planning Commission, No.216 Qingchun Road, Hangzhou 310006, China.
E-mail: yz1668@sina.com.cn

purifying drinking water, and rebuilding the local hospital were carried out by our team.

2. Medical emergency rescue measures

Medical treatment In Abuyong, common clinical projects and public health programs were carried out by our team. According to the needs of the local health system, we set up pediatrics, obstetrics and gynecology departments, respiratory medicine, orthopedics, infection, as well as blood tests, B-ultrasound, electrocardiogram (ECG) and other ancillary departments. A sterile room was set up, the room and medical equipment were carefully disinfected using adenosine triphosphate (ATP) bioluminescence assay to detect infection during surgery - 11 times forceps and 6 times surgical scissors were sampled before surgery, which showed that the forceps surface fluorescence was four times 1 relative light unit (RLU), and the remaining test results were 0 RLU, which was in line with requirements.

During the 10 days of joint operation, we provided medical assistance to about 200 patients per day, and a total of 1,831 cases and 2,144 outpatients were treated (Figure 1). Among the diseases diagnosed, the top 5 were tuberculosis, upper respiratory tract infection, skin infection, pregnancy and scabies (Figure 2). The blood tests, B-ultrasound, ECG and other laboratory examinations were carried out for more than 615 patients; by effective disinfection of operating room and medical equipment, 26 units of surgical operations were conducted successfully. Because of the large amount of patients, drugs we brought were not enough. So after consulting the embassy staff, many common drugs were bought, such as cloxacillin, erythromycin, paracetamol, amoxicillin, paracetamol, cotrimoxazole, and povidone iodine, mediplast, needles.

Besides, we also gave some guidance to the hospitals in Abuyong on the aspects of disinfection of medical pre-screening of clinics, obstetrics and the operating room, especially disinfecting support for the first medical surgery, disinfection testing, and sterilization of surgical instruments to prevent nosocomial infections.

Environmental disinfection and health education Microbiological indicators on surroundings were monitored by ATP bioluminescence assay of medical equipment and surgical instruments, while the quality of water was detected using a chlorine analyzer (H293711, Italy HANA) and density of mosquitoes was measured by visual method in the external environment (Figure 3). With one effervescent tablet (500mg/tablet) plus 1L water to allocate 500mg/L of disinfectant for residual spraying, and treatment tablets and medical instruments with wipe disinfection; and added chlorine to water which had inadequate residual chlorine by detection; the external environment insecticide used was deltamethrin (content of 2.5%, EC, Bayer UK). A cumulative 90,000 square meters in the external environment were disinfected, besides, more than 500 health education materials were handed out, which effectively prevented

Figure 1. The first case of hip tumor resection carried out by Chinese medical rescue team.

Figure 2. The team member disinfected and used insecticide around the camp.

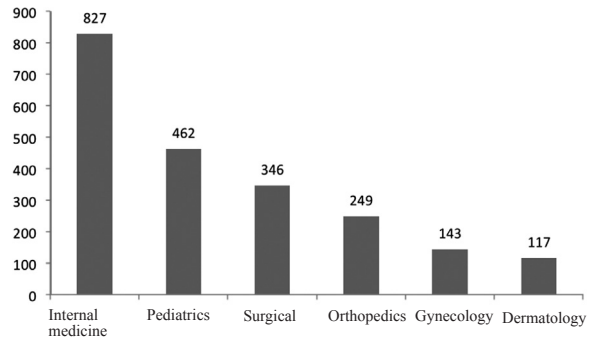

1	Tuberculosis	Skin infection	Pregnant
2	Lung infection	Surface mass	Menstrual disorders
3	Coronary heart disease	Skin laceration	Uterine fibroids
4	Hypertension	Spine disease	Pelvic masses
5	Peptic ulcer	Knee osteoarthritis	Gynecological inflammation

Figure 3. Classification of patients for the Chinese emergency rescue team diagnosis and treatment in Abuyong.

the occurrence of infectious diseases after Haiyan.

Purifying drinking water Because of Haiyan, running water, electricity, and communication were all interrupted, and there was a lack of enough drinking water. Thus, we immediately communicated with the local residents after arrival, and found that drinking water was mainly from wells and rivers without special disinfection. In addition, it was rainy season at that time when the amount of rain was three times more than normal per day. To ensure enough clean and healthy drinking water, chlorine was added and timely detected in water. The turbidity of untreated water was 3.62, with total chlorine zero. After estimation of the size and depth of the well, 30 disinfection tablets were put in, then we purified the water by polypropylene cotton, activated carbon and ultra filtration; after these measures, the turbidity of water declined to 0.2. As local residents and us shared the same well and did not like the sense of chlorine, we controlled the total chlorine to less than 0.2. Until December 1st, luckily local residents did not object drinking water with chlorine. When local residents got used to the sense, we increased the amount of disinfection tablets to 0.3 in tap water.

Rebuilding the the local hospital Because of the impact of the typhoon, the only one hospital - Abuyong Aeneral Hospital in Abuyong was on the verge of paralysis. The diagnostic equipment in hospital cannot work because of lack of power, which also brought great difficulty for rebuilding the local hospital system. On the recommendation of the local government, we took over the local hospitals to gradually restore their treatment capacity. We helped and trained them to carry out medical work after the disaster, when they had no drugs, no instruments and irregular medical materials, and also when we evacuated from Abuyong, we donated lots of prerequisite materials and medical supplies, such as generators, medical monitors, ECG, clinical urinary analyzers, infrared thermometers, oxygen generators, suction equipment, glucometers and operation lamps, disposable surgical packages, disposable surgical gowns, infusion apparatus, N95 masks, disposable latex gloves and a large quantity of pharmaceuticals.

3. Discussion

From SARS (2003) to Wenchuan earthquake (2008), from Yushu earthquake (2010) to Ludian earthquake (2014), from the supporting medical team fighting against Haiyan typhoon in Philippines in 2013 and that for Ebola in Africa in 2014, the Chinese rescue teams against public disasters have made great progress and played a more important role, not only for national medical emergency rescue, but also for international public health emergency rescue.

This international medical aid to the Haiyan typhoon in Philippines gained much support from the Chinese Government and many departments, including the Embassy, the Civil Aviation Bureau, the Customs Head Office, and General Administration of Quality Inspection. They facilitated material preparation, charter transportation and so on. Specific workers are assigned to accompany the medical team, help contact our own country and communicate with the local people. With their help, our medical team members could communicate fluently with the local government, local people and local army, and then participate in disaster relief activities together, which have improved efficiency and effectiveness of relief activities, as well as safety of the medical team.

Our experience suggests that the WHO guidelines (*2*) are sound and appropriate when there is a total collapse of the local medical infrastructure. When the local medical system was in paralysis or semi paralyzed, the cooperation between the rescue teams from other countries and the local medical institutes can help gain confidence of the local people to the foreign rescue teams on one hand, and on the other hand, the cooperation could contribute to the recovery of the local medical system.

In international rescue especially in typhoon rescue, the water would always be polluted. When self-brought water could not satisfy need during the long period of rescuing, turbidity meter and total chlorine meter could be used to test the total particulate matter and the total chlorine quickly. It would be easy to satisfy the need in a disaster area, if we filter the local water with PP, activated carbon and gradocol membranes.

The devastation in the Philippines is only one of many recent examples of destruction from weather phenomena (*3*), a special project of international medical emergency rescue should be set in countries' medical emergency rescue, and disaster emergency medical rescue should be reserved as a conventional capacity. Unfortunately, lopsided development of medicine is generally worldwide. Some countries with a low-level medical system are always subjected to natural disasters. They are not always capable of carrying out rescues. In such situations, border countries or even some developed countries should carry out international medical emergency rescue. With the development of international communication, such foreign medical emergency rescue would increase. Thus, medical emergency relief teams with miniaturized and portable equipment, with a capability of distant transportation and with standard logistic support should be built. When disasters happen, one country should bear the social and public opinion on long - term development with border countries in mind and act according to its ability.

We should also point out that there are still some shortages of Chinese medical rescue teams which have to improve the capacity of its own for all the 50 medical rescue staff - there are only 6 professional public health experts (6/50), who play an important role

in guaranteeing the public health of a rescue camping site (safety of drinking water and food, density control of vectors, *etc*.). Due to limited human resources and the local special environment, we could not be able to launch large-scale help in the rescue area, including case searching, safety of drinking water and food and other public health work.

Of course, we have shortages in collected data, which were produced during the process of rescue, such as, we do not have the density data of mosquitos before insecticide use, we also did not calculate the amount of disinfectant to use every day for living water disinfection.

In conclusion, the international emergency response to the Haiyan typhoon in Philippines contributed to reconstruct the local disaster health system by measures from international medical emergency rescue. To improve the capacity of international medical emergency rescue in disasters, the special project of international medical emergency rescue should be set in countries' medical emergency rescue, and disaster emergency medical rescue should be reserved as a conventional capacity.

References

1. WHO coordinates health relief after typhoon Haiyan. Bull World Health Organ 2013; 91:900-901.
2. WHO-PAHO guidelines for the use of foreign field hospitals in the aftermath of sudden-impact disasters. Washington, DC: Pan American Health Organization, 2003 (*http://www.who.int/hac/techguidance/pht/FieldHospitalsFolleto.pdf*). (accessed December 15, 2014)
3. Cranmer HH, Biddinger PD. Typhoon Haiyan and the professionalization of disaster response. N Engl J Med. 2014; 370:1185-1187.

(Received November 4, 2014; Revised December 21, 2014; Accepted December 23, 2014)

Subject Index (2014)

Reviews

Brief Reports

Original Articles

Evaluation of human D-amino acid oxidase inhibition by antipsychotic drugs *in vitro*.
Shishikura M, Hakariya H, Iwasa S, Yoshio T, Ichiba H, Yorita K, Fukui K, Fukushima T
2014; 8(3):149-154. (DOI: 10.5582/ bst.2014.01034)

Comparison of mechanisms underlying changes in glucose utilization in fasted rats anesthetized with propofol or sevoflurane: Hyperinsulinemia is exaggerated by propofol with concomitant insulin resistance induced by an acute lipid load.
Li X, Kitamura T, Kawamura G, Mori Y, Sato K, Araki Y, Sato R, Yamada Y
2014; 8(3):155-162. (DOI: 10.5582/ bst.2014.01060)

Relationship between T-SPOT.TB responses and numbers of circulating CD4+ T-cells in HIV infected patients with active tuberculosis.
Cai RT, Chen J, Guan LQ, Sun MY, Sun Y, Shen YZ, Zhang RF, Liu L, Lu HZ
2014; 8(3):163-168. (DOI: 10.5582/ bst.2014.01032)

Repeated doses of intravenous tranexamic acid are effective and safe at reducing perioperative blood loss in total knee arthroplasty.
Xu QT, Yang Y, Shi P, Zhou J, Dai WD, Yao ZJ, Zhang C
2014; 8(3):169-175. (DOI: 10.5582/ bst.2014.01063)

Effects of lifestyle factors on urinary oxidative stress and serum antioxidant markers in pregnant Japanese women: A cohort study.
Matsuzaki M, Haruna M, Ota E, Murayama R, Yamaguchi T, Shioji I, Sasaki S, Yamaguchi T, Murashima S
2014; 8(3):176-184. (DOI: 10.5582/ bst.2014.01014)

Pathological changes in primary cilia: A novel mechanism of graft cholangiopathy caused by prolonged cold preservation in a rat model of orthotopic liver transplantation.
Lu HW, Dong JH, Zhang YF, Li CH, Yu Q, Tang W
2014; 8(4):206-211. (DOI: 10.5582/bst.2014.01062)

Migration of breast cancer cells into reconstituted type I collagen gels assessed *via* a combination of frozen sectioning and azan staining.
Fukuda K, Kamoshida Y, Kurokawa T, Yoshida M, Fujita-Yamaguchi Y, Nakata M
2014; 8(4):212-216. (DOI: 10.5582/bst.2014.01090)

Ferulic acid combined with astragaloside IV protects against vascular endothelial dysfunction in diabetic rats.
Yin YH, Qi FH, Song ZH, Zhang B, Teng JL
2014; 8(4):217-226. (DOI: 10.5582/bst.2014.01081)

A simple, rapid, economical, and practical method for the determination of efavirenz in plasma of Chinese AIDS patients by reverse phase high-performance liquid chromatography with ultraviolet detector.
Yin K, Meng XM, Dong P, Ding TR, Shen L, Zhang L, Zhang RF, Cai WM, Lu HZ
2014; 8(4):227-234. (DOI: 10.5582/bst.2014.01002)

Involvement of the central monoaminergic system in the antidepressant-like effect of catalpol in mice.
Wang JM, Cui Y, Feng WS, Zhang YY, Wang GF, Wang XX, Zhou G
2014; 8(5):248-252. (DOI: 10.5582/bst.2014.01029)

Protection of *Angelica sinensis* (Oliv) Diels against hepatotoxicity induced by *Dioscorea bulbifera* L. and its mechanism.
Niu CW, Wang JM, Ji LL, Wang ZT
2014; 8(5):253-259. (DOI: 10.5582/bst.2014.01076)

Case Reports

Commentaries

Letter

BST
BioScience Trends

Guide for Authors

1. Scope of Articles

BioScience Trends is an international peer-reviewed journal. BioScience Trends devotes to publishing the latest and most exciting advances in scientific research. Articles cover fields of life science such as biochemistry, molecular biology, clinical research, public health, medical care system, and social science in order to encourage cooperation and exchange among scientists and clinical researchers.

2. Submission Types

Original Articles should be well-documented, novel, and significant to the field as a whole. An Original Article should be arranged into the following sections: Title page, Abstract, Introduction, Materials and Methods, Results, Discussion, Acknowledgments, and References. Original articles should not exceed 5,000 words in length (excluding references) and should be limited to a maximum of 50 references. Articles may contain a maximum of 10 figures and/or tables.

Brief Reports definitively documenting either experimental results or informative clinical observations will be considered for publication in this category. Brief Reports are not intended for publication of incomplete or preliminary findings. Brief Reports should not exceed 3,000 words in length (excluding references) and should be limited to a maximum of 4 figures and/or tables and 30 references. A Brief Report contains the same sections as an Original Article, but the Results and Discussion sections should be combined.

Reviews should present a full and up-to-date account of recent developments within an area of research. Normally, reviews should not exceed 8,000 words in length (excluding references) and should be limited to a maximum of 100 references. Mini reviews are also accepted.

Policy Forum articles discuss research and policy issues in areas related to life science such as public health, the medical care system, and social science and may address governmental issues at district, national, and international levels of discourse. Policy Forum articles should not exceed 2,000 words in length (excluding references).

Case Reports should be detailed reports of the symptoms, signs, diagnosis, treatment, and follow-up of an individual patient. Case reports may contain a demographic profile of the patient but usually describe an unusual or novel occurrence. Unreported or unusual side effects or adverse interactions involving medications will also be considered. Case Reports should not exceed 3,000 words in length (excluding references).

News articles should report the latest events in health sciences and medical research from around the world. News should not exceed 500 words in length.

Letters should present considered opinions in response to articles published in BioScience Trends in the last 6 months or issues of general interest. Letters should not exceed 800 words in length and may contain a maximum of 10 references.

3. Editorial Policies

Ethics: BioScience Trends requires that authors of reports of investigations in humans or animals indicate that those studies were formally approved by a relevant ethics committee or review board.

Conflict of Interest: All authors are required to disclose any actual or potential conflict of interest including financial interests or relationships with other people or organizations that might raise questions of bias in the work reported. If no conflict of interest exists for each author, please state "There is no conflict of interest to disclose".

Submission Declaration: When a manuscript is considered for submission to BioScience Trends, the authors should confirm that 1) no part of this manuscript is currently under consideration for publication elsewhere; 2) this manuscript does not contain the same information in whole or in part as manuscripts that have been published, accepted, or are under review elsewhere, except in the form of an abstract, a letter to the editor, or part of a published lecture or academic thesis; 3) authorization for publication has been obtained from the authors' employer or institution; and 4) all contributing authors have agreed to submit this manuscript.

Cover Letter: The manuscript must be accompanied by a cover letter signed by the corresponding author on behalf of all authors. The letter should indicate the basic findings of the work and their significance. The letter should also include a statement affirming that all authors concur with the submission and that the material submitted for publication has not been published previously or is not under consideration for publication elsewhere. The cover letter should be submitted in PDF format. For example of Cover Letter, please visit http://www.biosciencetrends.com/downcentre.php (Download Centre).

Copyright: A signed JOURNAL PUBLISHING AGREEMENT (JPA) form must be provided by post, fax, or as a scanned file before acceptance of the article. Only forms with a hand-written signature are accepted. This copyright will ensure the widest possible dissemination of information. A form facilitating transfer of copyright can be downloaded by clicking the appropriate link and can be returned to the e-mail address or fax number noted on the form (Please visit Download Centre). Please note that your manuscript will not proceed to the next step in publication until the JPA Form is received. In addition, if excerpts from other copyrighted works are included, the author(s) must obtain written permission from the copyright owners and credit the source(s) in the article.

Suggested Reviewers: A list of up to 3 reviewers who are qualified to assess the scientific merit of the study is welcomed. Reviewer information including names, affiliations, addresses, and e-mail should be provided at the same time the manuscript is submitted online. Please do not suggest reviewers with known conflicts of interest, including participants or anyone with a stake in the proposed research; anyone from the same institution; former students, advisors, or research collaborators (within the last three years); or close personal contacts. Please note that the Editor-in-Chief may accept one or more of the proposed reviewers or may request a review by other qualified persons.

Language Editing: Manuscripts prepared by authors whose native language is not English should have their work proofread by a native English speaker before submission. If not, this might delay the publication of your manuscript in BioScience Trends.

The Editing Support Organization can provide English proofreading, Japanese-English translation, and Chinese-English translation services to authors who want to publish in BioScience Trends and need assistance before submitting a manuscript. Authors can visit this organization directly at http://www.iacmhr.com/iac-eso/support.php?lang=en. IAC-ESO was established to facilitate manuscript preparation by researchers whose native language is not English and to help edit works intended for international academic journals.

4. Manuscript Preparation

Manuscripts should be written in clear, grammatically correct English and submitted as a Microsoft Word file in a single-column format. Manuscripts must be paginated and typed in 12-point Times New Roman font with 24-point line spacing. Please do not embed figures in the text. Abbreviations should be used as little as possible and should be explained at first mention unless the term is a well-known abbreviation (*e.g.* DNA). Single words should not be abbreviated.

Title Page: The title page must include 1) the title of the paper (Please note the title should be short, informative, and contain the major key words); 2) full name(s) and affiliation(s) of the author(s), 3) abbreviated names of the author(s), 4) full name, mailing address, telephone/fax numbers, and e-mail address of the corresponding author; and 5) conflicts of interest (if you have an actual or potential conflict of interest to disclose, it must be included as a footnote on the title page of the manuscript; if no conflict of

interest exists for each author, please state "There is no conflict of interest to disclose"). Please visit Download Centre and refer to the title page of the manuscript sample.

Abstract: The abstract should briefly state the purpose of the study, methods, main findings, and conclusions. For article types including Original Article, Brief Report, Review, Policy Forum, and Case Report, a one-paragraph abstract consisting of no more than 250 words must be included in the manuscript. For News and Letters, a brief summary of main content in 150 words or fewer should be included in the manuscript. Abbreviations must be kept to a minimum and non-standard abbreviations explained in brackets at first mention. References should be avoided in the abstract. Key words or phrases that do not occur in the title should be included in the Abstract page.

Introduction: The introduction should be a concise statement of the basis for the study and its scientific context.

Materials and Methods: The description should be brief but with sufficient detail to enable others to reproduce the experiments. Procedures that have been published previously should not be described in detail but appropriate references should simply be cited. Only new and significant modifications of previously published procedures require complete description. Names of products and manufacturers with their locations (city and state/country) should be given and sources of animals and cell lines should always be indicated. All clinical investigations must have been conducted in accordance with Declaration of Helsinki principles. All human and animal studies must have been approved by the appropriate institutional review board(s) and a specific declaration of approval must be made within this section.

Results: The description of the experimental results should be succinct but in sufficient detail to allow the experiments to be analyzed and interpreted by an independent reader. If necessary, subheadings may be used for an orderly presentation. All figures and tables must be referred to in the text.

Discussion: The data should be interpreted concisely without repeating material already presented in the Results section. Speculation is permissible, but it must be well-founded, and discussion of the wider implications of the findings is encouraged. Conclusions derived from the study should be included in this section.

Acknowledgments: All funding sources should be credited in the Acknowledgments section. In addition, people who contributed to the work but who do not meet the criteria for authors should be listed along with their contributions.

References: References should be numbered in the order in which they appear in the text. Citing of unpublished results, personal communications, conference abstracts, and theses in the reference list is not recommended but these sources may be mentioned in the text. In the reference list, cite the names of all authors when there are fifteen or fewer authors; if there are sixteen or more authors, list the first three followed by *et al.* Names of journals should be abbreviated in the style used in PubMed. Authors are responsible for the accuracy of the references. Examples are given below:

Example 1 (Sample journal reference):
Inagaki Y, Tang W, Zhang L, Du GH, Xu WF, Kokudo N. Novel aminopeptidase N (APN/CD13) inhibitor 24F can suppress invasion of hepatocellular carcinoma cells as well as angiogenesis. Biosci Trends. 2010; 4:56-60.

Example 2 (Sample journal reference with more than 15 authors):
Darby S, Hill D, Auvinen A, *et al.* Radon in homes and risk of lung cancer: Collaborative analysis of individual data from 13 European case-control studies. BMJ. 2005; 330:223.

Example 3 (Sample book reference):
Shalev AY. Post-traumatic stress disorder: diagnosis, history and life course. In: Post-traumatic Stress Disorder, Diagnosis, Management and Treatment (Nutt DJ, Davidson JR, Zohar J, eds.). Martin Dunitz, London, UK, 2000; pp. 1-15.

Example 4 (Sample web page reference):
Ministry of Health, Labour and Welfare of Japan. Dietary reference intakes for Japanese. *http://www.mhlw.go.jp/houdou/2004/11/h1122-2a.html* (accessed June 14, 2010).

Tables: All tables should be prepared in Microsoft Word or Excel and should be arranged at the end of the manuscript after the References section. Please note that tables should not in image format. All tables should have a concise title and should be numbered consecutively with Arabic numerals. If necessary, additional information should be given below the table.

Figure Legend: The figure legend should be typed on a separate page of the main manuscript and should include a short title and explanation. The legend should be concise but comprehensive and should be understood without referring to the text. Symbols used in figures must be explained.

Figure Preparation: All figures should be clear and cited in numerical order in the text. Figures must fit a one- or two-column format on the journal page: 8.3 cm (3.3 in.) wide for a single column, 17.3 cm (6.8 in.) wide for a double column; maximum height: 24.0 cm (9.5 in.). Please make sure that the symbols and numbers appeared in the figures should be clear. Please make sure that artwork files are in an acceptable format (TIFF or JPEG) at minimum resolution (600 dpi for illustrations, graphs, and annotated artwork, and 300 dpi for micrographs and photographs). Please provide all figures as separate files. Please note that low-resolution images are one of the leading causes of article resubmission and schedule delays. All color figures will be reproduced in full color in the online edition of the journal at no cost to authors.

Units and Symbols: Units and symbols conforming to the International System of Units (SI) should be used for physicochemical quantities. Solidus notation (*e.g.* mg/kg, mg/mL, mol/mm^2/min) should be used. Please refer to the SI Guide www.bipm.org/en/si/ for standard units.

Supplemental data: Supplemental data might be useful for supporting and enhancing your scientific research and BioScience Trends accepts the submission of these materials which will be only published online alongside the electronic version of your article. Supplemental files (figures, tables, and other text materials) should be prepared according to the above guidelines, numbered in Arabic numerals (*e.g.*, Figure S1, Figure S2, and Table S1, Table S2) and referred to in the text. All figures and tables should have titles and legends. All figure legends, tables and supplemental text materials should be placed at the end of the paper. Please note all of these supplemental data should be provided at the time of initial submission and note that the editors reserve the right to limit the size and length of Supplemental Data.

5. Submission Checklist

The Submission Checklist will be useful during the final checking of a manuscript prior to sending it to BioScience Trends for review. Please visit Download Centre and download the Submission Checklist file.

6. Online Submission

Manuscripts should be submitted to BioScience Trends online at http://www.biosciencetrends.com. The manuscript file should be smaller than 5 MB in size. If for any reason you are unable to submit a file online, please contact the Editorial Office by e-mail at office@biosciencetrends.com.

7. Accepted Manuscripts

Proofs: Galley proofs in PDF format will be sent to the corresponding author via e-mail. Corrections must be returned to the editor (proof-editing@biosciencetrends.com) within 3 working days.

Offprints: Authors will be provided with electronic offprints of their article. Paper offprints can be ordered at prices quoted on the order form that accompanies the proofs.

Page Charge: Page charges will be levied on all manuscripts accepted for publication in BioScience Trends ($140 per page for black white pages; $340 per page for color pages). Under exceptional circumstances, the author(s) may apply to the editorial office for a waiver of the publication charges at the time of submission.

(*Revised February 2013*)

Editorial and Head Office:
Pearl City Koishikawa 603
2-4-5 Kasuga, Bunkyo-ku
Tokyo 112-0003 Japan
Tel: +81-3-5840-8764
Fax: +81-3-5840-8765
E-mail: office@biosciencetrends.com

BST
BioScience Trends

JOURNAL PUBLISHING AGREEMENT (JPA)

Manuscript No.:

Title:

Corresponding Author:

The International Advancement Center for Medicine & Health Research Co., Ltd. (IACMHR Co., Ltd.) is pleased to accept the above article for publication in BioScience Trends. The International Research and Cooperation Association for Bio & Socio-Sciences Advancement (IRCA-BSSA) reserves all rights to the published article. Your written acceptance of this JOURNAL PUBLISHING AGREEMENT is required before the article can be published. Please read this form carefully and sign it if you agree to its terms. The signed JOURNAL PUBLISHING AGREEMENT should be sent to the BioScience Trends office (Pearl City Koishikawa 603, 2-4-5 Kasuga, Bunkyo-ku, Tokyo 112-0003, Japan; E-mail: **office@biosciencetrends.com**; Tel: **+81-3-5840-8764**; Fax: **+81-3-5840-8765**).

1. Authorship Criteria

As the corresponding author, I certify on behalf of all of the authors that:
1) The article is an original work and does not involve fraud, fabrication, or plagiarism.
2) The article has not been published previously and is not currently under consideration for publication elsewhere. If accepted by BioScience Trends, the article will not be submitted for publication to any other journal.
3) The article contains no libelous or other unlawful statements and does not contain any materials that infringes upon individual privacy or proprietary rights or any statutory copyright.
4) I have obtained written permission from copyright owners for any excerpts from copyrighted works that are included and have credited the sources in my article.
5) All authors have made significant contributions to the study including the conception and design of this work, the analysis of the data, and the writing of the manuscript.
6) All authors have reviewed this manuscript and take responsibility for its content and approve its publication.
7) I have informed all of the authors of the terms of this publishing agreement and I am signing on their behalf as their agent.

2. Copyright Transfer Agreement

I hereby assign and transfer to IACMHR Co., Ltd. all exclusive rights of copyright ownership to the above work in the journal BioScience Trends, including but not limited to the right 1) to publish, republish, derivate, distribute, transmit, sell, and otherwise use the work and other related material worldwide, in whole or in part, in all languages, in electronic, printed, or any other forms of media now known or hereafter developed and the right 2) to authorize or license third parties to do any of the above.

I understand that these exclusive rights will become the property of IACMHR Co., Ltd., from the date the article is accepted for publication in the journal BioScience Trends. I also understand that IACMHR Co., Ltd. as a copyright owner has sole authority to license and permit reproductions of the article.

I understand that except for copyright, other proprietary rights related to the Work (*e.g.* patent or other rights to any process or procedure) shall be retained by the authors. To reproduce any text, figures, tables, or illustrations from this Work in future works of their own, the authors must obtain written permission from IACMHR Co., Ltd.; such permission cannot be unreasonably withheld by IACMHR Co., Ltd.

3. Conflict of Interest Disclosure

I confirm that all funding sources supporting the work and all institutions or people who contributed to the work but who do not meet the criteria for authors are acknowledged. I also confirm that all commercial affiliations, stock ownership, equity interests, or patent-licensing arrangements that could be considered to pose a financial conflict of interest in connection with the article have been disclosed.

Corresponding Author's Name (Signature):

Date: